Orf protein modulates phage and bacterial pathways of genetic recombination

Bowers, Laura Yvonne

Orf protein modulates phage and bacterial pathways of genetic recombination

Laura Yvonne Bowers B.Sc (Hons)

John Snow College, University of Durham

Thesis submitted to the Department of Biological and Biomedical Sciences, University of Durham for the degree of Doctor of Philosophy

December 2008

Contents

Tables and Figures

Declaration

The work presented in this thesis is my own original research, except where indicated by statement or citation, and has not been submitted for any other degree.

Acknowledgements

I would like to thank my supervisor Dr Gary Sharples for giving me the opportunity to pursue my dream of a PhD. I would also like to thank Dr Fiona Curtis, Dr Patricia Reed and Dr Lindsay Wilson and all of the other lab members of the Wolfson Research Institute for their friendship and support. Many thanks to Diane Hart for the excellent technical assistance and for always being available to provide help and support. Thank you, also, to Melissa Sivaneson for her friendship and support throughout my PhD, not diminished by her move to France to pursue her own PhD.

My greatest thanks go to my family because without them this would not have been possible. Mum and Dad, you have made many sacrifices for me to pursue this PhD and for that I am so grateful; your continuous encouragement and support has been fantastic – thank you. Ali, as you keep telling me, you are the greatest sister. Thank you for your friendship, support and most of all for being you.
I would also like to thank my maternal grandparents, Miriam Joan Campbell and the late John Campbell, who provide the inspiration and encouragement to pursue every dream and give my all.

Finally, thanks to the Complex Regional Pain Syndrome team at the Royal National Hospital for Rheumatic Diseases, Bath and Carole Dyer. Without their help and support, the physical demands of this PhD may have proved many steps too far – literally!

Orf protein modulates phage and bacterial pathways of genetic recombination

Laura Yvonne Bowers
University of Durham

The emergence of novel pathogenic organisms due to the acquisition of virulence determinants from bacteriophages has generated significant interest in the pathways responsible for genomic rearrangements.

Phage λ encodes its own recombination system, the Red system, comprising Exo, β and γ proteins. In addition, λ encodes another recombinase, Orf, which participates in the initial stages of genetic exchange and supplies a function equivalent to that of the *Escherichia coli* RecFOR proteins. This thesis focuses on determining the function of Orf in phage and bacterial recombination pathways by analysing its impact on recombinases encoded by λ and *E. coli*.

Experiments revealed that Orf interacts with bacterial and phage recombination proteins in the initial exchange step of recombination, modulating the activities of both Exo and RecA. Orf, along with β, attenuates the 5'-3' exonuclease activity of Exo, a feature that depends largely on the ability of Orf to bind DNA. Orf also facilitates loading of RecA onto ssDNA pre-coated with SSB but only if a ssDNA:dsDNA intersection is incorporated in the substrate. A motif similar to that found at the BRCA2-Rad51 interface may be responsible for Orf mimicking a RecA monomer to initiate nucleoprotein filament formation. Significantly, this would direct recombination down the bacterial RecA pathway of break restoration rather than the phage Red pathway with potentially important consequences for the outcome of the exchange reaction.

Chapter 1

Introduction

1.1 Summary

Bacteriophages facilitate the dissemination of virulence factors within and between bacterial populations thus contributing to the evolution of new infectious diseases. They are important vehicles for gene transfer between bacterial species, with phage gene acquisition occurring *via* genomic rearrangements at sites of limited sequence homology. In addition to lysogenisation, bacteria may also acquire new genes by transduction, transposition and transformation (Brussow *et al*, 2004; Davison, 1999). If gene acquisition confers a selective advantage it is retained and transmitted to subsequent generations, potentially leading to the emergence of more virulent bacterial strains (Miao & Miller, 1999).

Members of the λ and λ-like (lambdoid) phage family are known to contribute significantly to the virulence of pathogenic *Escherichia coli* (Wagner & Waldor, 2002; Friedman & Court, 2001). These phages can pick up new genetic material by genome rearrangements mediated by the viral Red recombination system and these exchanges may be affected by another recombinase called Orf in phage λ. This study focuses on identifying and characterising the role of Orf protein in phage and bacterial recombination pathways. This chapter summarises the known genetic recombination pathways in *E. coli* and λ and discusses the potential role of Orf in bacterial and phage exchange reactions.

1.2 Bacterial and Bacteriophage Diversity

There are ~4,500 dsDNA phages capable of infecting a large and diverse range of bacteria, offering multiple opportunities for genome rearrangements and horizontal gene transfer (Hendrix, 2002; Hendrix *et al*, 1999). Regular genome reorganisation is crucial for phage evolutionary success, with phages closely related to λ having similar genomic organisations. Widespread mosaicism of genome content is evident, suggesting extensive horizontal exchange between phages in the lambdoid group (Hambly & Suttle, 2005; Hendrix, 1999). Diversity in phage and bacterial populations is achieved by a combination of point mutations, transposable elements and

recombination between homologous DNA sites (Ziebuhr *et al*, 1999). In addition, horizontal gene transfer involving plasmids, phages and other mobile elements contributes to bacterial diversity. A combination of legitimate and illegitimate recombination generates diversity in phage and bacteria, with illegitimate (non-homologous) recombination, where recombination takes place between two dissimilar sequences, giving rise to the mosaicism observed in lambdoid phage (Juhala *et al*, 2000; Szabo *et al*, 1999). The general processes involved in the generation of diversity are also the basis for the pathogen evolution as they provide the means for transmission of virulence determinants between phages and bacteria (Miao & Miller, 1999; Ziebuhr *et al*, 1999). Horizontal genetic exchange plays a key role in the acquisition of virulence determinants, as well as in generating diversity throughout phage and bacterial populations (Koonin *et al*, 2001; Maiden, 1998). Phage-mediated gene transfer occurs *via* transduction or lysogenic conversion (Miao & Miller, 1999; Cheetham & Katz, 1995); bacterial gene disruption can also occur by prophage integration into the bacterial genome (Serra-Moreno *et al*, 2006; Brussow *et al*, 2004).

1.3 Bacteriophage λ

Phage λ is a temperate *E. coli* bacteriophage (Lederberg, 1951) with a dsDNA genome of 48,502 base pairs (Echols & Murialdo, 1978). Phage λ can replicate in either a lytic or lysogenic state; lytic development results in cell lysis and the release of progeny phage, while lysogenic development involves integration of the phage genome into the bacterial chromosome. The prophage persists in a quiescent state, which is passively inherited, until environmental signals induce excision and a return to the lytic cycle (Court *et al*, 2007). Since its discovery, phage λ has proved to be a valuable model system leading to its characterisation at both genetic and biochemical levels (Murray & Gann, 2007; Echolas & Gingery, 1968). Phage λ has 67 predicted genes, with at least six of these implicated in recombination and responsible for the exchanges that create innovative combinations.

1.4 Genetic Recombination

Recombination is one of a triad of interconnected systems responsible for maintaining genomic integrity - the other two being DNA replication and repair (Kreuzer, 2005; Kowalczykowski, 2000). Recombination was defined by Clark, (1971) as any set of

pathways in which elements of nucleic acid interact with a resultant change of linkage of genes or parts of genes. Genetic or homologous recombination is differentiated from other recombination processes, e.g. illegitimate and site-specific recombination, which depend on short DNA sequences, by its requirement for more extensive regions of identical or near-identical sequence (Weinstock, 1996). Homologous recombination, exchanging DNA chains between duplex molecules plays a crucial role in the generation and maintenance of genomic integrity (Court *et al*, 2002, Cox *et al*, 2000; Kowalczykowski *et al*, 1994). One of its major functions is the non-mutagenic restoration of stalled or collapsed replication forks (Kreuzer, 2005; Cox, 1998). Repair of a damaged replication fork is thought to be important for every bacterial cell in every generation (Cox, 1998). Although recombination plays a critical role in repair of broken or damaged DNA as a consequence of exposure to endogenous or exogenous agents, unregulated recombination can lead to genome instability and, in higher organisms, carcinogenesis (Cox, 2007; Kreuzer, 2005; Morimatsu & Kowalczykowski, 2003; Anderson & Kowalczykowski, 1997).

The Holliday model, proposed by Robin Holliday in 1964 (Holliday, 1964) was the prototypic model for homologous recombination but failed to account for key factors, such as the initial transfer of a single strand. The Meselson-Radding (Aviemore) model was proposed in 1975 (Meselson & Radding, 1975), followed by the double-strand break model (Szostak *et al*, 1983) based upon initiation of recombination at a double-strand break (DSB). In this latter model, unlike the others, the DNA molecule being invaded provides the genetic information required to repair the DSB by two rounds of single-strand repair synthesis (Kowalczykowski *et al*, 1994).

Genetic recombination in phage λ proceeds *via* two different general recombination systems - Rec (supplied by the *E. coli* host) and Red (supplied by the phage) (Lam *et al*, 1974; McMilin *et al*, 1974; Stahl *et al*, 1974). This thesis focuses on the proteins involved in the initiation stage of these two recombination systems.

1.5 Genetic Recombination in *E. coli*

Homologous recombination has been extensively studied in *E. coli* and is crucial for multiple DNA repair pathways and restoration of stalled and collapsed replication

forks (Sherratt, 2003). The activities of enzymes involved in repair at gaps and ends are described below.

1.5.1 RecA

The 38 kD RecA protein (Figure 1.1) is required for almost all homologous recombination events (Sheridan *et al*, 2008; Cox, 2007; Kowalczykowski *et al*, 1994; Muniyappa *et al*, 1984) and mutations inactivating the *recA* gene confer severe defects in recombination and DNA repair (Clark, 1973; Franklin, 1967; Clark & Margulies, 1965). RecA is a DNA-dependent ATPase that assembles as a helical nucleoprotein filament on ssDNA, responsible for homologous pairing and strand exchange (Takahashi *et al*, 2007; Rajan *et al*, 2006; Mazin & Kowalczykowski, 1999; Muniyappa *et al*, 1984; Shibata *et al*, 1980; Shibata *et al*, 1979a/b). RecA is also required for regulating the SOS response, a group of genes induced following DNA damage. Binding of RecA to ssDNA mediates the autocatalysis of the LexA repressor, resulting in expression of the SOS regulon (Giese *et al*, 2008; Little, 1984, 1991). In phage λ, a similar effect occurs with cleavage of the cI repressor leading to induction of the prophage (Little, 1984).

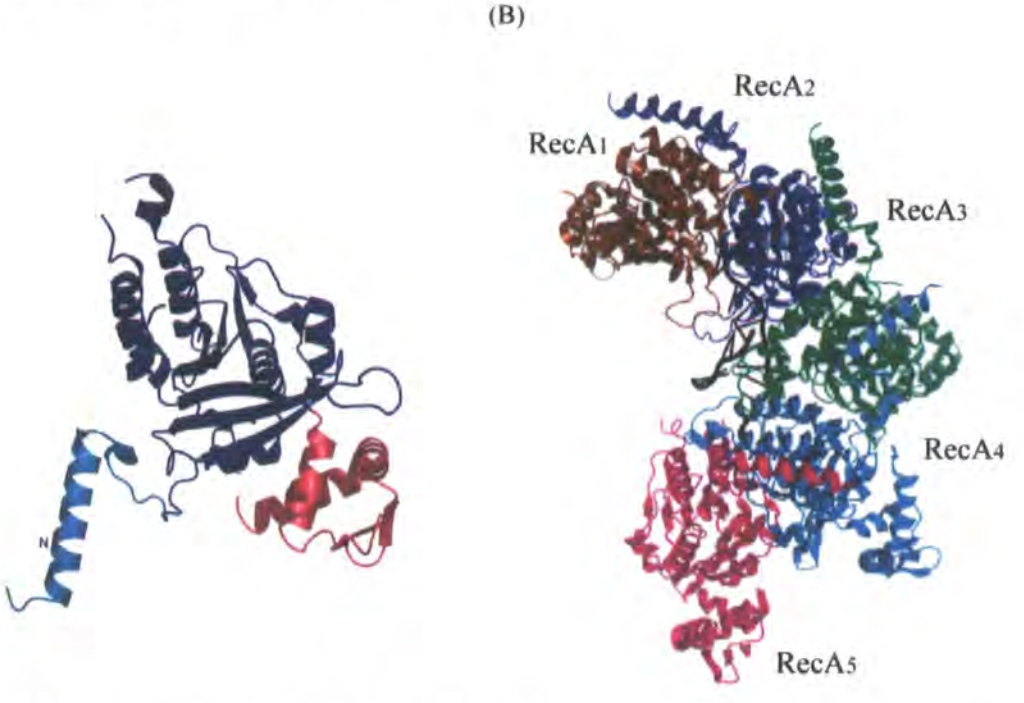

Figure 1.1. Structure of *Escherichia coli* RecA protein.
A) An *E. coli* RecA monomer (Story & Steitz, 1992; Story *et al*, 1992). The core domain is coloured blue, with N-terminus (teal) and C-terminus (pink). B) The post-synaptic nucleoprotein filament (Chen *et al*, 2008). The $RecA_5$-$(ADP\text{-}AlF_4\text{-}Mg)_5$-$(dT)_{15}$-$(dA)_{12}$ complex. Five RecA protomers are coloured rust, blue, green, cyan and magenta respectively. The DNA backbone is depicted in black.

RecA polymerises in a sequence dependent manner on ssDNA to form a right-handed dynamic helical filament, with six RecA monomers per turn (Biet *et al*, 1999; Dutreix, 1997; Tracy *et al*, 1997; Tracy & Kowalczykowski, 1996). RecA has a preference for GT-rich sequences such as the recombination hot spot χ (5'-GCTGGTGG-3') and CA dinucleotide repeats (Rajan *et al*, 2006). The RecA-ssDNA-ATP filament initiates a search for a homologous stretch of dsDNA and catalyses strand exchange in a polarised manner from 5'-3' with respect to the single strand within the filament; the initial, three-stranded, intermediate is known as a D-loop (Figure 1.2) (Takahashi *et al*, 2007; Umezu & Kolodner, 1994; Gupta *et al*, 1998; DasGupta & Radding, 1982). RecA is therefore a synapsis protein, with the ability to discriminate between homology and heterology during both pairing and strand exchange reactions (Amundsen & Smith, 2003; Bazemore *et al*, 1997; Kowalczykowski *et al*, 1994; Muniyappa *et al*, 1984; Wu *et al*, 1983).

Within a filament, RecA hydrolyses ATP in a reaction that is DNA-dependent (Cox *et al*, 2005). The ATP-dependency of RecA-DNA binding is explained by the allosteric coupling of RecA-ATP and RecA-DNA interactions, with cooperation bringing about alternative RecA-RecA interfaces and a conformational change to activate the filament for strand exchange (Chen *et al*, 2008; Renzette & Sandler, 2008; Shivashankar *et al*, 1999). Efficient recombination relies on the formation of RecA filaments where required but not otherwise, since this may produce inappropriate rearrangements (Anand *et al*, 2007). RecA filament assembly and disassembly are regulated at a number of levels notably by autoregulation, mediated by the C-terminus of RecA, and other *E. coli* proteins such as RecFOR (Morimatsu & Kowalczykowski, 2003), RdgC (Drees *et al*, 2006) and RecQ (Harmon & Kowalczykowski, 1998). Two others have direct effects, DinI (8 kD) stabilises the RecA-DNA filament while RecX (19.4 kD), encoded by a gene downstream of *recA*, acts as a negative modulator of RecA and is antagonised by DinI/RecF (Lusetti *et al*, 2006; Renzette *et al*, 2006; Drees *et al*, 2004a/b; Venkatesh *et al*, 2002).

1.5.2 SSB

The *ssb* gene product, single-stranded DNA binding protein (19 kD), was discovered in 1972 (Sigal *et al*, 1972) and belongs to the helix-destabilising class of proteins. SSB is an essential protein for DNA replication where it serves to prevent inter and

intra-strand annealing. SSB functions in homologous recombination by coating ssDNA exposed by the actions of helicases and nucleases (e.g. RecBCD and RecQJ) (Hatch *et al*, 2008; Kowalczykowski & Krupp, 1987; Muniyappa *et al*, 1984). The SSB-ssDNA complex usually prohibits RecA assembly but, at lower concentrations, stimulates RecA filament extension, as a consequence of removing the secondary structures which would normally impede filament growth (Lavery & Kowalczykowski, 1992; Kowalczykowski & Krupp, 1987). *In vitro* RecA ATPase activity can be inhibited or enhanced by SSB depending on factors such as the type of DNA substrate utilised (e.g. the presence of inverted repeats) and temperature (Shibata *et al*, 1980; Kowalczykowski & Krupp, 1987). *In vivo*, the presence of SSB reduces the efficiency of the homologous pairing promoted by RecA, however this problem is overcome by recombinases that stimulate RecA nucleation.

1.5.3 *E. coli* recombination pathways

In *E. coli*, collaboration between numerous proteins is required to initiate and then complete recombination, with two major pathways of recombination operating – RecBCD and RecFOR (Clark, 1971) (Figure 1.2). RecBCD (an exonuclease) is largely responsible for recombination at dsDNA breaks, while RecFOR deal with ssDNA gaps arising from replicational problems. Both tripartite assemblies aid RecA loading onto SSB-coated ssDNA. Once assembled, RecA-ssDNA filaments mediate homologous pairing and strand exchange (Takahashi *et al*, 2007; Renzette *et al*, 2008; Rajan *et al*, 2006; Mazin & Kowalczykowski, 1999). The requirement for RecBCD in dsDNA break repair can be circumvented by removing other exonucleases (encoded by *sbcB* and *sbcC* or *sbcD*) that lead to the preservation of substrates acted upon by RecQ, RecJ, RecF, RecO and RecR (Bidnenko *et al*, 1999; Lloyd & Buckman, 1985; Kuschner *et al*, 1971).

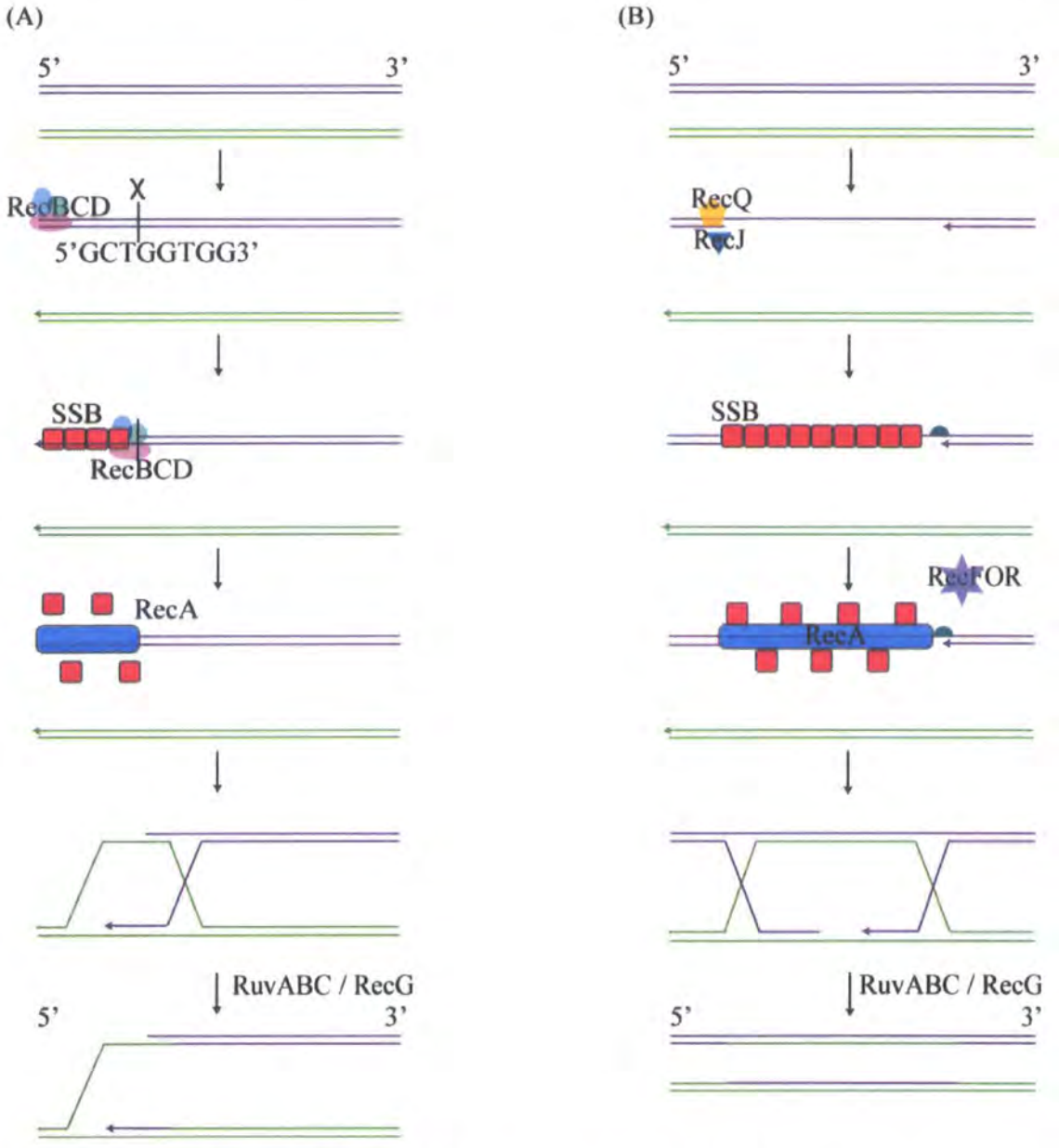

Figure 1.2. Model for two major pathways of homologous recombination in *E. coli*.
The RecBCD (A) and RecFOR (B) pathways both follow a similar approach with initiation by helicase and/or nuclease activities. SSB coats the exposed ssDNA and RecBCD or RecFOR facilitate RecA loading and displacement of SSB. RecA mediates homologous pairing and catalyses strand invasion and exchange with an intact sister duplex, leading to the formation of a Holliday junction. The Holliday junction can be resolved by duel strand scission mediated by the RuvABC complex or branch migration by the RecG helicase. Following resolution, DNA ligase seals any remaining nicks in the DNA.

1.5.3.1 RecBCD

The RecBCD holoenzyme is the main pathway of homologous recombination for the repair of dsDNA breaks in wild-type *E. coli* (Amundsen & Smith, 2003). It is a multifunctional 330 kD heterotrimeric protein complex (Figure 1.3), encoded by the *recB*, *recC* and *recD* genes (Sutherland *et al*, 2008; Wigley, 2007; Singleton *et al*, 2004; Arnold & Kowalczykowski, 2000; Roman *et al*, 1992).

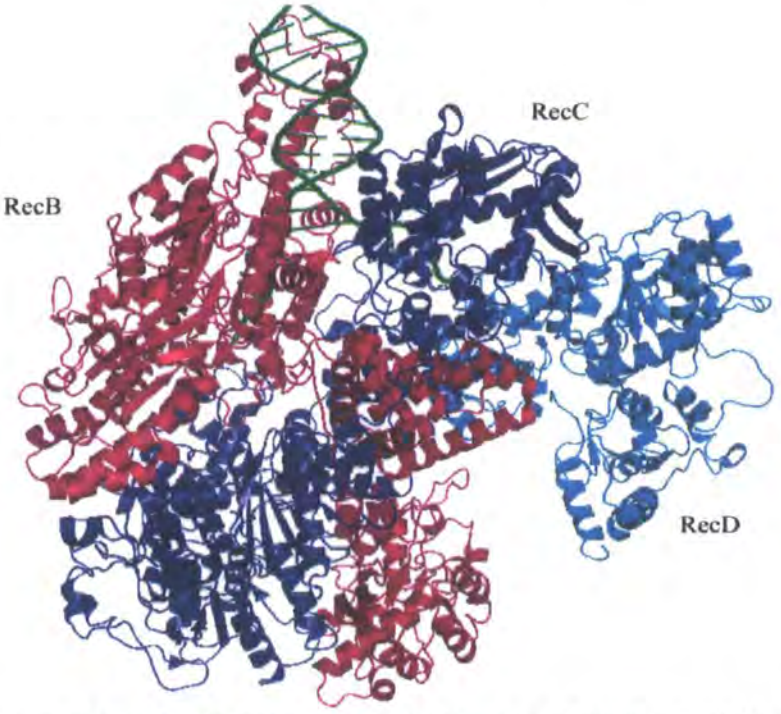

Figure 1.3. Structure of the RecBCD-DNA complex (Singleton *et al*, 2004). Bound DNA is shown in green.

RecBCD is a helicase and exonuclease, degrading both strands of blunt-ended dsDNA until it encounters the recombination hotspot χ (Chi; crossover hotspot instigator), consisting of the sequence 5'-GCTGGTGG-3. Recognition of χ attenuates the 5' strand nuclease activity of RecBCD to yield 3' ssDNA overhangs (Kowalczykowski, 2000; Bianco & Kowalczykowski, 1997). RecB is a 3'-5' slow helicase and multifunctional nuclease. RecC is important in χ recognition and RecD is a 5'-3' fast helicase and ssDNA-dependent ATPase (Singleton *et al*, 2004; Dillingham *et al*, 2003; Taylor & Smith, 2003). RecB and RecD comprise independently functioning motor subunits, each powered by the hydrolysis of ATP. Driven by these two motors, RecBCD, traverses the DNA at a rate greater than 1000 bp per second (Wigley, 2007;

Handa *et al*, 2005; Taylor & Smith, 2003; Korangy & Julin, 1994; Dixon & Kowalczykowski, 1993; Roman *et al*, 1992).

RecBCD helicase and nuclease activities unwind and digest DNA until χ is recognised and bound by RecC. The complex pauses and nuclease activity switches to favour 5'-3' in polarity (Spies *et al*, 2007; Handa & Kowalczykowski, 2006; Anderson & Kowalczykowski, 1997a/b; Anderson *et al*, 1997; Dixon & Kowalczykowski, 1993; Taylor & Smith, 1985). χ recognition elicits a change in lead motor subunit usage, thus regulating RecBCD translocation velocity. RecD helicase activity is faster prior to χ, however, following χ recognition, RecB predominates. As a consequence of the slower motor taking control, RecBCD translocation rate is reduced, possibly facilitating RecA loading (Spies *et al*, 2007; Spies *et al*, 2003; Bianco *et al*, 2001; Dixon & Kowalczykowski, 1995). RecBCD aids RecA assembly as a result of a conformational change bringing the RecA binding site close to the 3' ssDNA tail. Upon RecBCD-χ interaction, a nuclease dependent signal causes a change in RecD (a conformational alteration, rather than the ejection of RecD as proposed by Myers *et al*, 1995) and the RecB C-terminus is repositioned, revealing the RecA binding site in close proximity to the 3' tail (Spies *et al*, 2007; Wigley, 2007; Spies & Kowalczykowski, 2006; Handa *et al*, 2005; Amundsen *et al*, 2000; Anderson *et al*, 1997, 1999). RecBCD, in particular the 30 kD C-terminal region of RecB (Chang & Julin, 2001; Churchill & Kowalczykowski, 2000), then loads RecA to initiate recombination (Spies *et al*, 2005; Singleton *et al*, 2004; Amundsen *et al*, 2000; Churchill & Kowalczykowski, 2000). The final cleavage on the 3' ssDNA tail, performed by RecB following signalling by RecD (Amundsen *et al*, 2007), occurs at or within a few bases 3' of χ and the 3' tail is protected from further digestion (Taylor & Smith, 1999; Taylor & Smith, 1992). The χ sequence allows RecBCD to recognise chromosomal DNA and protect it from degradation. Double-strand breaks accumulate in *recBC* deficient cells and show a dramatic reduction in recombination and increased sensitivity to DNA damaging agents (Handa & Kowalczykowski, 2006; Amundsen *et al*, 2000; Arnold & Kowalczykowski, 2000; Kuzminov *et al*, 1994).

Facilitated loading of RecA is an essential function of the RecBCD holoenzyme and allows RecA to overcome its competitive disadvantage against SSB for binding to ssDNA, thus facilitating the initiation of recombination (Spies *et al*, 2007; Joo *et al*,

2006; Spies & Kowalczykowski, 2006; Arnold & Kowalczykowski, 2000; Anderson & Kowalczykowski, 1997; Kowalczykowski & Krupp, 1987).

1.5.3.2 RecFOR

The RecFOR pathway complements the RecBCD pathway in *E. coli*, preferentially repairing ssDNA gaps. The RecFOR pathway is equally as important as the RecBCD to the bacterium in fulfilling the major function of recombination, repairing stalled or collapsed replication forks (Cox *et al*, 2000; Kuzminov, 1999). Unlike the RecBCD pathway, where helicase, nuclease and RecA loading functions are all supplied by the RecBCD holoenzyme, the RecFOR pathway utilises individual components - RecQ (helicase; Umezu *et al*, 1990), RecJ (nuclease; Lovett & Kolodner, 1989) and RecFOR (facilitation of RecA loading; Morimatisu & Kowalczykowski, 2003).

The RecF, RecO and RecR proteins (Figure 1.4), as distinct RecOR and RecFR complexes, modulate both assembly and disassembly of RecA filaments (Inoue *et al*, 2008; Bork *et al*, 2001; Shan *et al*, 1997). The 40 kD RecF protein (Horii & Clark, 1973) has weak ATPase activity and binds ssDNA with an apparent stoichiometry of 1 RecF monomer per 15 nucleotides (Webb *et al*, 1995, 1999; Sandler *et al*, 1992; Madiraju & Clark, 1991; Griffin & Kolodner, 1990). RecF is thought to direct RecA loading to the edges of ssDNA gaps in duplex DNA (Morimatsu & Kowalczykowski, 2003) by specifically binding to dsDNA-ssDNA junctions (Hedge *et al*, 1996a). In the presence of ATP, RecF also binds dsDNA, with ATP hydrolysis leading to dissociation from DNA (Madiraju & Clark, 1992). RecF apparently has multiple functions, working with RecOR in some processes and independently in others (Rangarajan *et al*, 2002; Sandler, 1996).

The 26 kD RecO protein (Kolodner *et al*, 1985) is comprised of three domains and possesses sites for interaction with both DNA and other proteins (Leiros *et al*, 2005; Makharashvili *et al*, 2004). RecO possesses ATP-independent ssDNA strand annealing activity (Luisi-DeLuca, 1995; Luisi-DeLuca & Kolodner, 1994), a reaction that is enhanced when RecO forms a complex with SSB (Kantake *et al*, 2002). The crystal structure reveals potential sites of interaction with other proteins and DNA, consistent with specific contacts between RecO and SSB (Koroleva *et al*, 2007; Leiros *et al*, 2005). RecR inhibits DNA annealing promoted by RecO-SSB,

suggesting RecR and SSB compete for RecO binding (Kantake *et al*, 2002; Umezu & Kolodner, 1994).

The 22 kD RecR protein (Mahdi & Lloyd, 1989) forms a tetrameric ring with a central hole large enough to accommodate dsDNA, although *E. coli* RecR on its own is unable to bind DNA (Lee *et al*, 2004; Webb *et al*, 1995). RecR forms alternative complexes with RecF and RecO and both proteins compete for binding *via* the RecR toprim domain (Honda *et al*, 2006; Rangarajan *et al*, 2002; Bork *et al*, 2001). RecR probably tethers the two other proteins together at sites of DNA damage and acts as a dsDNA clamp in readiness for loading of RecA onto SSB-coated ssDNA (Lee *et al*, 2004).

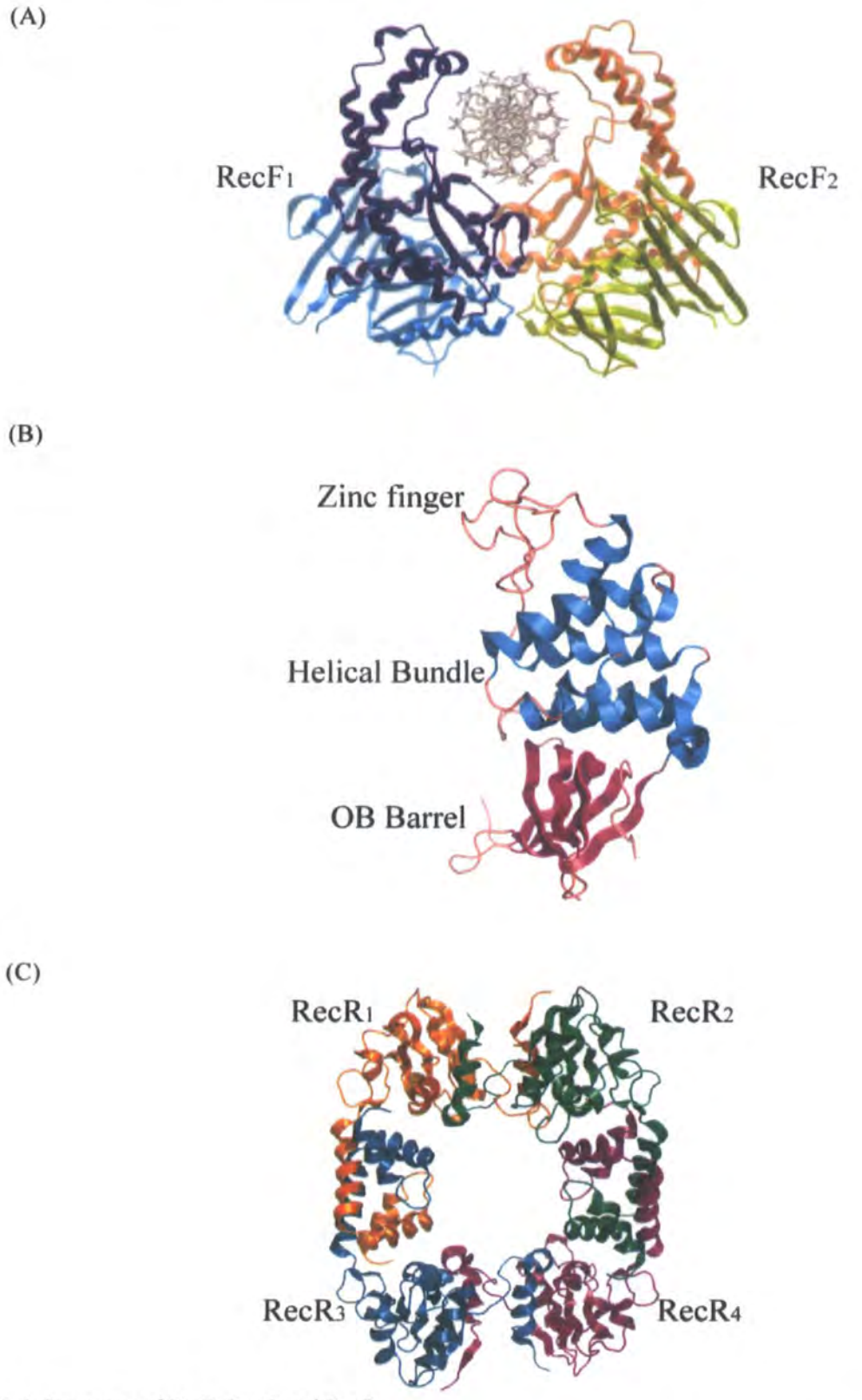

Figure 1.4. Structures of RecF, RecO and RecR.
A) Model of the RecF dimer bound to dsDNA (Koroleva *et al*, 2007). Lobe I and II of one monomer are coloured yellow and orange, respectively, with lobe I and II of the second monomer coloured cyan and dark blue. B-form dsDNA is shown in grey. B) RecO monomer (Leiros *et al*, 2005). Helices are shown in cyan and β strands in magenta; the zinc finger motif is a black sphere (which cannot be visualised in this diagram). C) RecR tetramer (Lee *et al*, 2004). RecR monomers are depicted orange, green, purple and teal respectively.

The RecOR complex stimulates RecA binding to SSB-coated ssDNA by binding to SSB and forming a RecO-RecR-SSB complex. RecOR continues to be associated with RecA after nucleation, potentially stabilising the filament as a result of a RecR-induced conformational change in RecO (Inoue *et al*, 2008; Bork *et al*, 2001; Shan *et al*, 1997; Umezu & Kolodner, 1994; Umezu *et al*, 1993). However, it has also been suggested that RecO and RecR may interact directly with RecA during the filament nucleation process and alter the conformation of RecA so that the C-terminus of RecA is no longer inhibitory (Eggler *et al*, 2003). While RecO and RecR are both required to facilitate RecA loading, the presence of RecF tends to inhibit this reaction (Shan *et al*, 1997; Umezu & Kolodner, 1994). RecF functions on its own to inhibit RecA filament formation (Xu & Marians, 2003; Umezu *et al*, 1993; Madiraju & Clark, 1991). However, Morimatsu & Kowalczykowski, 2003, demonstrated that RecF could enhance RecOR-mediated loading of RecA onto SSB-coated ssDNA when a gapped duplex substrate was employed (a result confirmed by Lusetti *et al*, 2006). RecF and RecR form a complex in an ATP and DNA-dependent fashion, with the complex primarily binding dsDNA and limiting RecA filament extension (Webb *et al*, 1995, 1997, 1999). RecR stimulates RecF ATPase activity but reduces RecF transfer rate from one DNA to another (Webb *et al*, 1995, 1999). However RecF, like SSB, antagonises RecX, a protein that inhibits RecA filament extension resulting in net filament disassembly (Baitin *et al*, 2008; Lusetti *et al*, 2006).

Despite the interactions noted between RecF, RecO and RecR (Hegde *et al*, 1996b) physical evidence for a RecFOR complex has yet to be found (Inoue *et al*, 2008). Lusetti *et al*, 2006 suggest that the RecF, RecO and RecR proteins are all required for RecA filament assembly but do not necessarily act together. RecOR could mediate RecA nucleation onto SSB-coated DNA, while RecF facilitates RecA filament extension by antagonising RecX. Inoue *et al*, 2008 concur, suggesting that the RecOR complex is responsible for displacing SSB from ssDNA, with RecF being required when a gapped DNA substrate is used to allow ssDNA-dsDNA junction specific loading of RecA.

1.6 λ Red Recombination

Bacteriophage λ possesses its own recombination system, the Red system, composed of the *exo*, *beta* and *gam* genes, which are clustered in the P_L operon and therefore

expressed early in the phage's transcriptional program (Poteete, 2001; Stahl, 1998). The Red system was identified following the discovery that λ could recombine normally in recombination-deficient *recA*, *recB* and *recC* strains (reviewed in Clark, 1973). Mutations in *exo* and *beta* eliminated homologous recombination in *recA* mutant strains confirming the involvement of the λ Red system (Franklin, 1967).
The phage Red system differs from *E. coli* RecA-dependent recombination by its ability to catalyse efficient recombination between very short regions (<50 bp) of sequence homology (Court *et al*, 2002). The pathways of recombination available to phage λ are described in section 1.7.

The 16 kD Gam protein (Figure 1.5) exists as a dimer in solution and associates with the *E. coli* RecBCD complex, inhibiting its activities by preventing binding to DNA (Court *et al*, 2007; Murphy, 1991, 2007; Karu *et al*, 1975). Gam also inhibits SbcCD, another host nuclease involved in recombinational repair (Kulkarni & Stahl, 1989). Red-mediated recombination requires Gam to preserve the linear concatemeric products of λ rolling-circle replication, arising from displacement of the 5' end of the leading strand in the θ replication mode from destruction by RecBCD and SbcCD (Stahl *et al*, 1997).

The 24 kD Exo protein or λ exonuclease binds free dsDNA ends and degrades a single strand in the 5'-3' direction, releasing 5' mononucleotides at a rate of ~12-16 nucleotides per second (Perkins *et al*, 2003; Subramanian *et al*, 2003; Matsuura *et al*, 2001; Mitsis & Kwagh, 1999; Cassuto & Radding, 1971; Little, 1967; Radding *et al*, 1966). Exo requires both Mg^{2+} and a 5'-terminal phosphate for activity and targets dsDNA ends (Cassuto & Radding, 1971; Little, 1967) it does not degrade at nicks or gaps in dsDNA or attack ssDNA substrates (Sriprakash *et al*, 1975; Carter & Radding, 1971). Three Exo monomers assemble to form a toroid with a funnel-shaped central channel capable of accommodating dsDNA at one end (30 Å) and ssDNA at the other (15 Å) (Figure 1.5) (Kovall & Matthews, 1998, 1997). The structure of Exo fits with it encircling its DNA substrate and remaining bound while hydrolysing nucleotides in a highly processive manner (Perkins *et al*, 2003; Subramanian *et al*, 2003; Kovall & Matthews, 1998). The degradation of the 5' strand by Exo produces long 3' ssDNA overhangs to which RecA can bind, therefore with Gam blocking the exonuclease

activities of RecBCD at DNA ends, Exo acts as an efficient replacement for the production of ssDNA for recombination.

The 29 kD β protein binds ssDNA and promotes annealing of complementary ssDNA strands (Kmiec & Holloman, 1981). Although β does not bind dsDNA directly, it remains tightly associated with the duplex product of annealing (Karakousis *et al*, 1998; Li *et al*, 1998). As well as promoting renaturation, β interacts with Exo and forms a complex in which β modulates the nucleolytic and recombination promoting activities of Exo (Tolun, 2007 *cited Poteete, 2008*; Muniyappa & Radding, 1986; Cassuto & Radding, 1971; Cassuto *et al*, 1971). β is capable of performing activities resembling those of both RecA and SSB, bringing ssDNA molecules together and reducing secondary structure in ssDNA (Li *et al*, 1998; Muniyappa & Radding, 1986). β can promote strand exchange in one direction by displacing a strand of dsDNA providing the substrate is AT-rich. However, it cannot mediate duplex strand invasion reactions typical of RecA and is unable to form D-loops (Rybalchenko *et al*, 2004; Li *et al*, 1998; Muniyappa & Radding, 1986).

β belongs to a family of annealing proteins, which includes RecT from the *E. coli* cryptic Rac prophage and RAD52 from eukaryotes (Iyer *et al*, 2002; Singleton *et al*, 2002). Analysis suggests β, RecT and RAD52 share a structurally similar mode of ssDNA binding and annealing (Wu *et al*, 2006; Singleton *et al*, 2002; Passy *et al*, 1999). β forms multisubunit rings in solution and in the presence of ssDNA, with the larger form of rings (~185-210 Å in diameter) being active in the initial catalysis of annealing. When two complementary strands of ssDNA are annealed or dsDNA is present, β forms left-handed helical filaments, possibly by the merging of rings (Passy *et al*, 1999). Study of the predicted binding regions of β and RAD52 (Figure 1.5) suggests that each β subunit contains a stable N-terminal core and a flexible central domain, which come together in the binding of DNA. This stabilises the central region and a flexible C-terminal domain, which is disordered and does not participate in DNA binding (Wu *et al*, 2006, Singleton *et al*, 2002; Mythili *et al*, 1996). The structure of RAD52 indicates the ssDNA binding site is a positively charged groove around the central hub, which binds the phosphodiester backbone of ssDNA and leaves nucleotide bases accessible for annealing to complementary ssDNA (Singleton

et al, 2002). The structure of β protein has yet to be elucidated, however, study of β by electron microscopy (Passy *et al*, 1999) and of the potential DNA interaction sites of both β and RAD52 (Wu *et al*, 2006; Singleton *et al*, 2002) provide some insight into the potential mechanisms by which β interacts with ssDNA and promotes strand annealing.

(A)

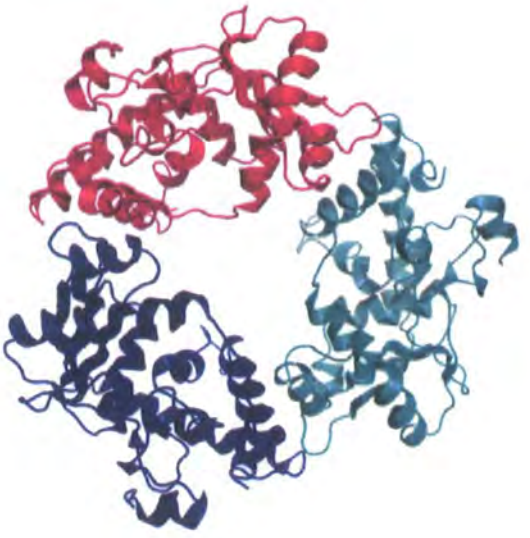

(B)

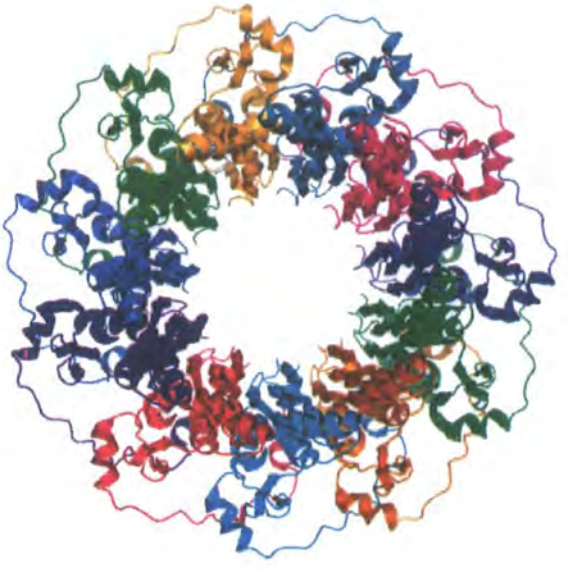

(C)

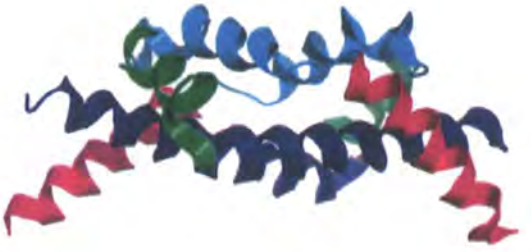

Figure 1.5. Structure of λ Exo, human Rad52 and λ Gam.
A) The trimeric λ exonuclease (Kovall & Matthews, 1997). Monomers are depicted in magenta, blue and cyan. B) Structure of the $Rad52_{1-209}$ undecamer ring (Singleton *et al*, 2002), viewed along the 11-fold symmetry axis. A similar ring-like structure may be adopted by β protein. C) Orthorhombic crystal structure of Gam (Court *et al*, 2007). The four helices are shown in magenta, cyan, green and blue.

1.7 Recombination pathways in λ

Homologous recombination occurs during the lytic cycle of phage λ, through expression of the *red* genes, irrespective of the recombination status of its host (Franklin, 1967). Double-strand breaks (DSB), which are processed by the Red pathway, may occur in λ as a result of restriction cleavage, replication fork collapse (to form rolling circles) or λ terminase cutting at the *cos* site before phage packaging (Sharples *et al*, 1998; Poteete & Fenton, 1993; Thaler *et al*, 1987a). In situations where normal phage DNA replication is absent or severely restricted the λ Red system, together with RecA, is able to promote high frequency recombination providing one partner in the cross has a DSB (Poteete & Fenton, 1993; Stahl *et al*, 1990).

The strand annealing and strand invasion pathways are active during phage λ recombination. Both recombination pathways require the presence of Exo and β (Muyrers *et al*, 2000) to facilitate the restoration of a genomic dsDNA break by exchange with a second λ genome (Stahl *et al*, 1997). RecA is responsible for the strand invasion route, which requires Exo to expose 3' ssDNA overhangs for binding; it is possible that β contributes to these reactions. Once assembled, RecA promotes homologous pairing and catalyses strand exchange to form branched recombination intermediates (Passy *et al*, 1999; Stahl *et al*, 1997) (Figure 1.6). Following D-loop formation several options for resolution are available. The D-loop possesses a 3'-end that can prime DNA replication, with extensive DNA synthesis providing a potential escape route. Alternatively, strand cleavage within the D-loop could generate a splice-type recombination intermediate (Hill *et al*, 1997). If a Holliday junction is created by further strand exchange into the adjacent dsDNA of the invading molecule it can be resolved to restore each chromosome in an intact state (Takahashi & Kobayashi, 1990; Szostak *et al*, 1983). In the presence of RecA, the strand invasion pathway is favoured, whereas in its absence, recombination by strand annealing predominates (Stahl *et al*, 1997).

Strand annealing initiates in the same manner as strand invasion, with Exo producing a 3' ssDNA overhang, however in this case the strand is paired by β to a complementary strand from another molecule (Kmiec & Holloman, 1981).

Continuing degradation by Exo trims the joint resulting in excess 3' ssDNA branches being assimilated into the dsDNA. DNA ligase seals the nicked duplex, completing the process and allowing the fused genomes to be packaged (Muniyappa & Radding, 1986; Cassuto & Radding, 1971; Cassuto *et al*, 1971). Strand annealing was proposed as a mechanism for Red recombination because recombination between λ chromosomes depended to a significant extent on DNA replication (Stahl *et al*, 1974). It was thought that phage DNA replication was required to generate sufficient DSBs distributed over the λ genome to provide suitable substrates for Red-mediated recombination (Thaler *et al*, 1987b). However, recently it has been proposed that replication plays a more substantial role in Red-mediated recombination than is accounted for by either the strand invasion or strand annealing pathways (Poteete, 2008). The alternative replisome invasion (template switch) model (Figure 1.7) requires Exo degrading dsDNA to give 3' ssDNA overhangs bound by β protein. β is then hypothesised to anneal the 3' tail of the linear DNA to complementary sequences in the lagging strand template of a replication fork, with the 3' ended strand positioned to displace the original template for the leading strand polymerase to induce a template switch. A nuclease, as yet unspecified, makes a single-stranded incision at the branch point, releasing the lagging strand arm and the remainder of the originally replicating chromosome, while the replication fork continues in the same direction on its new template. A second template switch, at the other end of the linear DNA is also required to account for Red-mediated, RecA-independent, gene replacement events (Poteete, 2008). This mechanism has yet to be thoroughly investigated but merits for consideration alongside strand invasion and strand annealing pathways.

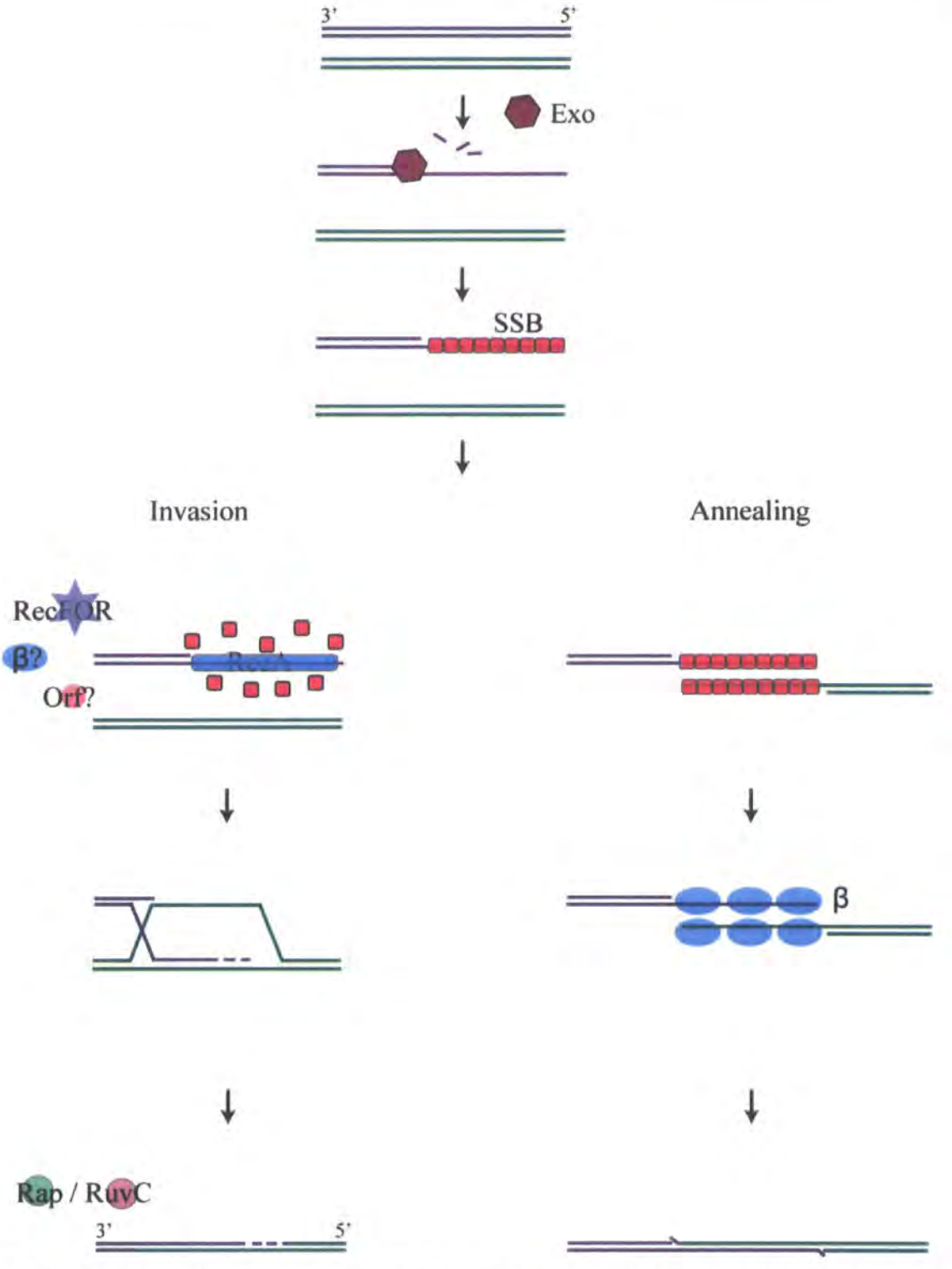

Figure 1.6. Model for strand invasion and strand annealing, the predominant pathways for recombination in phage λ.
Exo degrades DNA and degrades dsDNA ends in the 5'-3' direction to give 3' ssDNA overhangs which become coated in SSB. In the invasion pathway, RecFOR (and possibly β and Orf) facilitate loading of RecA onto the SSB coated DNA where it mediates homologous pairing and catalyses strand exchange; the recombination intermediate can be resolved by Rap or RuvC. The annealing pathway is RecA-independent and proceeds with β protein coating the 3' ssDNA overhangs and promoting annealing of homologous ssDNA. DNA ligase seals any remaining nicks in the DNA.

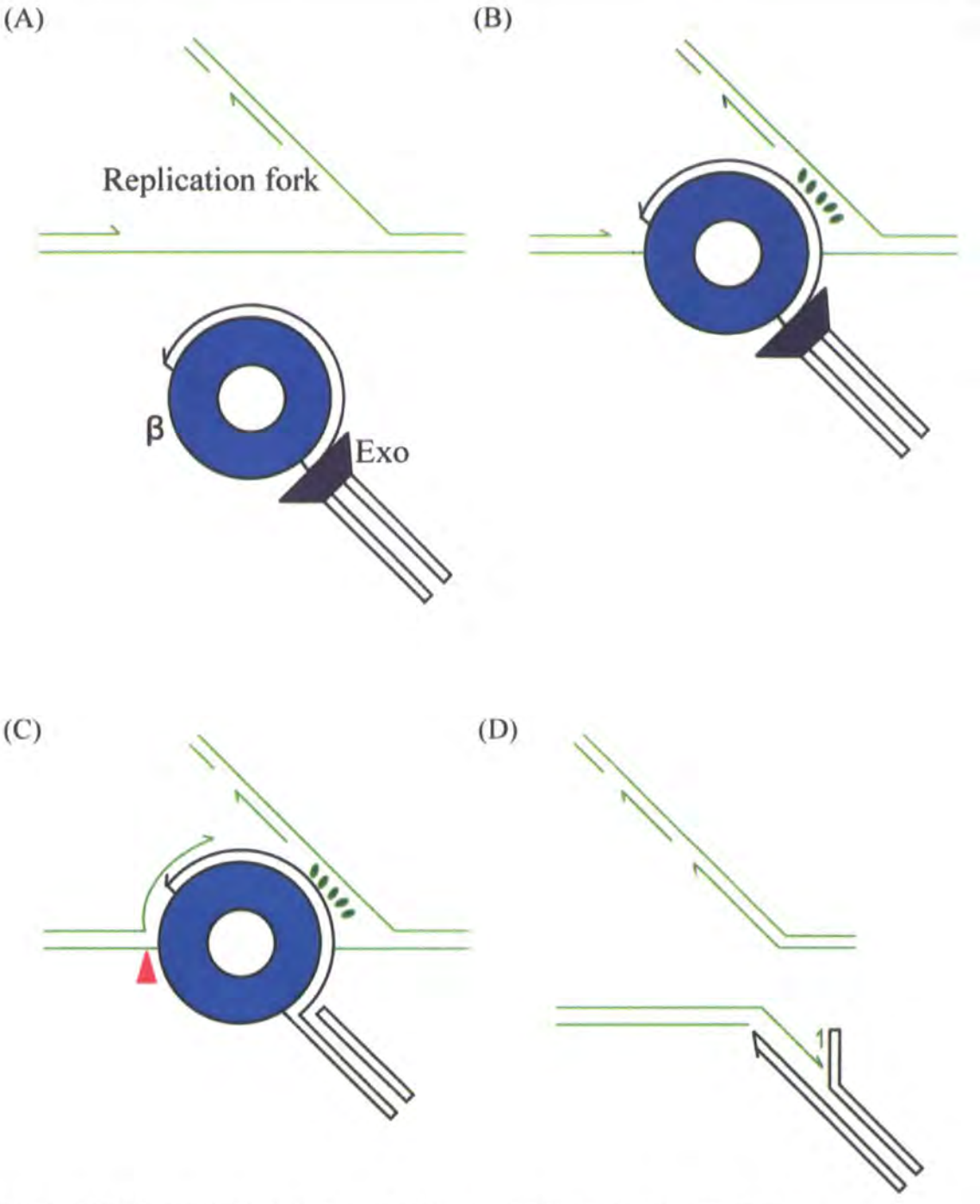

Figure 1.7. Red-mediated replisome invasion (template switch) model (Poteete, 2008).
A) A replication fork moving through λ DNA, left to right is shown in green. A dsDNA end processed by Exo is shown in black and white, with the 3' overhang wrapped around a β ring (blue). B) β anneals the captive strand to complementary bases, on the strand serving as a template for lagging strand synthesis, which are exposed by the replisome. C) β positions the invading strand to act as the new template for leading strand synthesis and a joint molecule is formed. The joint molecule is resolved by an endonucleolytic cleavage (pink triangle) and Exo either falls off or is removed. D) The detached lagging strand arm and unreplicated remainder of the right side of the parent chromosome are shown in the upper drawing. The incoming DNA, which is now serving as the template for both leading and lagging strand synthesis and the transferred replication fork moving in the same genetic direction on its new template are shown in the lower diagram.

1.8 Role of λ Orf in recombination

Phage λ has another recombination function known as *orf* (formerly *ninB*), which can replace the *recF*, *recO* and *recR* functions in λ, but not bacterial, recombination (Sawitzke & Stahl, 1992, 1994). The *orf* gene resides in the *ninR* region of phage λ, located between replication functions (O and P) and the regulator of late transcription (Q) (Hollifield *et al*, 1987; Kroger & Hobom, 1982). The *nin* region is dispensable for the growth of λ in the laboratory, however, the ten open-reading frames in this region are under positive selection. Although *nin* genes differ between phage, with 30-50 genes encountered within the lambdoid gene pool, each phage does retain approximately ten genes in this region (Juhala *et al*, 2000). It is likely that *nin* genes supply a particular set of capabilities, allowing the phage to adapt to an ecological niche. The functions of most *ninR* genes are unknown, however *orf* (*ninB*) and *rap* (*ninG*), and potentially *ninH*, are known to bind DNA and are likely participants in genetic recombination (Tarkowski *et al*, 2002; Sawitzke & Stahl, 1992, 1994).

Orf is a functional analogue of the *E. coli* RecF, RecO and RecR proteins (Maxwell *et al*, 2005) replacing RecFOR in λ crosses but not in host conjugational recombination (Sawitzke & Stahl, 1992, 1997). Orf encourages the formation of exchanges close to an initiating DSB in both the RecFOR and Red pathways (Tarkowski *et al*, 2002; Sawitzke & Stahl, 1997). It can partially substitute for *recFOR* mutants in *E. coli* recombination when Exo and β are present (i.e. Red-mediated) (Poteete, 2004). The Orf crystal structure reveals a homodimer arranged as a toroid, with a shallow U-shaped cleft perpendicular to the central cavity (Maxwell *et al*, 2005). The diameter of the central cavity is sufficient to accommodate ssDNA throughout but dsDNA only at the widest end (Figure 1.8). Orf preferentially binds ssDNA over dsDNA and forms complexes with gapped substrates and oligonucleotides containing 5' and 3' ssDNA overhangs with no obvious preference (Maxwell *et al*, 2005). The structure of Orf and its ability to bind gapped duplex DNA suggests that the U-shaped cleft may be the site of DNA binding. However, residues lining the central cavity are conserved in Orf homologues and many are positively charged suitable for binding of the phosphodiester backbone. If DNA is bound with this hole, the Orf dimer would have to open so that it could bind to substrates with dsDNA at each end (Reed, 2006). Orf

also associates with SSB in far-western and yeast-two hybrid assays (Maxwell *et al*, 2005).

(A)

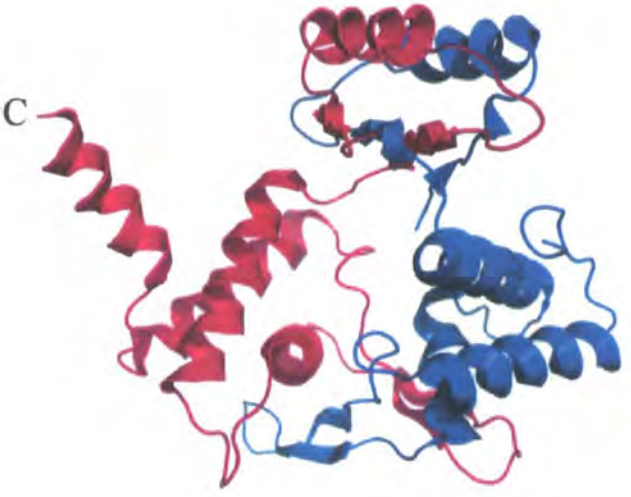

(B)

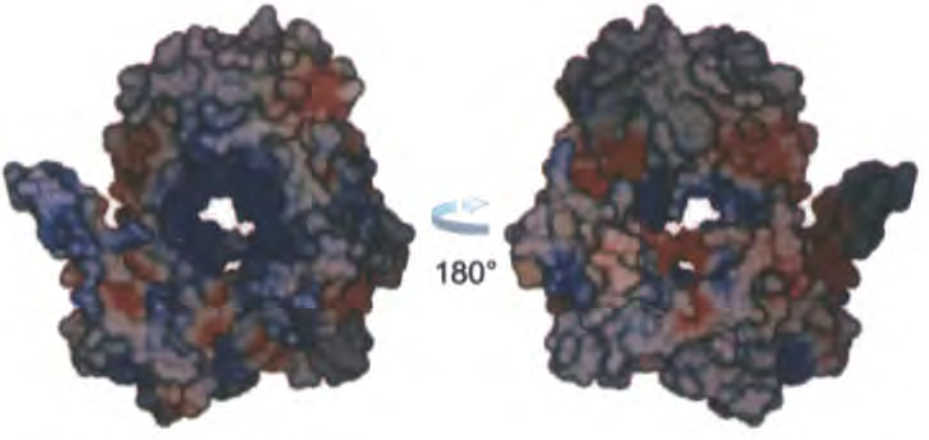

Figure 1.8. Structure of λ Orf (Maxwell *et al*, 2005).
A) Ribbon structure of Orf dimer with monomer one shown in magenta and monomer two in cyan. B) Electrostatic surface representation of the Orf dimer. Views of the central channel, the potential DNA binding site, from the top (left) and bottom (right) of the dimer are shown. Positively-charged residues are in blue and negatively charged residues in red.

As discussed earlier, RecFOR act during the initial stages of recombination to overcome the inhibitory effect of SSB by facilitating RecA loading onto ssDNA (Morimatsu & Kowalczykowski, 2003). The ability of Orf to substitute for RecFOR, under certain conditions *in vivo*, and interact with both ssDNA and SSB (Maxwell *et al*, 2005) indicates it may perform the same mechanistic function.

1.9 Thesis Objectives

The objective of this work is to further our understanding of how the λ Orf protein influences initial stage recombination events by interacting with bacterial and phage recombinases. Biochemical experiments will be performed to study the impact of Orf on RecA-mediated strand exchange in the presence or absence of SSB protein. The possible involvement of Orf and β in regulating the nuclease activity of Exo will also be investigated. In addition, two distantly-related members of the Orf family, *Escherichia coli* cryptic prophage DLP12 Orf151 and *Staphylococcus aureus* phage ϕETA Orf20, will be purified and their properties compared with λ Orf. The results should offer fresh insight into the molecular mechanisms of phage λ recombination and how these exchange events contribute to the emergence of new pathogenic bacteria.

Chapter 2

Materials and Methods

2.1 Computer Software

The text for this thesis was prepared in Microsoft Word, with figures produced and prepared in Adobe Illustrator and Adobe Photoshop respectively. Microsoft Excel was used for numerical analysis of data and graph production. Images of protein structures were generated using PyMol (DeLano, W.L. The PyMol Molecular Graphics System (2002), http://www.pymol.org). Protein sequences were obtained from the National Centre for Biotechnology Information (NCBI, www.ncbi.nlm.nih.gov) and protein structures obtained from the Protein Data Bank (www.rcsb.org/pdb). Densitometry calculations were performed using Image J (W. Rasband, National Institutes of Health).

2.2 Materials

2.2.1 Chemicals and reagents

Analytical grade chemicals and reagents used in this study were obtained from Amersham Biosciences, BDH Laboratory Supplies, Difco, Fischer Science, Invitrogen, New England Biolabs, Novagen and Sigma-Aldrich. Water used in this study was deionised and filtered, and when required, was sterilised by autoclaving at 121°C for 15 min except in the case of enzyme activity assays where pure ionized water obtained from Severn Biotech was used.

2.2.2 Growth media and antibiotics

Luria-Bertani (LB) broth composition 10 g Difco tryptone, 5 g Difco yeast extract, 0.5 g NaCl and 2 ml 1 M NaOH (pH7) made up to 1 L with SDW and autoclaved at 121°C for 15 min; LB media was solidified with 15 g/l Difco agar.

BL21-SI strains were cultured in LB media made without NaCl. Strains carrying a pMALc2 expression vector were cultured in LB broth containing 2 g/l glucose.

Mu broth composition 10 g Difco tryptone / peptone, 5 g Difco yeast extract, 10 g NaCl and 2 ml 1 M NaOH (to pH 7) made up to 1 L with SDW.

Antibiotic stocks were prepared in sterile distilled water, unless otherwise indicated, filtered and stored at 4°C before being added to media at the following concentrations: ampicillin (Ap) at 150 μg/ml, chloramphenicol (Cm) at 50 μg/ml and kanamycin (Km) at 40 μg/ml.

2.2.3 Bacterial strains and plasmids

Figure 2.1. Genotype and sources of *E. coli* strains

Strain	Relevant genotype	Source, reference(s), or construction
AB1157	*F⁻ thr-1 ara-14 leuB6 Δ(gpt-proA)62 lacY1 tsx-33 supE44 galK2 λ⁻ rac⁻ hisG4 rfbD1 mgl-51 rpsL31 kdgK51 cyl-5 mtl-1 argE3 thi-1 qsr⁻*	(Bachman,1996)
DH5α	*F'/endA1, hsdR17(r_K-m_K), glnV44, thi-1, recA1, gyrA (Nal^r), relA1, Δ(lacIZYA-argF)U169, deoR, (ϕ80dlacΔ(lacZ)M15)*	(Hanahan,1983)
BL21 (DE3)	*F⁻ ompT hsdS$_B$($r_B^-m_B^-$) gal dcm (λclt857 lacUV5-T7 gene 1 ind1 Sam7 nin5)*	(Studier & Moffatt, 1986)
BL21-AI	*F⁻ ompT hsdS$_B$($r_B^-m_B^-$) gal dcm araB::T7RNAP-tetA*	(Invitrogen, 2005)
BL21-SI	*F⁻ ompT lon hsdSB($r_B^-m_B^-$) gal dcm endA proU-T7 RNAP:: malQ-lacZ Tet^s*	(Hanahan, 1983) and US Patent
BL21-Codonplus	*F⁻ ompT hsdS($r_B^-m_B^-$) dcm$^+$ Tet^R galλ(DE3) endA Hte [argU ileY leuW Cam^R]*	(Weiner, 1994)

Figure 2.2. Plasmids

Plasmid	Description	Source / Reference
pMALc2	Expression vector for tagging proteins with maltose binding protein (MBP), Ap^R	New England Biolabs
pUC18	Cloning vector, Ap^R	MBI Fermentas
pT7-7	Expression vector with T7 ϕ10 promoter, Ap^R	(Tabor and Richardson,1985)
pET14b	Expression vector for tagging proteins with N-terminal His_6, Ap^R	Novagen
pET22b	Expression vector for tagging proteins with N-terminal His_6, Ap^R	Novagen
pET24a	Expression vector, Km^R	Novagen
pGEX-6P-1	Expression vector for tagging proteins with Glutathione S-transferase (GST), Ap^R	Amersham Biosciences
pLysS	Encodes T7 lysozyme active against T7 RNA polymerase, Cm^R	(Studier & Moffatt, 1986)
pLB100	*E. coli orf151* in pUC18, Ap^R, (EcoRI-BamHI)	This work
pLB101	*E. coli orf151* in pMALc2, Ap^R, (EcoRI-BamHI)	This work
pLB104	*S. aureus* phage ϕETA *orf20* in pET22b, Ap^R, (NdeI-HindIII)	This work
pLB105	*S. aureus* phage ϕETA *orf20*Δc82 in pMALc2, Ap^R, (EcoRI-HindIII)	This work
pLB107	λ *orf* in pGEX-6P-1, Ap^R, (EcoRI-SalI)	This work
pLB108	*E. coli orf151* in pGEX-6P-1, Ap^R, (EcoRI-SalI)	This work
pFC109	λ *ninH* in pT7-7, Ap^R (NdeI/HindIII)	Dr F.A. Curtis
pFC110	λ *ninH* in pET14b, Ap^R (NdeI/HindIII)	Dr F.A. Curtis
pFC130	*E. coli recA* in pT7-7, Ap^R (NdeI/BamHI)	Dr F.A. Curtis
pFC154	λ *exo* in pT7-7, Ap^R (NdeI/BamHI)	Dr F.A. Curtis

pFC155	λ *bet* in pT7-7, Ap^R (NdeI, BamHI)	Dr F.A. Curtis
pCC146	*E. coli ssb* in pET22b, Ap^R	(Cadman and McGlynn, 2004)
pPR109	λ *orfΔc6* in pT7-7, Ap^R (NdeI/BamHI)	Dr P. Reed
pPR110	λ *orfΔc19* in pT7-7, Ap^R (NdeI/BamHI)	Dr P. Reed
pPR111	λ *orfΔc6* in pET14b, Ap^R (NdeI/BamHI)	Dr P. Reed
pPR112	λ *orfΔc19* in pET14b, Ap^R (NdeI/BamHI)	Dr P. Reed
pPR113	*S. aureus* phage ϕETA *orf20* in pMALc2 (EcoRI-HindIII), Ap^R	Dr P. Reed
pPR114	λ *orf* in pMALc2 (EcoRI-BamHI), Ap^R	Dr P. Reed

2.2.4 Oligonucleotides

DNA oligonucleotides (HPSF-purified) were purchased from MWG-Biotech AG and supplied as a precipitate and resuspended in appropriate volume of TE (10 mM Tris-HCl pH 8.0, 1 mM EDTA) before use.

Figure 2.3. Oligonucleotides for PCR amplification

Name	Nucleotide sequence (5'-3')	Restriction site
Orf151-2	GACGATTTGGATCCCTGTAGATGTG	BamHI
Orf151-3	CGGAGGGAATTCATGAACCTCTCAC	EcoRI
NinB-1	GAGAGGGAACATATGAAAAAACTAA	NdeI
NinB-2	CCTGCCACCGGATCCACTAACGACA	BamHI
MBP-ETA20-1	ACGTGGAATTCATGCAATACATTAC	EcoRI
MBP-ETA20ΔC82	TTACAAGCTTGCGCTAGATTGTAGC	HindIII
ETA20-1	ACGTGGTTCATATGCAATACATTAC	NdeI
ETA20-2	CTTCCGCCAAGCTTACGATTAGGAG	HindIII
Exo-1	TGGCCATATGACACCGGACATTATC	NdeI
Exo-2	TGACGATCCGTCATCGCCATTGCTC	BamHI
Bet-1	TAAAACATATGAGTACTGCACTCGC	NdeI
Bet-2	TGCAGGATCCTGTCCGGTGTCATGC	BamHI

Figure 2.4. Oligonucleotides for assays

Name	Sequence (5'-3')	Length (nt)	Reference
NH7	GGCGACGTGATCACCAGATGATTGCTAGGCATGCTTTCCGCAAGAGAAGC	50	(Whitby, 1996)
NH8	GGCTTCTCTTGCGGAAAGCATGCCTAGCAATCCTGTCAGCTGCATGGAAC	50	(Whitby, 1996)
NH9	GGTTCCATGCAGCTGACAGGATTGCTAGGCTCAAGGCGAACTGCTAACGG	50	(Whitby, 1996)
NH10	ACCGTTAGCAGTTCGCCTTGAGCCTAGCAATCATCTGGTGATCACGTCGC	50	(Whitby, 1996)
NH11	GCTTCTCTTGCGGAAAGCATGCCTAGCAATCATCTGGTGATCACGTCGCC	50	(Whitby, 1996)
X174-LYB-1	GGACTCAGATAGTAATCCACGCTCT	25	This work
X174-LYB-2	GGTACTGAATCTCTTTAGTCGCAGTAGG	28	This work
X174-LYB-3	GAACTAAGTCAACCTCAGCACTAACC	26	This work
X174- LYB-4	CATTAGCTGTACCATACTCAGGCAC	25	This work
FAC1	AACGTCATAGACGATTACATTGCTAGGACATCTTTGCCCACGTTGACCCA	50	Dr F.A. Curtis
RGL14	TGGGTCAACGTGGGCAAAGATGTCCTAGCAATGTAATCGTCTATGACGTT	50	Prof. R.G. Lloyd
GF-51	CTACCGGTTGGTCACGGGTGACCATTGCTGAAAAACTCGGCGGCAAACAGC	51	Dr J. Yates

2.3 Biological Techniques

2.3.1 Propagation and maintenance of bacterial strains

"Overnight" cultures for routine use (expansion of population) were prepared by suspension of a single colony in 5 ml broth (LB/Mu), containing the required antibiotic(s) in order to maintain plasmids, and overnight incubation at 37°C, with gentle aeration. Strains prepared this way were suitable for storage for periods of 2-4 weeks at 4°C; longer-term storage was achieved by the addition of 80% glycerol to a final concentration of 40% with storage at -20°C.

Strains grown on solid media were streaked on LB/Mu agar plates, using disposable sterile plastic loops, to obtain single colonies; plates were incubated at 37°C for 8-16 hrs and then stored for up to 3 weeks at 4°C.

2.3.2 Harvesting bacterial cells from liquid culture

Centrifugation was employed in the harvesting of cells from liquid culture. Small volume samples (≤1.5 ml) were centrifuged in a MSE Micro Centaur bench-top centrifuge at 4000-6000 rpm (low speed) or 13000 rpm (high speed). Larger volumes were harvested at 4°C in Beckman Coulter Avanti J-E centrifuge (JA-20 or JA-10 Rotor) or Beckman-Coulter AVANTI J20-XP Centrifuge (JLA 8:1000 Rotor).

2.3.3 Competent cells

A calcium chloride protocol (Sambrook, 2001) was used to obtain chemically competent *E. coli* cells, which were snap frozen in dry ice and stored in 40 µl aliquots at -80°C.

2.3.4 Transformation of bacteria

Bacterial transformation was achieved using the heat-shock method. 1-2 µl of stock-sample plasmid DNA was added to 40 µl of competent cells and the mixture incubated on ice for 30 min, transferred to a heat block at 42°C for 1 min and then returned to ice for 1 min prior to addition of 500 µl SOC (2% Difco tryptone, 0.5% Difco yeast extract, 10 mM NaCl, 2.5 mM KCl, 10 mM $MgCl_2$, 20 mM $MgSO_4$ and 20 mM glucose) or LB and incubation at 37°C for 30-90 min. Following incubation, cells were harvested in a MSE Micro Centaur bench-top centrifuge at 6000 rpm and

resuspended in 100 µl fresh LB before being spread on appropriate selective media and incubated at 37°C overnight.

2.4 DNA preparation and analysis

2.4.1 Polymerase Chain Reaction (PCR)

Amplification of DNA for cloning purposes was performed by PCR, in a Techgene Thermocycler, according to the manufacturers instructions and using the buffers provided in the PCR kit (Invitrogen). Reactions typically comprised *ca.* 100 pmoles of each oligonucleotide, template DNA (1 µl in 50 µl), 2 mM of each of the four dNTPs, 2.5 units Platinum Pfx DNA polymerase (Invitrogen), 1 x final concentration of standard and enhancer reaction buffers and 1 mM $MgSO_4$. Reaction programmes employed varied and were modified, along with reaction components, if problems were encountered. A typical programme consisted of a three-step cycle (repeated ~30 times) with denaturation at 94°C for <40 sec, annealing at 45-70°C (temperature dependent on T_m of primers-usually 5°C less than the T_m) for ~40 sec and extension at 68°C for 1-3 min (1 min for every kb amplified).

PCR reactions on genomic DNA were carried out as above, except 1 colony was picked from an agar plate with a sterile disposable plastic loop and transferred into 100 µl of SDW and heated to 95°C for 2 min. After cooling and vortexing, 1 µl of this solution was added to the PCR reaction.

2.4.2 Purification of DNA

Small scale plasmid DNA extractions (1-100 ml cultures) and the purification of PCR and digestion products from agarose gel slices were performed using Qiagen supplied kits and protocols, with recovered DNA being stored in EB buffer (10 mM Tris-HCl pH 8.5) at -20°C.

2.4.3 Restriction Digestion

Restriction enzymes (Invitrogen), stored at -20°C were used with the appropriate reaction buffer (supplied by the manufacturer). Reactions were incubated at 37°C in a water bath for >1.5 hours. Digestion products were analysed by agarose gel. DNA fragments were excised and purified using Qiagen kits.

2.4.4 Ligation

Ligations containing a 5:1, 10:1 or 25:1 ratio of insert:vector were carried out using T4 DNA ligase (Invitrogen) and incubated for >30 min at room temperature before use in the transformation of bacteria with appropriate antibiotic selection.

2.4.5 Electrophoresis

a) Agarose gel electrophoresis

Carried out using 0.8-2% agarose-TBE gels containing 0.2 μg/ml ethidium bromide (EtBr), and prepared by melting powdered agarose in Tris-borate EDTA buffer (90mM Tris-borate pH 7.5, 2 mM EDTA) in a microwave. Molten agar was allowed to cool to ~55°C before addition of EtBr and pouring into the gel tank apparatus. DNA samples were mixed with loading dye (0.25% bromophenol blue, 0.25% xylene cyanol, 15% Ficoll type 400) to a final concentration of 20% before electrophoresis at 50-100 V for 30-90 min in TBE buffer. A λBstEII ladder was typically used as a marker.

b) SDS-polyacrylamide gel electrophoresis (SDS-PAGE)

Standard SDS-PAGE apparatus and protocols (BioRad Mini Protean III) were employed for 12.5-15% polyacrylamide gels made with 29:1 acrylamide-bisacrylamide (Sigma) in Tris-glycine running buffer (25 mM Tris-HCl, 250 mM glycine, 0.01% SDS). SDS-loading dye (100 mM Tris-HCl pH 6.8, 200 mM dithiothreitol, 4% SDS, 0.2% bromophenol blue, 20% glycerol) was added to protein samples, which were then incubated at 100°C for 2 min prior to loading and the gel being run at 200 V for ~1 hr. Gels were stained at room temperature with Coomassie blue (200 ml Methanol, 200 ml dH_2O, 80 ml acetic acid, 0.48 g Coomassie Blue R-250) and destained in 20% methanol, 10% acetic acid for 1-2 hrs.

c) Native PAGE

10% polyacrylamide gels in TBE buffer in a BioRad Protean II system were used to purify ^{32}P-labelled oligonucleotides and annealed substrates. Samples were mixed with loading dye, applied to the gel and electrophoresised with buffer recirculation.

Low-ionic strength (LIS) 4% polyacrylamide gels were used in DNA gel retardation assays. Electrophoresis took place in LIS buffer (6.7 mM Tris-HCl, 3.3 mM sodium

acetate, 2 mM EDTA) with loading dye omitted from the samples but added to the first lane of the gel as a marker.

2.4.6 Preparation of gapped DNA substrates

Sequences of oligonucleotides, X174-LYB1, X174-LYB2, X174-LYB3 and X174-LYB4, are complementary to the ϕX174ss virion DNA sequence at position 333-358, 1880-1908, 3692-3718 and 4734-4759, respectively. The LYB4000 substrate was prepared by incubating a solution containing 500 μM nucleotide ϕX174ss virion DNA and 0.035 μM (molecule concentration) of all four oligonucleotides in 10 mM Tris-HCl pH 8.0, 50 mM NaCl at 70°C for 3 min, followed by cooling to 25°C over a period of 1 hr. The LYB2000 substrate was prepared using the same procedure, except only two oligonucleotides (X174-LYB1 and X174-LYB3) were included in the annealing mixture.

2.4.7 5'-end labelling of DNA substrates and DNA substrate assembly

a) ^{32}P-labelling

NH7, ssDNA oligonucleotide, was 5'-end labelled using T4 polynucleotide kinase (Invitrogen) and γ-^{32}P ATP (Amersham Pharmacia). The mix comprised: 3 μl NH7 (100 ng/μl), 4 μl 5x Forward Reaction Buffer (350 mM Tris-HCl pH 7.6, 50 mM $MgCl_2$, 500 mM KCl, 5 mM 2-mercaptoethanol), 1 μl T4 polynucleotide kinase, 2 μl γ-^{32}P ATP and 10 μl SDW. Reactions were incubated at 37°C for 1 hr followed by 15 min at 65°C to inactivate the kinase. Following the addition of 30 μl SDW, the mixture was purified using a Micro Bio-spin column (BioRad) to separate labelled DNA from unincorporated ^{32}P ATP; the sample was made up to 50 μl with SDW and 90% recovery of oligonucleotide was assumed as defined by the manufacturer.

b) Annealing

Labelled oligonucleotides (NH7) were annealed with their complementary partners, to form J11/X, Flayed Duplex (FD) and Duplex Linear (DL) conformations, in SSC buffer (150 mM NaCl, 15 mM sodium citrate pH7.0). J11 contains an 11 bp core of homology flanked by regions of heterology (G.J. Sharples). Reactions were heated to 92°C for 2 min and then cooled on a heat block (Techne Dri-Block DB-2D) for ~2 hr before loading dye (5 μl) was added and products separated on a native

polyacrylamide gel (10% polyacrylamide in TBE buffer) for 180 min at 190 V. The gel was exposed to X-ray film and the bands corresponding to the required products excised and eluted by soaking in TE buffer (10 mM Tris-HCl, pH 8.0, 1 mM EDTA) at 4°C, overnight. The radioactivity recovered was measured in a Scintillation counter (Perkin Elmer 1450 Microbeta Wallac Trilux) and compared to that of the original labelled oligo, the concentration of which was known, to estimate the concentration of the DNA substrates recovered.

2.4.8 DNA Sequencing

Nucleotide sequencing was performed by the DBS Genomics sequencing service at the University of Durham.

2.5 Protein Overexpression and Purification

2.5.1 Protein overexpression

Target proteins cloned into pMALc2, pGEX-6P-1, pET14b, pET22b and pUC18 vectors were overexpressed in DH5α, BL21-AI, -SI, BL21 (DE3) pLysS or Codon plus backgrounds. Protein overexpression was performed in 500 ml or 1 L of fresh media, in 1 L or 2 L baffled flasks. Media was supplemented with the appropriate antibiotics and inoculated with 5-15 ml of an overnight culture. Cells were incubated at 37°C with vigorous aeration (180 rpm) to an absorbance (A_{650nm}) of ~0.5 as determined by a Spectronic 20+ spectrophotometer. Cultures were then induced by addition of IPTG (to 1 mM), NaCl (300 mM) or arabinose (100 mM) before a further 3 hr incubation at 37°C, 180 rpm (or overnight at 25°C, 140 rpm). Cells were harvested by centrifugation at 6000 rpm (JLA8:1000 rotor) at 4°C for 8-10 min.

2.5.2 Protein purification

Further detail on the purification protocols employed in this study are incorporated within the relevant chapters.

a) Purification Buffers

All buffers were derived from those detailed below with the necessary modifications to salt, pH, glycerol, imidazole, maltose and magnesium as appropriate:

Buffer A: 20 mM Tris-HCl pH 8.0, 1 mM EDTA, 0.5 mM dithiothreitol (DTT), 10% glycerol

Lysis Buffer: 100 mM Tris-HCl pH 8.0, 2 mM EDTA, 5% Glycerol

Nickel column Equilibration Buffer: 50 mM sodium phosphate (NaH_2PO_4) pH 8.0, 300 mM NaCl, 10 mM imidazole.

Nickel column Elute Buffer: 50 mM sodium phosphate pH 8.0, 300 mM NaCl, 250 mM imidazole

Amylose Column Buffer: 20 mM Tris-HCl pH 8.0, 200 mM NaCl, 1 mM EDTA.

Storage Buffer: 20 mM Tris-HCl pH 8.0, 1 mM EDTA, 0.5 mM dithiothreitol (DTT), 50% glycerol

b) Cell lysis and buffer exchange protocol

Cells were disrupted using either sonication (MSE Soniprep 150), at an amplitude of 7-7.5 in 20 second bursts or by cell disruption (Constant Cell Disruption System) at 15 Psi and 25 Psi. In both cases samples were kept on ice to limit localised heating. The cell lysate was centrifuged at 3 g for 20 min. The supernatant containing soluble proteins was dialysed into an appropriate buffer, following cell disruption and after purification columns by buffer exchange through dialysis tubing (17.5 mm, Medicell International Ltd), for 3-4 hrs at 4°C with stirring.

c) Chromatography

Ion exchange and affinity chromatography were performed at 4°C using matrices prepared and used according to the manufacturer's instructions and buffers described in section 2.5.2 (a). The following matrices were used in purification protocols: amylose resin (Amersham Biosciences), heparin agarose (Sigma), His-select nickel affinity gel (Sigma), phenyl-sepharose (Amersham Biosciences), phosphocellulose (Amersham Biosciences), Q-sepharose fast flow (Amersham Biosciences), Reactive Blue 4 powder (Sigma) and ssDNA cellulose powder (Sigma). Prior to use, matrices provided as suspensions were washed with distilled water and equilibrated with the appropriate buffer, whereas powdered matrices were prepared by addition of appropriate buffer followed by periods of absorption, mixing and removal of fines; matrices were then poured into the required column and equilibrated with appropriate buffer before addition of the sample. The flow through was collected and the column washed with appropriate buffer before elution, usually on a salt gradient. However in the case of amylose resin and His-select nickel affinity gel, the elution buffer contained 10 mM maltose or 250 mM imidazole, respectively.

2.5.3 Protein concentration estimations

The BioRad Protein Assay Kit – a modified version of the Bradford Assay, was used to estimate protein concentration, by following absorbance at 595 nm in a Cecil CE3041 Spectrophotometer. Bovine Serum Albumin (BSA) was used as a standard.

2.6 Biochemical Assays

2.6.1 ATPase Assays

a) NADH-oxidation-coupled spectrophotometric assay

This assay couples the formation of ADP, generated from the hydrolysis of ATP by RecA, to the oxidation of NADH to NAD^+. Hence the ATP hydrolysis rate was calculated as the initial steady state reaction velocity (μM/min), with the concentration of NADH oxidised divided by the change in time, assuming an extinction coefficient of 1.21 $mM^{-1}cm^{-1}$ for NADH at 380 nm. ϕX174, LYB4000 or LYB2000 DNA (final concentration of 5 μM;N) was incubated with SSB in 450 or 900 μl of reaction buffer (20 mM Tris-acetate pH 7.5, 10 mM magnesium acetate, 1 mM DTT, 5% Glycerol, 100 μg/μl BSA, 1 mM ATP, 1.5 mM phosphoenolpyruvate, 2 mM NADH, 20 units/ml pyruvate and 20 units/ml lactate dehydrogenase) at 30°C for 5 min. Additional proteins (excluding RecA) such as Orf, were preincubated in 50-100 μl buffer at 30°C for 5 min before mixing with the SSB-ssDNA complex and further incubation for 10 min at 30°C. Sample mixtures containing a final volume of 500-1000 μl were transformed to micro-quartz cuvettes and reactions initiated by addition of 3.6 μM (f.c.) RecA and any change in absorbance at 380 nm recorded for 15 min in a JASCO V-550 spectrophotometer.

b) Colourimetric phosphate-detection assay - Biomol Green Assay

Biomol green (Biomol), an analogue of malachite green, was employed as a single-point colourimetric assay for free phosphate in solution. Reactions were performed at 25°C in a clear, flat-bottom 96-well microplate and contained 0.5 μM RecA, 2 μM (N) LYB4000 DNA and 500 μM ATP in 1x assay buffer (25 mM Tris acetate pH 7.5; 5% glycerol; 10 mM magnesium acetate; 1 mM DTT) with a final volume of 100 μl. ATPase reactions (order of addition: DNA, SSB then Orf) were initiated by the addition of RecA and terminated at intervals by the addition of 200 μl Biomol Green reagent. The plate was incubated for 20 min at room temperature prior to reading the absorbance of the solutions at 625 nm in a Biotek Synergy HT microplate reader. To determine the amount of phosphate released during the ATPase reaction, the absorbances measured for the solution in the wells were compared to those of a series of phosphate standards to determine the phosphate concentration at the different time points of the reaction and thus obtain ATP hydrolysis rates.

c) MESG-phosphorolysis-coupled Assay

The EnzChek Phosphate Assay Kit (Molecular Probes) was employed to detect free phosphate in solution generated during ATP hydrolysis by RecA. Reactions were performed in clear, flat-bottom 96-well microtitre plates with a final reaction volume of 100 µl and absorbance measured using a Biotek Synergy HT microplate reader (360 nm). Reactions contained 0.5 µM RecA, 15 µM (N) LYB4000 DNA, 1 mM ATP, 0.2 mM MESG and 0.1 U PNP in 1x assay buffer (Molecular Probes). All components except RecA and ATP were added (order of addition: DNA, SSB then Orf) and the plate incubated for 5 min at 27°C. RecA was then added and the plate incubated for a further 5 min at 27°C before the reaction was initiated by the addition of ATP and the absorbance (360 nm) monitored every 15 sec for 30 min in the microplate reader. The rate of ATP hydrolysis was calculated by determining the amount of phosphate present at specified time points (using a standard phosphate curve, prepared alongside each assay) and dividing the change in phosphate by each time point to give ATP hydrolysis values in µM/min.

2.6.2 Enzyme Linked Immunosorbent Assays (ELISA)

Protein in PBS (or PBS alone for negative controls) was applied to flat bottom Immulon-2HB microtitre plates (Thermo Scientific), covered and incubated for 16 hrs at 37°C. Wells were washed with PBS containing 0.3% Tween-20 (Sigma) and then incubated for 1 hr at 37°C in this buffer (block) containing 5% milk powder. After washing, a second GST-tagged protein diluted in block buffer was added to the appropriate wells and the plates incubated at 37°C for 1 hr. Wells were washed again prior to addition of 1:1000 dilution of HRP-anti-GST antibody (Sigma) and the plate incubated (1 hr, 37°C). Appropriate controls were included at each stage.

After a further wash treatment, tetramethylbenzidine (TMB) (Sigma) was added to each well and allowed to develop at room temperature before the intensity of the colour reaction was measured at A_{620nm} in an Anthos htII plate reader.

2.6.3 Fluorescent Dye Displacement Assays

a) 4'6-Diamidino-2-phenylindole (DAPI) Assay

The degradative activity of Exo on linear λ DNA (dsDNA) was investigated by measuring the fluorescence change of dye-labelled DNA in a JASCO FP750

spectrofluorimeter (Ex. 345 nm; Em. 467 nm). λ DNA (48502 bp: Fermentas) was incubated at 65°C for 10 min in buffer (20 mM CHES pH 9.4, 1 mM DTT) to ensure linearity before mixing it in assay buffer (20 mM CHES pH 9.4, 2.5 mM $MgCl_2$, 1 mM DTT, 200-400 nM DAPI) to give a concentration of 2 μM (nucleotide). The fluorescence change on addition of DNA was recorded before addition of secondary proteins (if any) and Exo with fluorescence changes recorded for a further 10 min.

b) Hoechst 33258 (H33258) Assay

Assays were performed as described 2.6.3(a) with H33258 (300 nM) replacing DAPI (300 nM) in the assay buffer and spectrofluorimeter settings changed to Ex.344 nm; Em.487 nm.

c) Stopped Flow Assays employing DAPI

i) λ Exo

Exonuclease activity on linear λ DNA was investigated by detecting a change of fluorescence when Exo protein was mixed with DAPI-labelled DNA in an Applied Photophysics pbp Spectrakinetic stopped flow machine (Ex. 345 nm; Em. >420 nm) employing Spectrakinetic workstation v4 56-1 software.

λ DNA was prepared by heating to 65°C for 4 min in buffer – DAPI (20 mM CHES pH9.4, 2.5 mM $MgCl_2$, 1 mM DTT) before being placed on ice ready for use.

Samples contained 300 nM DAPI and 2 μM (N) λDNA (a final reaction concentration 1 μM(N)) and Exo at various concentrations. Samples were mixed at 37°C and any fluorescence change observed recorded for 200-1000 sec and compared to the DNA mixed with Buffer containing 300 nM DAPI.

ii) λ β

The ssDNA annealing activity of β was examined in the presence of two 50-mer oligonucleotides (FAC1 and RGL14) in the stopped-flow device as described for Exo in 2.6.3(i). However, in this case the reactions (in buffer containing 300 nM DAPI) contained 0.2 μM FAC1 (f.c. 0.1 μM) or 0.2 μM RGL14 (f.c. 0.1 μM) mixed with 0.2 μM His-β (f.c. 0.1 μM). Fluorescence changes were observed for 200 sec after mixing of protein and DNA samples.

2.6.4 DNA binding assays

Protein interactions with unlabelled DNA were performed by mixing λBstEII DNA (MBI Fermentas) with increasing concentrations of protein (31.25-500 nM) in binding buffer (50 mM Tris-HCl pH 8.0, 5 mM EDTA, 1 mM DTT, 100 μg/ml BSA, 5% glycerol). Controls without protein were carried out in parallel and subjected to the same reaction conditions and treatment. Binding mixtures were incubated at 4°C for 15 min prior to loading on 0.8% agarose gel. Electrophoresis was at 80 V for 1-2 hrs and DNA visualised by staining with ethidium bromide and exposure to UV light.

Protein binding to radio-labelled DNA was performed by mixing ^{32}P-labelled DNA with increasing concentrations of protein (200-800 nM) in binding buffer (50 mM Tris-HCl pH 8.0, 5 mM EDTA, 1 mM DTT, 100 μg/ml BSA, 5% glycerol). Reactions were incubated at 4°C for 15 min. A sample of 12 μl from each reaction was applied to a 4% LIS (Low ionic strength) gel and subjected to electrophoresis at 160 V for 60 min. The gels were dried onto 3MM paper in a Gel Dryer (BioRad) and labelled DNA visualised by autoradiography.

2.6.5 Nuclease assays

a) MBP-ETA20 / MBP-ETA20ΔC82 Assays

Nuclease assays (20 μl) were performed by mixing λBstEII DNA, ϕX174RF DNA or ϕX174 Virion DNA obtained from New England Biolabs with increasing concentrations of protein (31.25-500 nM) in nuclease buffer (50 mM Tris-HCl pH 8.0, 1 mM DTT, 100 μg/ml BSA) containing 1 mM $MgCl_2$. Reactions were incubated at 37°C for 30 min prior to addition of stop buffer (20 mM Tris-HCl pH 8.0, 0.5% v/v SDS, 20 mM EDTA, 2 mg/ml proteinase K) and incubation for a further 10 min at 37°C. Samples were mixed with loading dye and subjected to agarose gel electrophoresis at 80 V for 2 hr.

b) λ Exo Assays

Nuclease assays (100 μl) were performed by mixing 5 μM (N) λ DNA (Fermentas) with 0.001375 μl Exo (New England Biolabs) in buffer (67 mM Glycine-KOH pH 9.4 at 25°C, 2.5 mM $MgCl_2$, 50 μg/ml BSA) at 37°C. All components with the exception of Exo were mixed (order of addition: DNA, SSB, β, Orf then RecA) and

preincubated at 37°C for 5 min. Reactions were started by the addition of Exo. At appropriate time intervals, 15 µl was removed and mixed with stop buffer (20 mM Tris-HCl pH 8.0, 0.5% v/v SDS, 20 mM EDTA,
2 mg/ml proteinase K) and incubation continued for 10 min at 37°C. Samples were subjected to agarose gel electrophoresis as in 2.6.5(a). Densitometry calculations were performed using Image J.

Chapter 3

Purification of Orf and other recombination proteins

3.1 Introduction

Genetic evidence indicates that λ Orf influences the initial stage of genetic exchange, substituting for RecFOR in λ Red-mediated recombination and promoting bacterial recombination in cells expressing the Red system (Poteete, 2004; Tarkowski *et al*, 2002; Sawitze & Stahl, 1992, 1994). In order to investigate the biochemical properties of Orf and other λ and *E. coli* recombinases and assess any protein-protein interactions between them, several relevant proteins were overexpressed and purified.

To investigate any interactions and effects of λ Orf with host and phage recombination proteins, Red pathway proteins, λ Exo and β protein were overexpressed as N-His_6 fusions. Both *E. coli* SSB and RecA were purified using published protocols.

Three Orf family proteins, λ Orf, *Escherichia coli* cryptic prophage DLP12 Orf151 and *Staphylococcus aureus* phage ϕETA Orf20, were purified to facilitate comparison of the properties of these distantly related putative orthologues. Orf151, from the *E. coli* cryptic prophage DLP12 shares only 16% overall identity with λ Orf, however, structural analysis indicates Orf151 and λ Orf share a similar architecture (Reed, 2006). Similarly, *Staphylococcus aureus* phage ϕETA Orf20 is a distantly-related homologue of Orf, however, it carries an additional conserved C-terminal extension that matches the HNH family of nucleases (Mehta *et al*, 2004; Yamaguchi *et al*, 2000). ETA20 and a truncated protein, ETA20ΔC82, lacking the 82 C-terminal residues containing the HNH domain, were overexpressed and purified to examine the importance of the nuclease domain on ETA20 function.

3.2 Maltose-binding protein (MBP-) tagged λ Orf and *Escherichia coli* cryptic prophage DLP12 Orf151

Purification of wild-type and His-tagged MBP-Orf151 had previously been hampered by the fact that a large proportion of the protein precipitated with the cell debris after

lysis (Reed, 2006). In an effort to alleviate this problem an Orf151 construct fused to MBP was made. Attachment of a soluble globular domain (MBP) can enhance the solubility of intractable proteins and also allows for purification in a single step using amylose affinity resin (Sambrook, 2001). Similar solubility problems encountered with Orf were overcome by construction of an MBP-Orf fusion (Reed, 2006).

3.2.1 Construction of an MBP-Orf151 fusion

The *orf151* gene was amplified from *E. coli* K12 genomic DNA using oligonucleotides Orf151-2 and Orf151-3, designed to introduce flanking restriction sites for insertion in the appropriate orientation in pMALc2. The resulting clone (pLB101) fuses MBP (the *malE* product) to the N-terminus of Orf151. A deletion within the signal sequence of the *malE* gene leads to cytoplasmic expression of the MBP-Orf151 fusion protein (New England Biolabs). Nucleotide sequencing of pLB101 confirmed that no mutations within the *orf151* gene had been introduced by PCR.

3.2.2 Overexpression of MBP-Orf151

E. coli DH5α was transformed with pLB101 as described in Chapter 2. Cells were grown in 1 L of LB broth containing glucose, to limit expression of amylase, which could interfere with purification by degrading the amylose present in the affinity resin. Overexpression of MBP-Orf151 was induced by addition of IPTG (0.3 mM) at an absorbance of 0.5 (A_{650nm}). Uninduced and induced samples were analysed by SDS-PAGE and a band of ~60 kD corresponding to the MBP-Orf fusion protein was observed following IPTG addition (Figure 3.1).

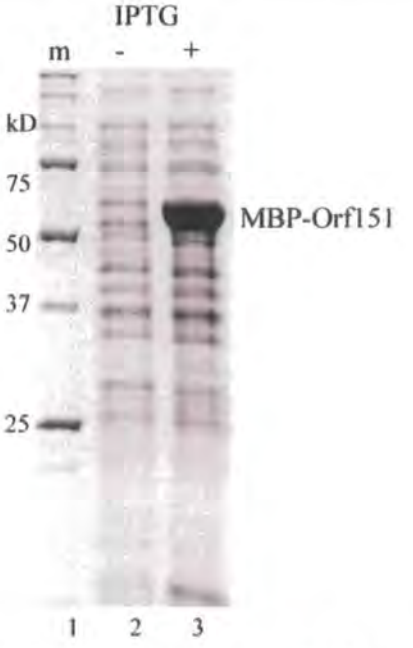

Figure 3.1. Overexpression of MBP-Orf151. Lane 1, molecular weight (MW) markers; Lane 2, uninduced DH5α pLB101; Lane 3, IPTG-induced DH5α pLB101.

3.2.3 Purification of MBP-Orf151

Overexpressed cells harvested by centrifugation (3 g) were resuspended in 10 ml of column buffer and lysed by sonication before samples of the supernatant and pellet were analysed by SDS-PAGE (Figure 3.2, lanes 4 and 5). The cell lysate containing MBP-Orf151 was applied to an amylose column and eluted with buffer containing 10 mM maltose. The majority of the MBP-Orf151 protein appeared in the first two fractions (Figure 3.2, lanes 9-10). A total of 26.25 mg of purified MBP-Orf151 was recovered at a concentration of 17.5 mg/ml. Following purification, a single band of ~60 kD was visualised by SDS-PAGE; purified MBP-Orf151 was aliquoted and stored at -80°C.

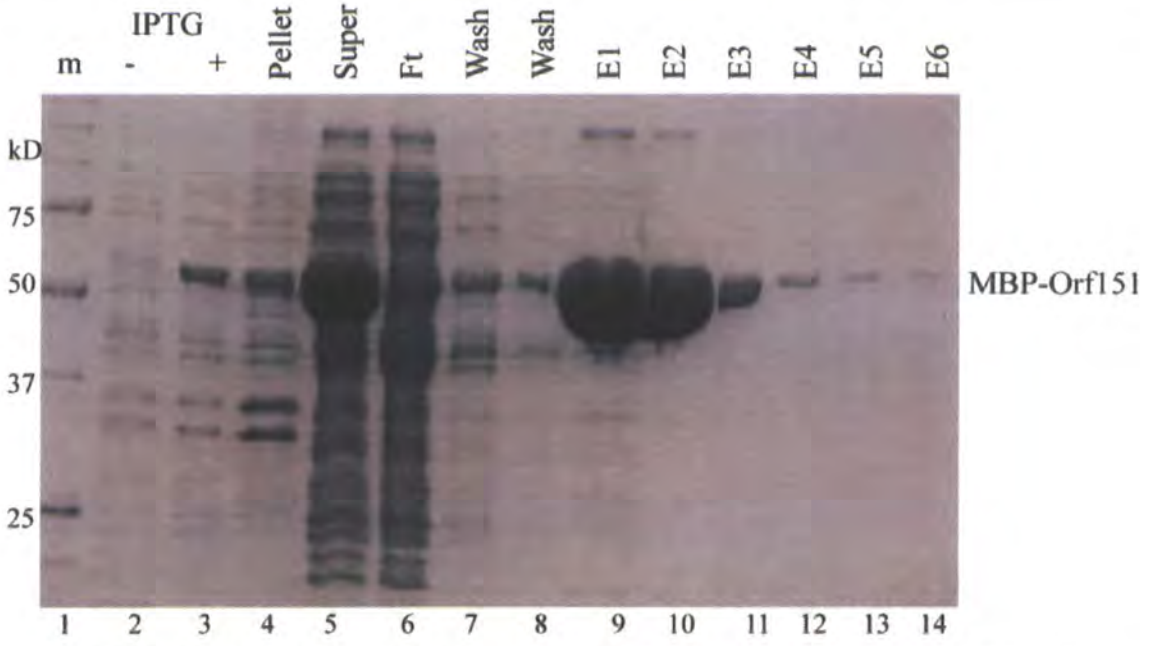

Figure 3.2. Purification of MBP-Orf151 by amylose affinity chromatography. Lane 1, MW markers; Lanes 2 and 3, uninduced and induced DH5α pLB101; Lane 4, pellet following cell lysis; Lane 5, supernatant following cell lysis; Lane 6, flow-through from column; Lanes 7 and 8, wash fractions; Lanes 9-14, consecutive fractions from the column, eluted in the presence of 10 mM maltose.

3.3 Glutathione S-transferase (GST-) tagged λ Orf and *Escherichia coli* prophage DLP12 Orf151

The MBP-Orf and MBP-Orf151 proteins were sufficiently pure to use in biochemical assays. However, to perform ELISA, and obtain alternatively tagged proteins for other studies, GST-tagged proteins were also generated.

3.3.1 Construction and overexpression of GST-Orf and GST-Orf151 fusions

N-terminal GST fusions of Orf and Orf151 were constructed by subcloning the *orf* and *orf151* genes in pPR114 and pLB101, respectively, into pGEX-6P-1 using EcoRI and SalI restriction sites to give pLB107 (GST-Orf) and pLB108 (GST-Orf151). *E. coli* BL21 Codon Plus carrying pLB107 and pLB108 were grown in 6 L of Mu broth, containing ampicillin. Overexpression of GST-Orf and GST-Orf151 was induced by addition of IPTG and samples were analysed by SDS-PAGE. Bands of ~43 kD corresponding to the GST-Orf and GST-Orf151 fusion protein were observed (Figure 3.3 A and B).

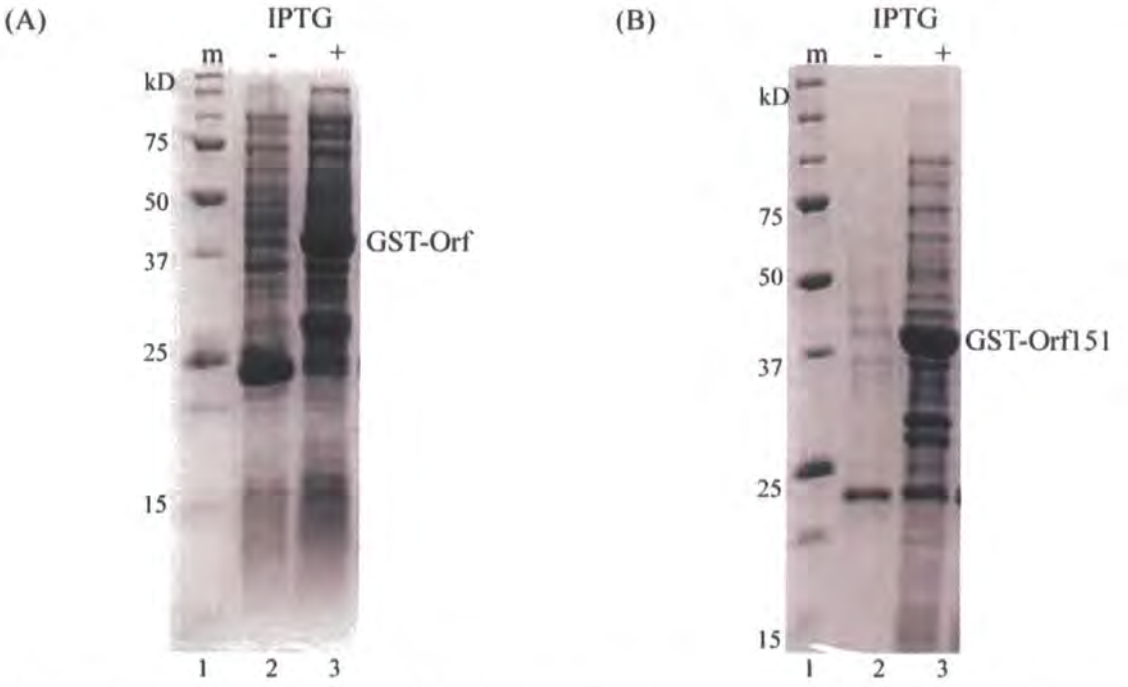

Figure 3.3. Overexpression of GST-Orf (A) and GST-Orf151 (B). Lane 1, MW markers; Lane 2, uninduced BL21 C^+ pLB107/8; Lane 3, IPTG-induced BL21 C^+ pLB107/8.

3.3.2 Purification of GST-Orf and GST-Orf151

Cells were lysed as described in the materials and methods section and the cell lysate, containing GST-Orf or GST-Orf151 in PBS, was mixed with approximately 4 ml of pre-equilibrated glutathione sepharose resin. A column was poured with the mixture and the flow through collected before the matrix was washed with PBS. Bound proteins were eluted from the glutathione sepharose matrix in the presence of 10 mM glutathione. The majority of both GST-Orf and Orf151 appeared in elution fractions 1-4 (Figure 3.4 A and B), however, contaminating proteins were evident so additional chromatography steps were performed.

(A)

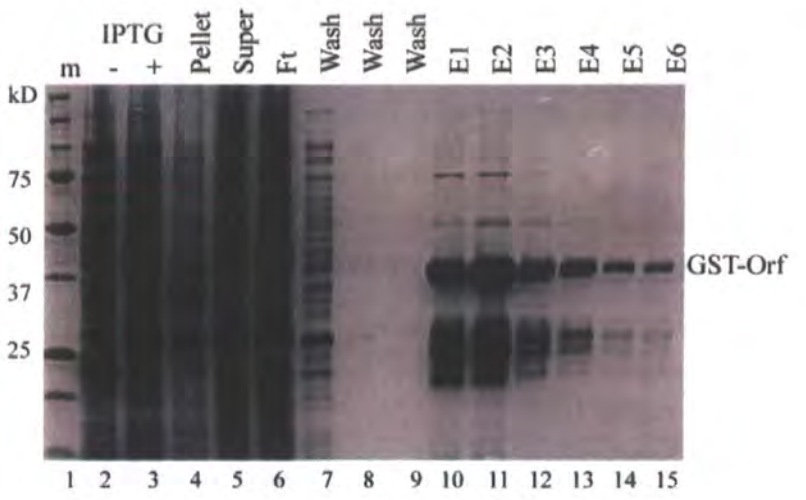

(B)

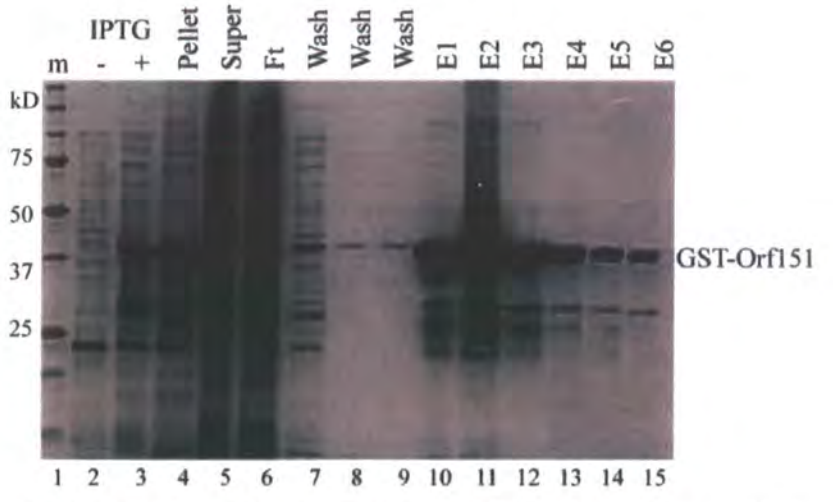

Figure 3.4. Purification of GST-Orf and GST-Orf151 by glutathione sepharose affinity chromatography. Lane 1, MW markers; Lanes 2 and 3, uninduced and induced BL21 C^+ pLB107/8; Lane 4, pellet following cell lysis; Lane 5, supernatant following cell lysis; Lane 6, flow-through from column; Lanes 7, 8 and 9, wash fractions; Lanes 10-15, consecutive fractions from the column, eluted in the presence of 10 mM glutathione.

Dialysed fractions from the glutathione sepharose column were applied to a 2 ml heparin agarose column. Neither GST-Orf nor GST-Orf151 bound well to this column and this step did not significantly improve the purity of samples. Flow-through samples from the heparin column were applied to a 2 ml Q-sepharose fast flow column. GST-Orf appeared in the flow through and between 0.3-0.4 M KCl. The unbound sample was dialysed to give GST-Orf1 and elution fractions pooled and dialysed as GST-Orf2. In contrast, GST-Orf151 bound well to this column, with the majority of GST-Orf151 eluting in a broad peak at 0.35-0.65 M KCl. The purified GST-Orf and GST-Orf151 proteins were analysed by SDS-PAGE (Figure 3.5) and

stored in aliquots at -80°C. A total of 27 mg purified GST-Orf (6 mg/ml) and 32 mg GST-Orf151 (16.2 mg/ml) was recovered. The samples contain trace amounts of GST and Orf/Orf151 probably due to proteolytic cleavage at the linker between the two domains.

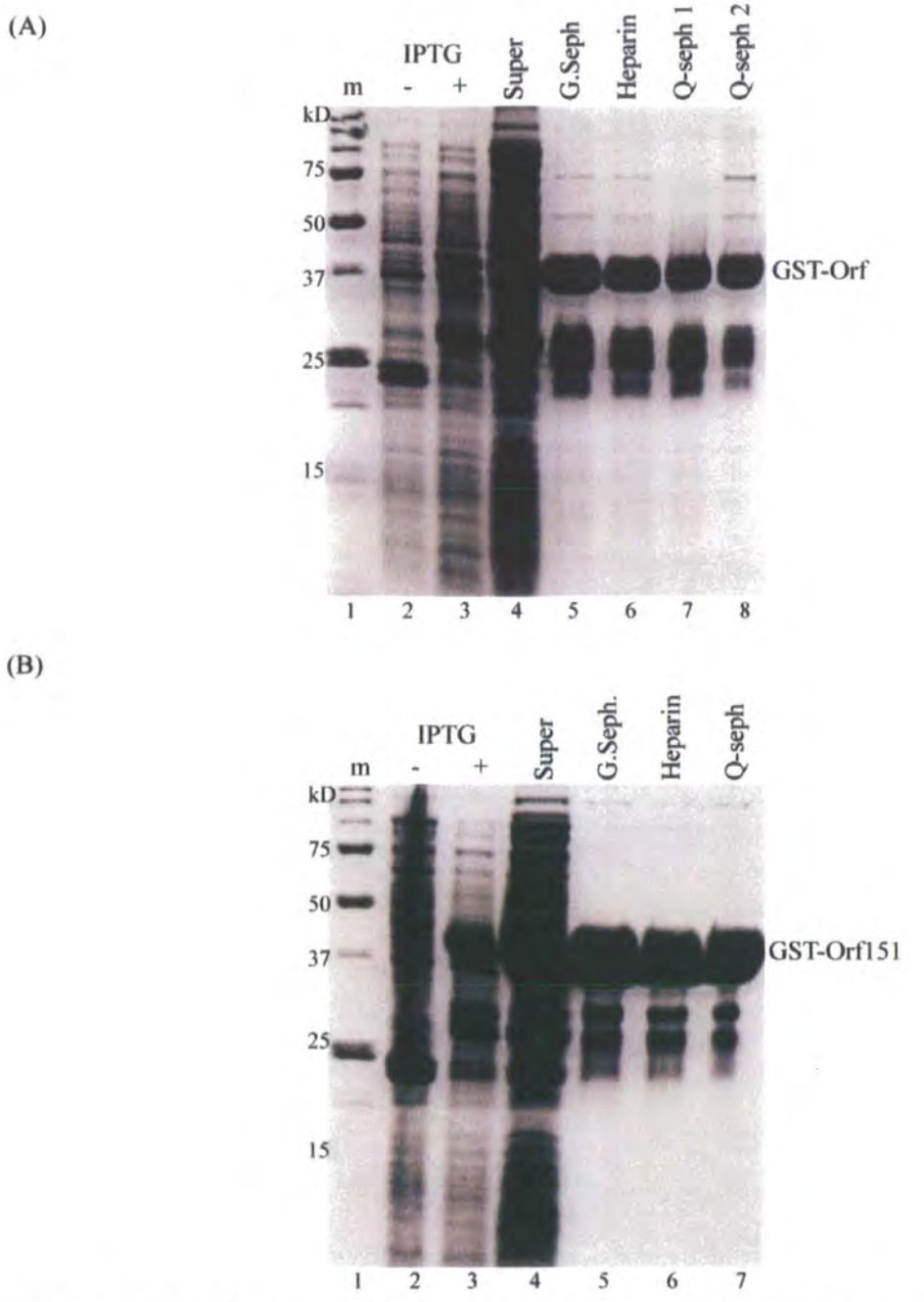

Figure 3.5. Purification steps for GST-Orf (A) and GST-Orf151 (B). Lane 1, MW markers; Lanes 2 and 3, uninduced and induced BL21 C^+ pLB107/8; Lane 4, supernatant following cell lysis; Lane 5, sample from glutathione sepharose column; Lane 6, sample from heparin column; Lanes 7 and 8, samples from Q-sepharose fast flow column.

3.4 *Staphylococcus aureus* phage ϕETA Orf20 (ETA20 & ETA20ΔC82)

3.4.1 Cloning of ETA20 and ETA20ΔC82

The *eta20 and eta20ΔC82* genes were amplified from *S. aureus* phage ϕETA genomic DNA (a gift from M. Sugai, Department of Microbiology, Hiroshima University, Japan) using oligonucleotides ETA20-1 and ETA20-2 and MBP-ETA20-1 and MBP-ETA20ΔC82 respectively. These oligonucleotides were designed to introduce flanking restriction sites, an NdeI (ETA20) or EcoRI (ETA20ΔC82) site at the 5'end of the gene and a HindIII site at the 3' end. The ETA20 clone was made by Dr F. A. Curtis. Insertion of the PCR products in pMALc2, pre-cut with NdeI/EcoRI and HindIII, fused MBP (the *malE* product) to the N-terminus of ETA20 (pPR113) and ETA20ΔC82 (pLB105). The integrity of the cloned genes was confirmed by nucleotide sequencing.

3.4.2 Overexpression of MBP-ETA20 and MBP-ETA20ΔC82

E. coli BL21 Codon Plus containing pPR113 was grown in 4 L of Mu broth, containing ampicillin and chloramphenicol and expression induced as before. A band of ~69 kD corresponding to MBP-ETA20 was detected by SDS-PAGE (Figure 3.6). MBP-ETA20ΔC82 was overexpressed in a similar fashion from 4 L of *E. coli* DH5α pLB105 cells and a band of ~65 kD corresponding to the MBP-ETA20ΔC82 fusion protein was observed (Figure 3.6).

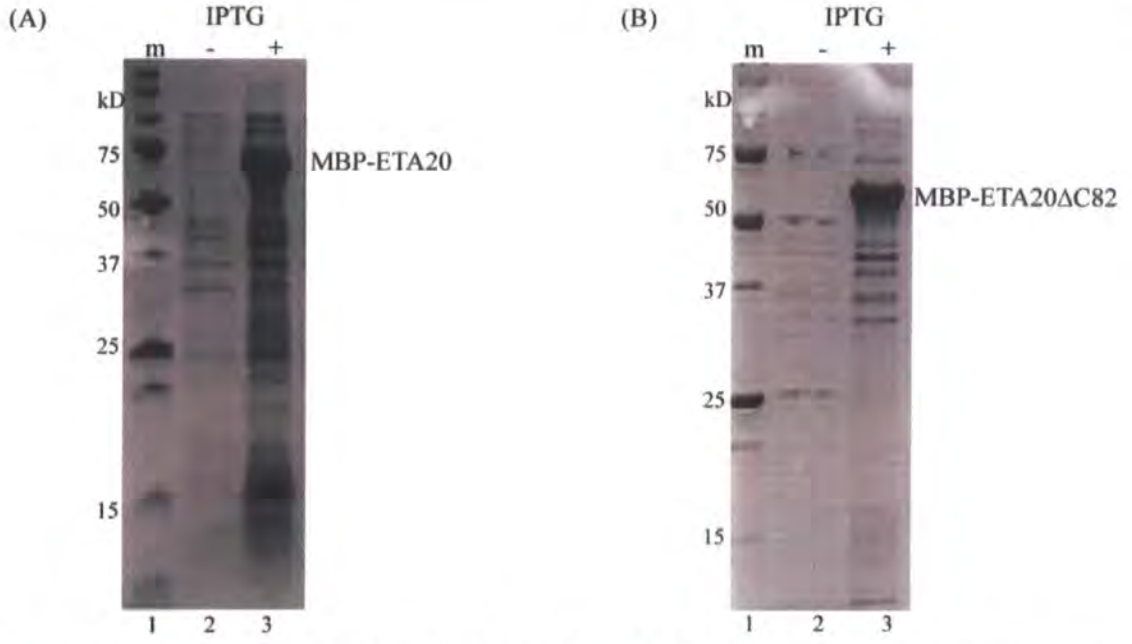

Figure 3.6. Overexpression of MBP-ETA20 (A) and MBP-ETA20ΔC82 (B). Lane 1, molecular weight (MW) markers; Lane 2, uninduced BL21 C^+ pPR113 / DH5α pLB105; Lane 3, IPTG-induced BL21 C^+ pPR113 / DH5α pLB105.

3.4.3 Purification of MBP-ETA20 and MBP-ETA20ΔC82

a) MBP-ETA20

Overexpressed cells (4 L) were harvested and lysed according to the methodology described in Chapter 2. The cell lysate containing MBP-ETA20 in column buffer was applied to approximately 8 ml of pre-equilibrated amylose resin. The majority of the MBP-ETA20 protein appeared in the first elution fraction when bound proteins were eluted from the amylose matrix in the presence of 10 mM maltose (Figure 3.7, lanes 8-13). The protein was not sufficiently pure so further chromatography steps were employed.

The dialysed MBP-ETA20 fractions from the amylose column were applied to a 2 ml heparin agarose column, however the protein failed to bind the column. The flow through was next applied to a 2.5 ml reactive blue-4 column where, once again, the protein failed to bind. A further step of Q-sepharose ion exchange chromatography at pH 7.0 (1 ml) was therefore undertaken. In addition to appearing in the flow through, MBP-ETA20 eluted from the Q-sepharose matrix between 0.2-0.45 M KCl. The elution fractions were pooled and dialysed as MBP-ETA20(1) and the flow through as MBP-ETA20(2). The purified MBP-ETA20(1) (4.25 mg/ml) was stored in aliquots at

-80°C. The sample contains some free MBP protein and trace minor contaminating proteins (Figure 3.9).

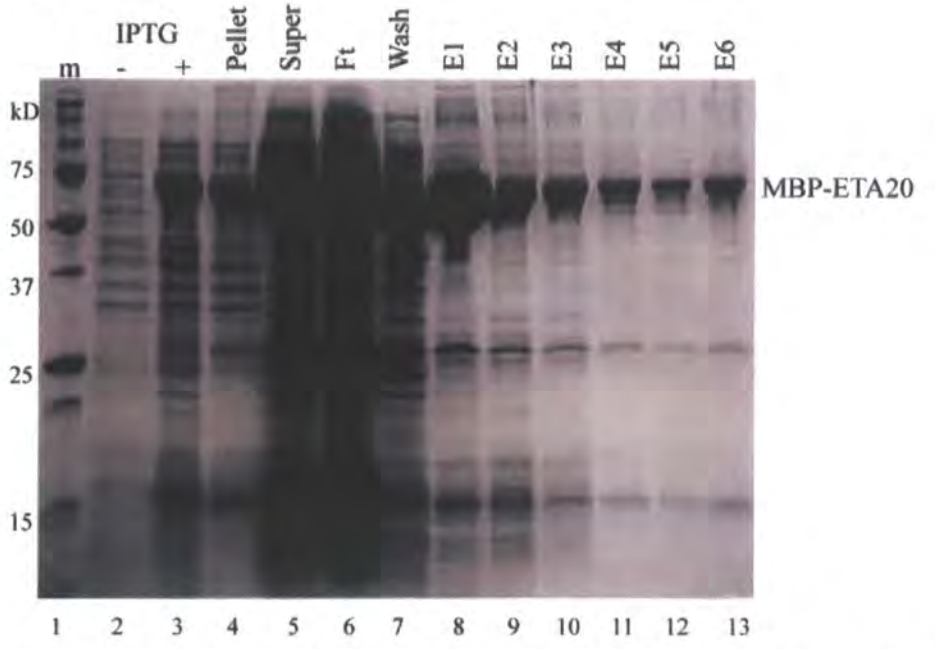

Figure 3.7. Purification of MBP-ETA20 by amylose affinity chromatography. Lane 1, MW markers; Lanes 2 and 3, uninduced and induced BL21 C^+ pPR113; Lane 4, pellet following cell lysis; Lane 5, supernatant following cell lysis; Lane 6, flow-through from column; Lane 7, wash fraction; Lanes 8-13, consecutive fractions from the column, eluted in the presence of 10 mM maltose.

b) MBP-ETA20ΔC82

The cell lysate containing MBP-ETA20ΔC82 was mixed with approximately 2 ml of amylose resin. From the resulting column, the majority of MBP-ETA20ΔC82 appeared in the first two fractions (Figure 3.8), however protein was not sufficiently pure at this stage necessitating additional purification steps.

MBP-ETA20ΔC82-containing fractions from amylose chromatography were applied to a 1 ml Q-sepharose fast flow ion exchange chromatography column. Bound protein eluted from the column between 0.3-0.5 M KCl but still retained contaminating proteins. Pooled fractions were also passed through heparin agarose, phosphocellulose and reactive blue-4 columns where, although the protein failed to bind, several contaminating proteins were eliminated. The purified MBP-ETA20ΔC82 (0.65 mg/ml) was stored in aliquots at -80°C. It contains some free MBP protein and trace minor contaminants as with the MBP-ETA20 protein (Figure 3.9).

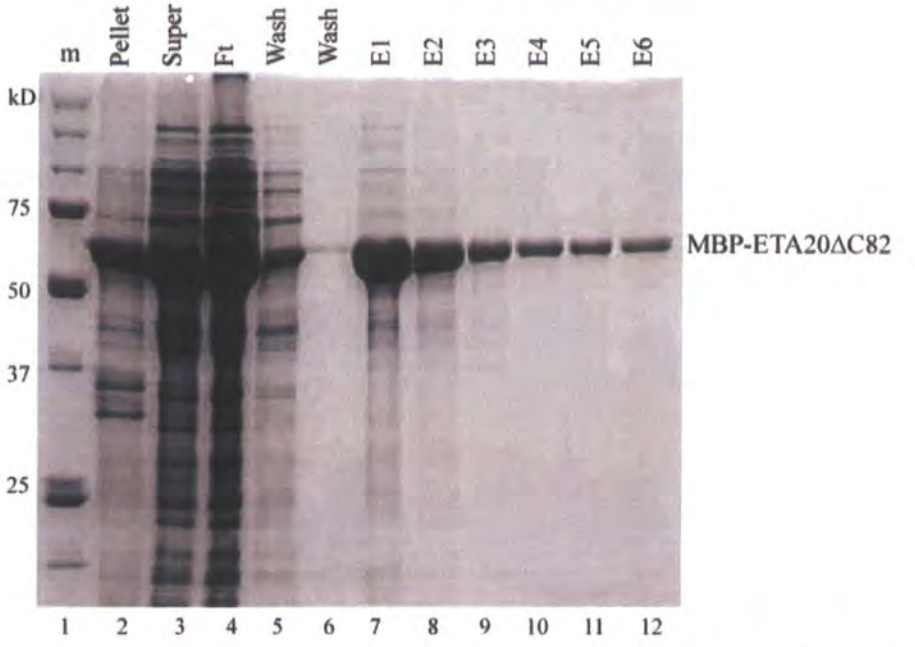

Figure 3.8. Purification of MBP-ETA20ΔC82 by amylose affinity chromatography. Lane 1, MW markers; Lane 2, pellet following cell lysis; Lane 3, supernatant following cell lysis; Lane 4, flow-through from column; Lanes 5 and 6, wash fractions; Lanes 7-12, consecutive fractions from the column, eluted in the presence of 10 mM maltose.

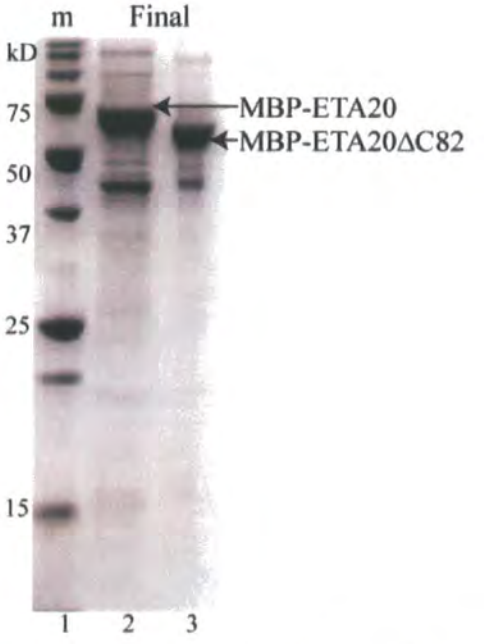

Figure 3.9. Purified MBP-ETA20 and MBP-ETA20ΔC82 (5 μg) at 4.25 mg/ml and 0.65 mg/ml respectively. Lane 1, MW markers; Lane 2, purified MBP-ETA20; Lane 3, purified MBP-ETA20ΔC82. Proteins were visualised on 12.5% SDS-PAGE stained with Coomassie Blue.

3.5 *E. coli* RecA and SSB

E. coli RecA and SSB were purified according to published protocols (Cadman & McGlynn, 2004; Cox *et al*, 1981). The RecA used in this study was prepared by Dr F.A. Curtis. The final gel filtration step in the SSB purification scheme was omitted.

3.6 λ Exo and λ β proteins

His_6-tagged Exo and β fusion protein constructs were obtained from Dr F.A. Curtis. *E. coli* BL21 Codon Plus containing pFC154 / pFC155 were overexpressed, as described in Chapter 2, and uninduced and induced samples analysed by SDS-PAGE (Figure 3.10 A and B).

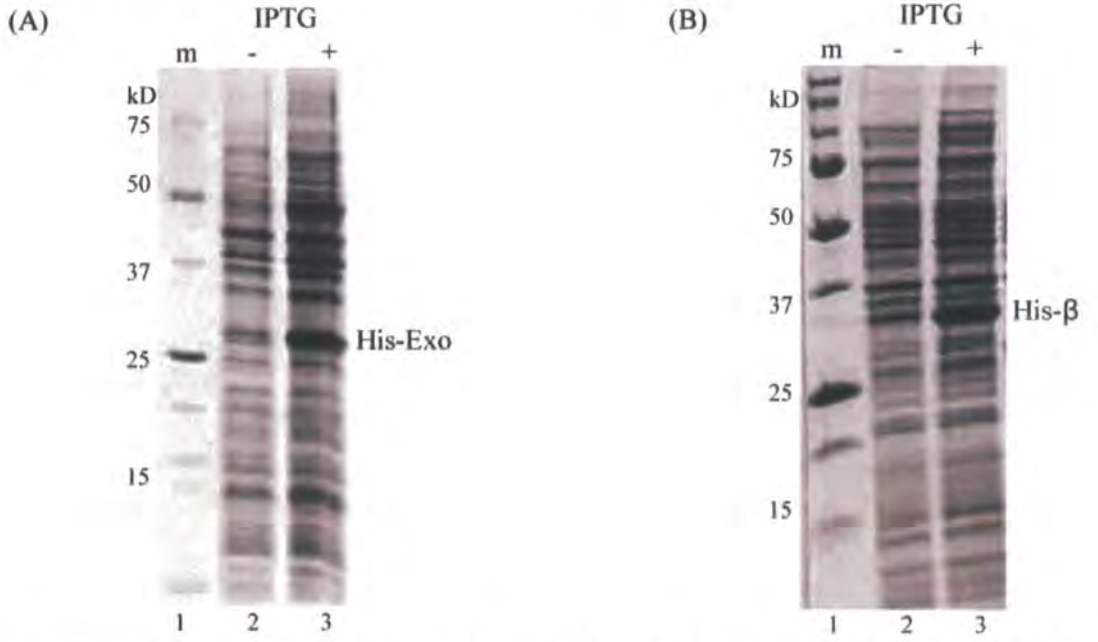

Figure 3.10. Overexpression of His-Exo (A) and His-β (B). Lane 1, molecular weight (MW) markers; Lane 2, uninduced BL21 C^+ pFC154/5; Lane 3, IPTG-induced BL21 C^+ pFC154/5.

Cells were lysed as described previously and purified on a 2 ml His-select nickel affinity gel column. Bound proteins were eluted in the presence of 250 mM imidazole; the majority of the His-Exo appeared in the first elution fraction, with His-β appearing in elution fractions 1 -3, which were pooled for dialysis (Figure 3.11). A total of 1.5 mg of Exo was obtained but was only ~90% pure, therefore the majority of Exo assays performed in this work employed wild-type Exo protein purchased from New England Biolabs.

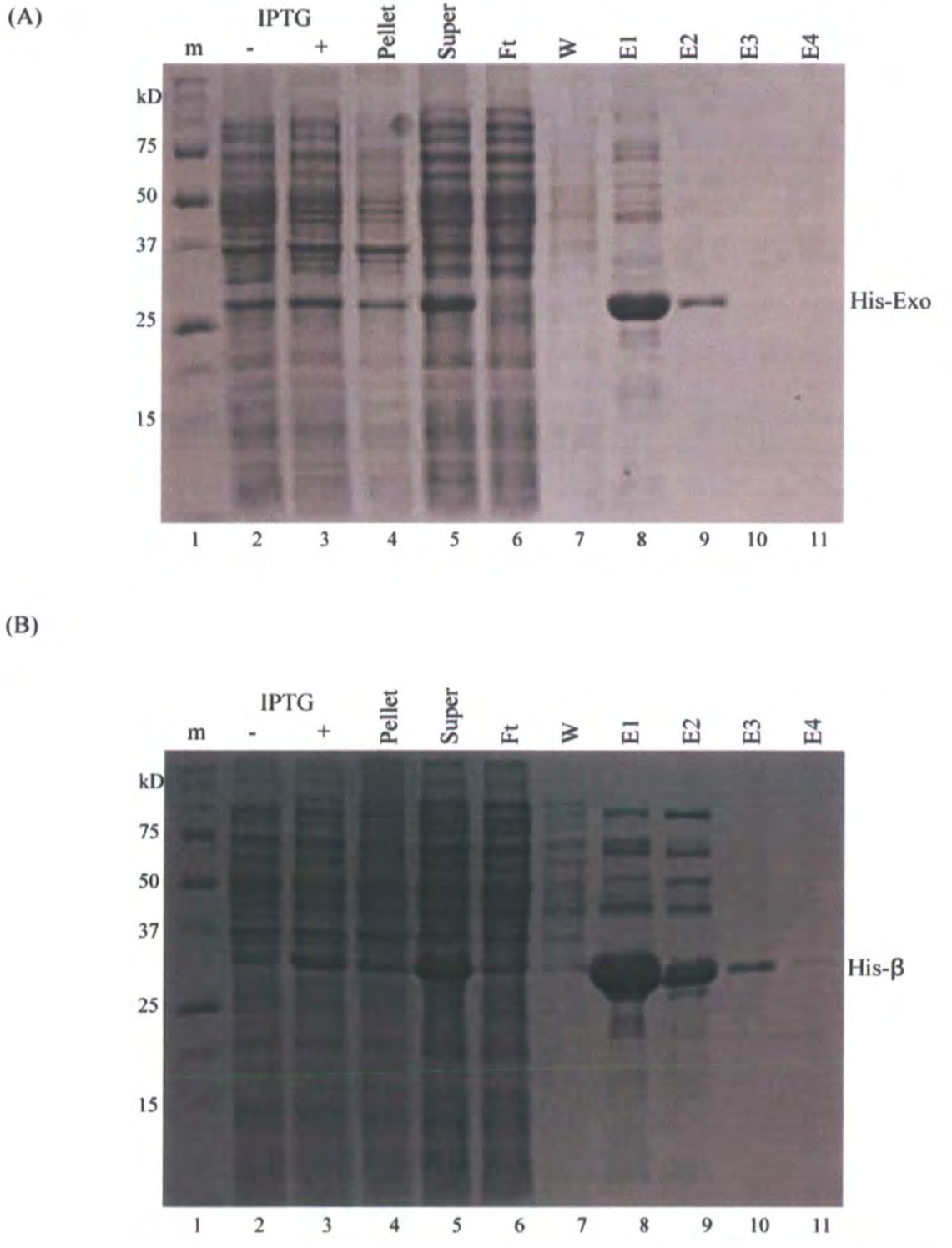

Figure 3.11. Purification of His-Exo (A) and His-β (B) by nickel affinity chromatography. Lane 1, MW markers; Lanes 2 and 3, uninduced and induced BL21 C^+ pFC154/5; Lane 4, pellet following cell lysis; Lane 5 supernatant following cell lysis; Lane 6, flow-through from column; Lane 7, wash fraction; Lanes 8-11, consecutive fractions from the column, eluted in the presence of 250 mM imidazole.

His-β protein appeared in elution fractions 1-3 from the nickel column alongside other contaminants, although several of these could be stable multimers of β protein. The pooled elution fractions were applied to a 1 ml Q-sepharose fast flow column and β

eluted between 0.35-0.45 M KCl. These fractions were also passed through heparin and phosphocellulose columns, which β failed to bind. The samples of β were dialysed into storage buffer and stored in aliquots at -80°C. The protein is approximately 95% pure (Figure 3.12).

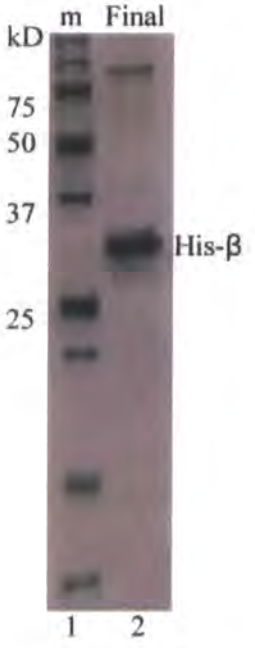

Figure 3.12. Purified His-β (5 μg). Lane 1, MW markers; Lane 2 purified His-β.

3.7 λ NinH

The *ninH* gene, is an uncharacterized open reading frame of 60 residues located immediately downstream of *rap* (*ninG*) in the *ninR* region of λ. The protein resembles the Fis protein, a non-specific DNA binding protein with multifunctional roles in various DNA transactions (Pratt *et al*, 1997; Safo *et al*, 1997). To investigate the function of this protein it was purified to homogeneity. Experiments by Dr F.A. Curtis confirmed that NinH binds to a range of single-stranded and double-stranded DNA substrates.

3.7.1 Purification of NinH

E. coli BL21-AI cells containing pFC109 were grown in LB broth (12 L) and NinH expression induced by addition of arabinose (Figure 3.13). Cells were lysed using standard procedures and the supernatant applied to a 10 ml Q-sepharose fast flow column; the majority of the NinH protein appeared in the flow through and wash fractions. Samples containing NinH were loaded onto a 3 ml dsDNA cellulose column and bound proteins eluted in a 0.2-1 M salt gradient. The majority of the NinH protein

eluted between 0.35-0.5 M KCl. Pooled fractions were applied to a 1 ml heparin agarose column and NinH eluted from the column in a broad peak at 0.4-0.8 M KCl. The protein was sufficiently pure for further analysis and was stored in aliquots at -80°C. A total of 1.6 mg purified NinH at 1 mg/ml was recovered (Figure 3.14).

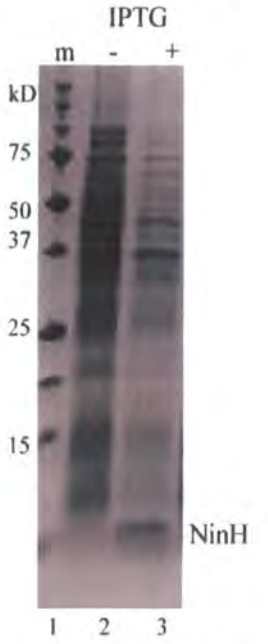

Figure 3.13. Overexpression of NinH. Lane 1, molecular weight (MW) markers; Lane 2, uninduced BL21-AI pFC109; Lane 3, IPTG-induced BL21-AI pFC109.

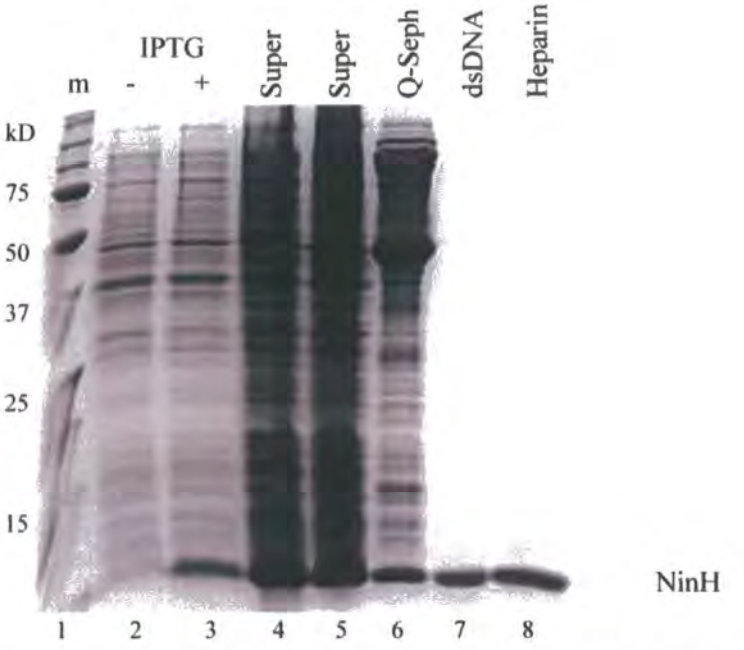

Figure 3.14. Purification steps for NinH. Lane 1, MW markers; Lanes 2 and 3, uninduced and induced BL21-AI pFC109; Lane 4, supernatant following cell lysis; Lane 5, supernatant following cell lysis; Lane 6, sample from Q-sepharose column; Lane 7, sample from dsDNA column; Lane 8, sample from heparin column.

3.8 Discussion

This chapter describes the cloning, overexpression and purification of *E. coli* and λ proteins either known or implicated in the initial stages of genetic recombination. Purification of these proteins was undertaken to facilitate investigations into the possible interactions between λ Orf and other λ and host functions *in vitro*. Two distantly related Orf homologues, Orf151 and ETA20, were purified to compare their properties with λ Orf. In addition, λ NinH was obtained for future laboratory investigations into its possible function in λ site-specific or genetic recombination pathways. The functional analysis of these λ and *E. coli* proteins are presented in the remaining chapters of this thesis.

Chapter 4

Influence of Orf, β, SSB and RecA proteins on Exo activity

4.1 Introduction

The Red system, comprising *exo*, *beta* and *gam* gene products, is employed when phage λ enters the lytic phase and is active at double-strand DNA breaks, such as those occurring when the phage terminase cleaves at the *cos* site (Tarkowski, *et al*, 2002). Genetic evidence indicates that λ Orf influences the initial stage of genetic exchange (Poteete, 2004; Tarkowski *et al*, 2002; Sawitze & Stahl, 1992, 1994) by substituting for *E. coli* RecFOR, which facilitate loading of RecA onto gapped DNA (Morimatsu & Kowalczykowski, 2003; Poteete, 2001; Sawitzke & Stahl, 1992). Orf has been proposed to act in loading or unloading β, RecA or SSB proteins at the ssDNA:dsDNA interface (Poteete, 2004). Orf binds preferentially to ssDNA (Maxwell *et al*, 2005) and yeast-two hybrid studies (M.D. Watson, unpublished results) highlighted potential interactions between Orf and Exo, β and SSB. To investigate the extent of Orf's involvement in phage λ recombination, further evidence of a physical interaction between Orf and Exo was sought. In addition, the effect of λ Orf and β and *E. coli* RecA and SSB on DNA degradation by Exo was examined. The results of the assays performed are described in this chapter.

4.2 Orf interacts weakly with Exo

An enzyme linked immunosorbent assay (ELISA) was used to confirm the potential interaction between Orf and Exo. An N-terminal GST (Glutathione-S-transferase) Orf fusion was purified as described in Chapter 3. Following preliminary experiments to determine optimum conditions, assays were performed with 5 μg/ml Exo (10.42 μM) with purified GST-Orf at 0.367 - 11.74 μM. Antibodies to the GST moiety were used to detect GST-Orf binding to the untagged Exo protein bound to an Immulon plate (described Chapter 2). A positive Orf-Exo association was detected at GST-Orf concentrations greater than 2.93 μM (Figure 4.1). No interactions were evident in control reactions with the individual Exo and GST-Orf proteins. Inclusion of a 51-mer oligonucleotide significantly reduced the protein-protein interaction (Figure 4.1)

indicating that DNA binding by Orf or Exo, or both, can affect their stable association. These results, in combination with yeast two-hybrid experiments, suggest that Orf and Exo do associate and that this may be important during the initial stage of genetic exchange.

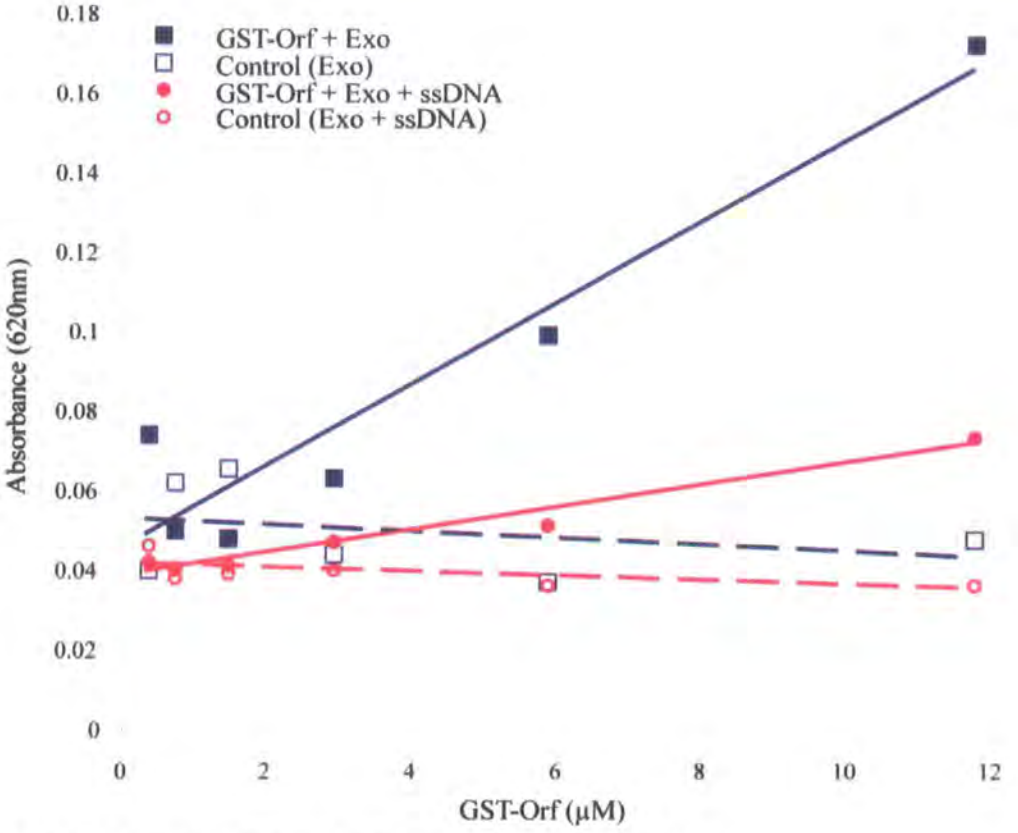

Figure 4.1. GST-Orf interacts with Exo in the presence or absence of DNA.
Binding mixtures contained 10.42 μM Exo and 0.367, 0.734, 1.47, 2.93, 5.87 and 11.74 μM GST-Orf. A 51-nt ssDNA substrate was included at 0.5 μg/ml. Data are the mean of three experiments.

4.3 Orf modulates the nuclease activity of Exo on linear λ DNA

Initial attempts to examine the impact of Orf on Exo activity were performed using λ DNA labelled with 4'6-diamidino-2-phenylindole (DAPI) or Hoechst 33258 (H33258) and measuring any fluorescence change using a fluorimeter and by stopped-flow fluorescence spectroscopy (Chapter 2, section 2.6.3). DAPI and H33258 interact preferentially with duplex DNA by binding the minor groove (Breusegem *et al*, 2002; Kubota *et al*, 2000). Binding of DAPI and H33258 to DNA results in a ~6 fold increase in fluorescence (Zaitsev & Kowalczykowski, 1998) and this feature was to be utilised to measure a fluorescence decrease as Exo processivity removed the 5' strand from linear DNA. Unfortunately, binding of these fluorescent dyes inhibited

the nuclease activity of Exo. An alternative approach using ethidium-stained agarose gels to monitor Exo nuclease activity was therefore devised.

Assays were performed with $7.7x10^{-4}$ U/ml Exo (New England Biolabs) and 5 μM (N) λ DNA in the reaction buffer provided by the manufacturer (Chapter 2, section 2.6.5(b)). Appropriate control assays were performed in parallel, confirming that the observed degradation was solely due to Exo activity. Under the conditions used, Exo reduced the quantity of linear λ DNA by approximately 5-fold in 10 minutes (Figure 4.2). The extent of degradation was quantified by densitometry as described in Chapter 2 (Figure 4.2B). MBP-Orf, β, RecA and SSB proteins did not exhibit any nuclease activity when incubated individually with DNA in the absence of Exo (Figure 4.2 and data not shown). Addition of purified MBP or storage buffer (0.2 M KCl, 20 mM Tris-HCl pH 8.0, 1 mM EDTA, 0.5 mM DTT, 50% glycerol) to Exo reactions did not affect the rate of Exo nuclease activity (Figure 4.2).

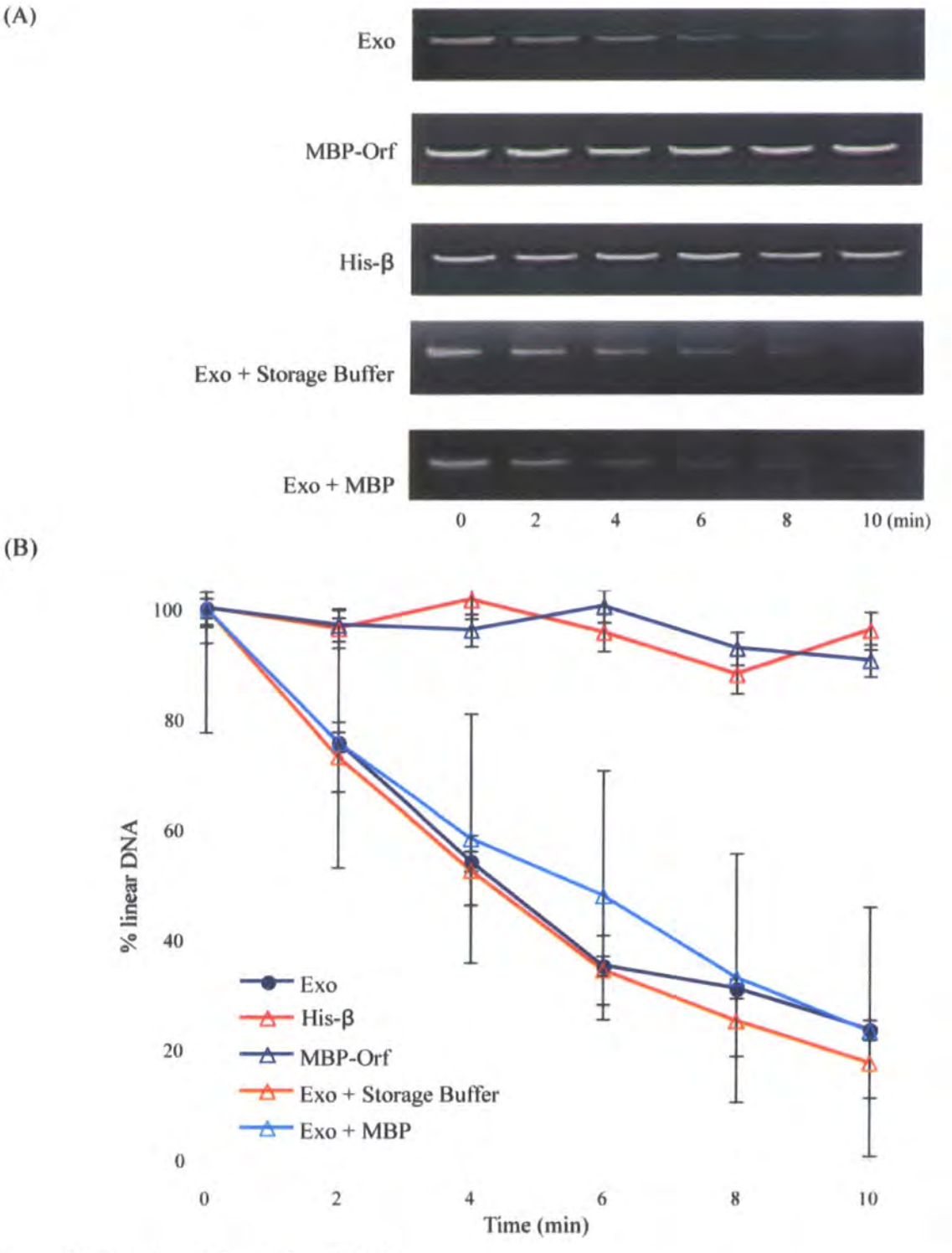

Figure 4.2. Exo degradation of linear λ DNA.
A) 1.5% agarose gels showing degradation of λ DNA by Exo ($7.7x10^{-4}$ U/μl). Control experiments were performed in parallel. MBP-Orf, MBP and His-β at 100 nM were added prior to addition of Exo. B) Densitometry (Image J data) analysis of exonuclease assays. Data are the mean of two independent experiments.

The Exo nuclease experiments were repeated to evaluate any effect of the MBP-Orf protein on DNA degradation. Inclusion of 50 nM MBP-Orf has no effect on Exo nuclease activity (Figure 4.3). However, when 100 nM or 400 nM MBP-Orf was

used, the assays revealed a significant inhibition of Exo activity; MBP-Orf at 100 nM reduced the amount of λ DNA destroyed in 10 min from 23.44% to 68.39% (Figure 4.3). Incorporation of His-Orf protein has a similar inhibitory effect on Exo activity (data not shown).

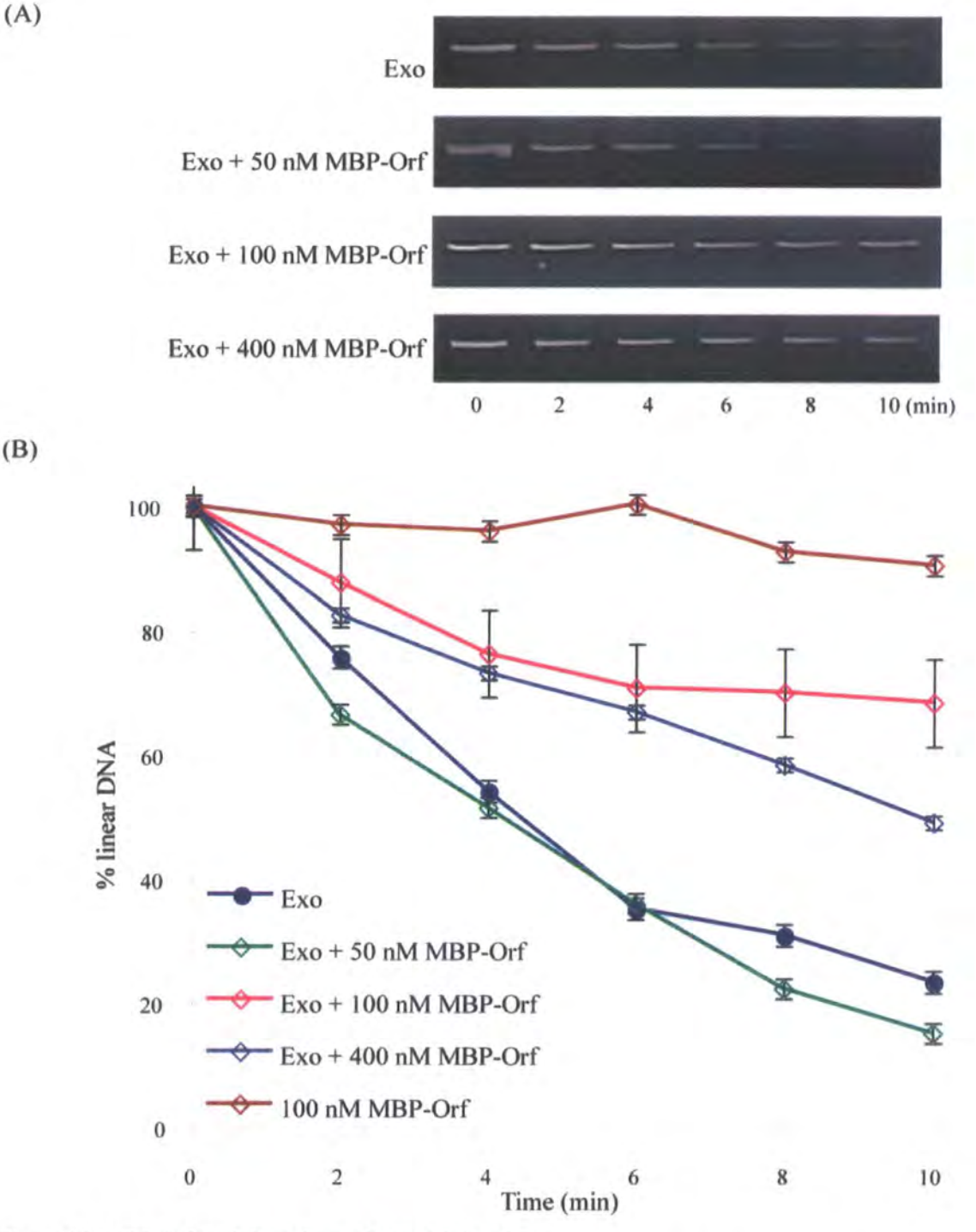

Figure 4.3. MBP-Orf modulates the nuclease activity of Exo.
A) Assays were performed at 37°C and contained 7.7×10^{-4} U/μl Exo and 5μM λ DNA with 0, 50, 100 and 400 nM MBP-Orf protein. B) Quantification of DNA degradation gels, using Image J. Data are the mean of two independent experiments.

To examine the importance of Orf DNA binding on the inhibition of Exo activity, several MBP-Orf mutants known to impair DNA binding were used. Mutations in the C-terminal region (OrfΔC6 and OrfW141F) confer a slightly reduced ssDNA binding capability relative to the wild-type Orf protein. A larger deletion at the C-terminus (OrfΔC19) and a substitution mutation (OrfR103E) completely abolish Orf binding to ssDNA (F.A. Curtis and G.J. Sharples, unpublished results). MBP-OrfΔC6 and MBP-OrfW141F mutant proteins inhibited Exo activity to a similar extent as the wild-type MBP-Orf, although they allowed more degradation at the 10 min period (from 68.39% linear DNA remaining with wt MBP-Orf to 53.3% and 52.4% linear DNA remaining with MBP-OrfΔC6 and MBP-OrfW141F, respectively) (Figure 4.4). This overall reduction in their inhibitory effect could be due to their reduced capacity to bind ssDNA. Interestingly, MBP-OrfΔC19 and MBP-OrfR103E were significantly less able to restrict the nuclease activity of Exo (ΔC19 and R103E showed 35.2% and 30.3% linear DNA remaining at 10 min, respectively) (Figure 4.4). Taken together, the results suggest that the ability of Orf to bind DNA is important for its inhibitory effect on Exo activity. However, there must be some other factor involved since MBP-OrfΔC19 and MBP-OrfR103E are still able to limit the nuclease activity of Exo despite their inability to bind DNA (Figure 4.4).

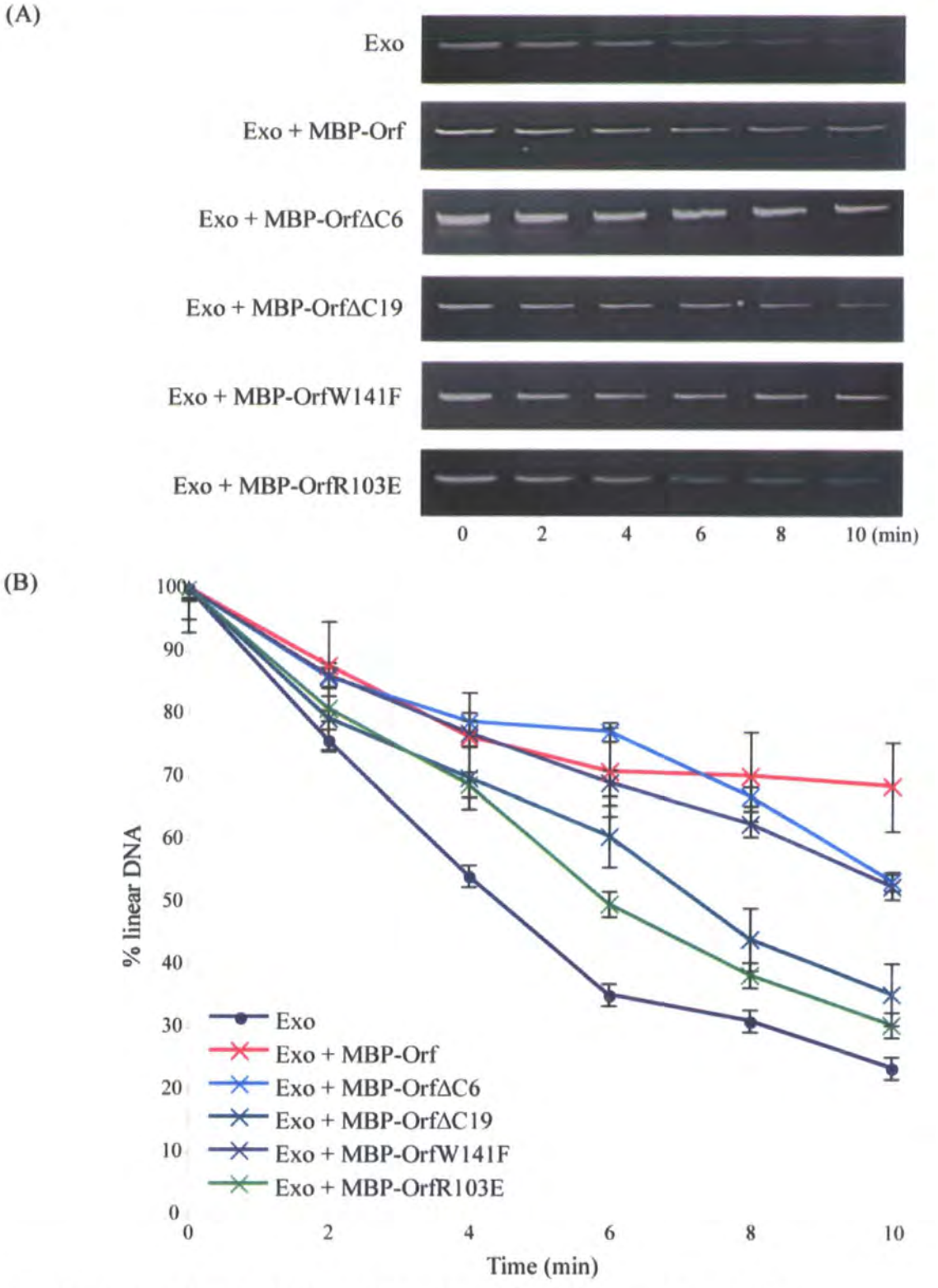

Figure 4.4. Impact of MBP-Orf C-terminal mutant proteins on the nuclease activity of Exo.
A) Assays comprised 7.7×10^{-4} U/μl Exo and 5 μM λ DNA with 100 nM of each MBP-Orf protein.
B) Quantification of DNA degradation gels using Image J. Data are the mean of two independent experiments.

To probe the effect of Orf on Exo nuclease activity in a more complex and potentially realistic context, β protein was incorporated in the assays. Inclusion of β protein into

the Exo reaction slightly reduced the nuclease activity of Exo. However, the addition of both β and Orf resulted in 82.5% linear DNA remaining at 10 min, similar to reactions without Exo present (Figure 4.5). The data suggest a synergistic interaction between β and Orf that serves to protect linear λ DNA from destruction by Exo. This could be brought about by direct Orf-Exo and β-Exo interactions and/or binding to DNA substrate in some fashion to impede exonuclease progression.

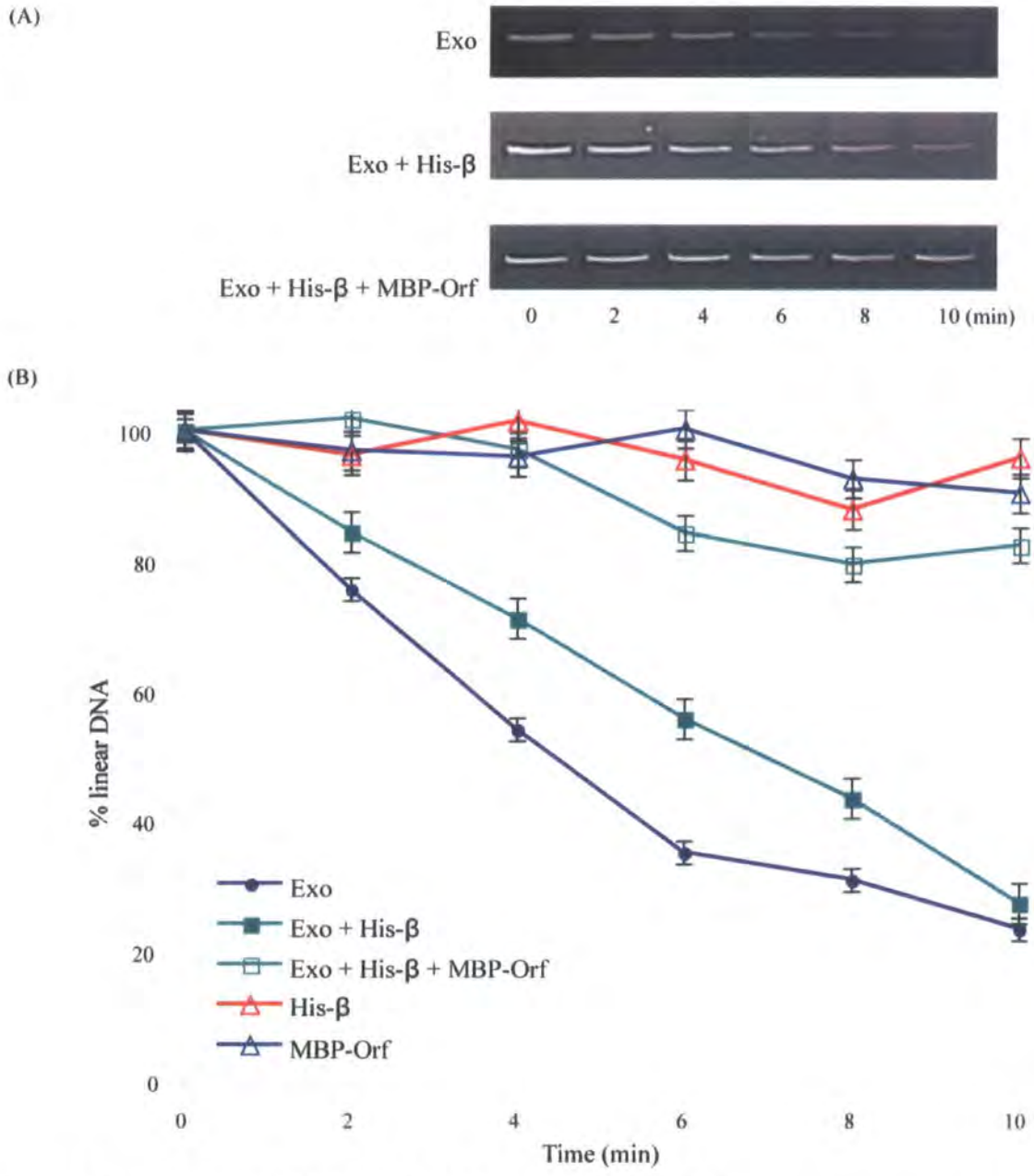

Figure 4.5. Impact of MBP-Orf and His-β on the nuclease activity of Exo.
A) Assays comprised $7.7x10^{-4}$ U/μl Exo and 5 μM λ DNA with 0, 100 and 200 nM β with or without 100 and 200 nM MBP-Orf protein. B) Quantification of DNA degradation gels using Image J. Data are the mean of two independent experiments.

4.4 SSB enhances Exo nuclease activity

The ability of Orf to replace the different functions of the RecFOR proteins in λ recombination is consistent with loading or unloading β, SSB or RecA at the ssDNA:dsDNA interface. The effect of *E. coli* SSB protein on Exo nuclease activity was therefore investigated. No nuclease activity was detected when the linear λ DNA substrate was incubated with SSB alone (data not shown). Addition of SSB to Exo nuclease reactions did result in significantly more DNA degradation (Figure 4.6); this increase in nuclease rate was further stimulated by higher concentrations of SSB protein (data not shown). The inclusion of 100 nM MBP-Orf to assays containing Exo and 20 nM SSB eliminated this increased rate of degradation, returning the level of nuclease activity to levels akin to Exo alone (Figure 4.6). This effect may simply be a balance of stimulatory (SSB) and inhibitory (Orf) effects. However, mixing Exo, MBP-Orf, β and SSB proteins together produced a significant increase in degradation, even greater than that seen with just Exo and SSB (Figure 4.6). This is puzzling since MBP-Orf and β together have such a negative effect on Exo activity and perhaps suggests that a more complex set of interactions is important during these early presynaptic steps.

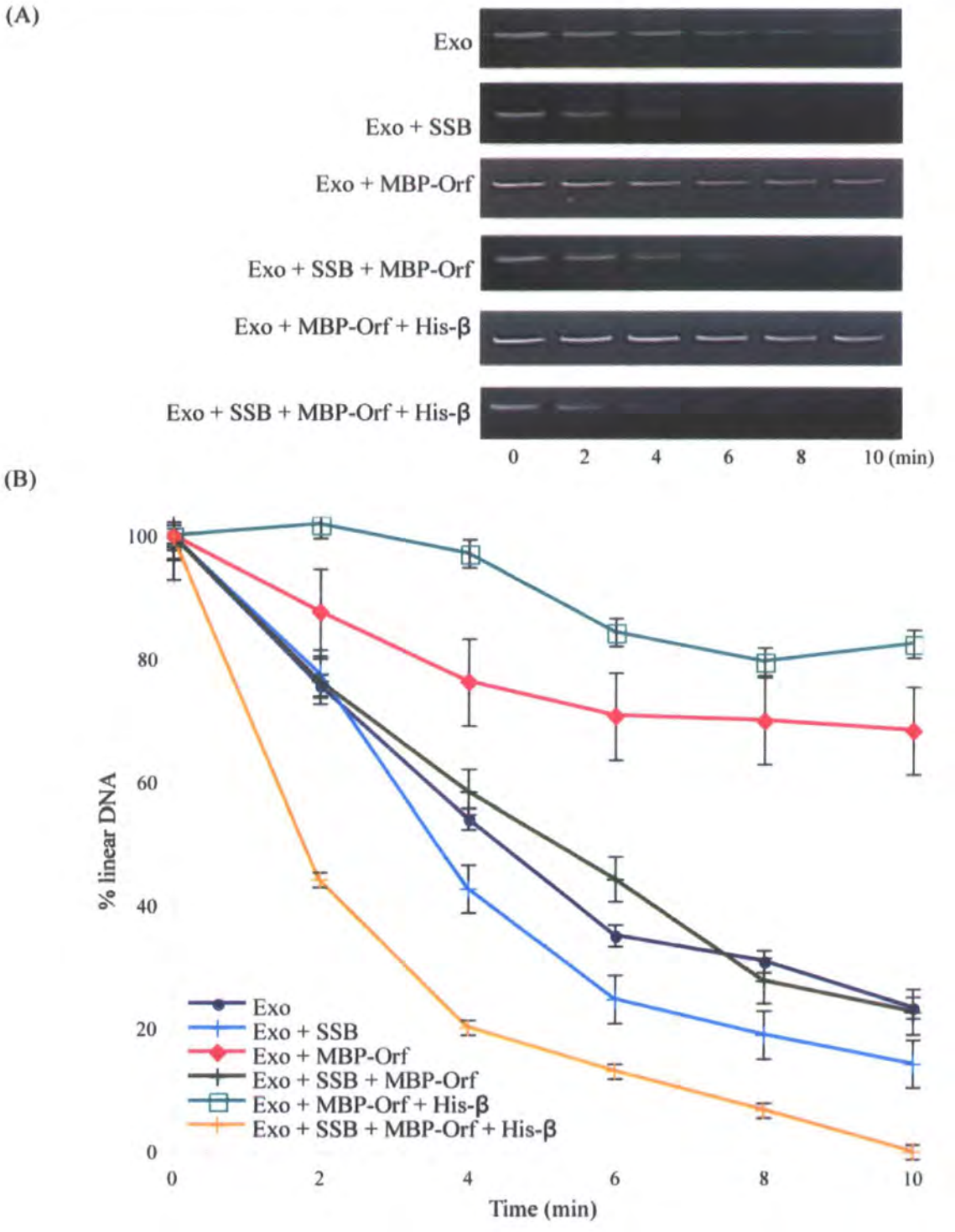

Figure 4.6. SSB enhances the nuclease activity of Exo.
A) Assays comprised 7.7×10^{-4} U/μl Exo and 5 μM λ DNA with 20 nM SSB and 100 nM of Orf and β. B) Quantification of DNA degradation gels using Image J. Data are the mean of two independent experiments.

4.5 Impact of RecA on Exo nuclease activity

The Red pathway provides a RecA-independent mechanism for generating packageable genomes during phage λ lytic growth. Genetic and biochemical evidence

supports the involvement of Orf in loading the bacterial RecA recombinase onto SSB-coated DNA as an alternative approach for strand exchange. Which pathway is favoured in whatever context is unclear. Given the potential interactions between Orf and RecA, the effect of RecA, together with the other relevant phage and bacterial partners on the nuclease activity of Exo was investigated. As before, control reactions confirmed that neither RecA nor ATP resulted in DNA degradation. Similarly, the presence of ATP, required for RecA strand exchange, did not influence Exo nuclease activity (data not shown). The presence of RecA in the absence of ATP (i.e. an inactive filament) did increase Exo activity. However, once RecA was activated by the addition of ATP, the Exo nuclease activity was attenuated by 15.81% (Figure 4.7 A and B). Addition of MBP-Orf (100 nM) to assays containing RecA, attenuated Exo nuclease activity by a further 38.84% (Figure 4.7B). However, addition of β to assays with RecA and Orf further reduced Exo nuclease activity with 61.7% of the linear DNA remaining at 10 min, a level midway between that obtained when RecA was present alone and RecA with Orf (Figure 4.7 A and B). These results generally fit with additive effects due to each of the inhibitory components, although it would have been expected that the combination of RecA, Orf and β would have the greatest negative effect.

To investigate further the influence of RecA on Exo activity in a situation more likely to be representative of *in vivo* conditions, the assays were repeated in the presence of SSB. SSB is one of the key modulators of RecA filament formation, responsible for strongly inhibiting the nucleation phase of RecA filament assembly but stimulating the extension phase by removing DNA secondary structures that would impede filament growth (Kowalczykowski & Krupp, 1987). The inhibitory effect of SSB on RecA filament assembly is overcome by RecFOR (Bork *et al*, 2001; Umezu & Kolodner, 1994). Hence if Orf can substitute for RecFOR in λ-λ recombination (Maxwell *et al*, 2005; Poteete, 2004), Orf would be expected to modulate assembly of RecA in the presence of inhibitory amounts of SSB during the initial exchange step of recombination. Inclusion of SSB in assays containing RecA had minimal effect on Exo activity (Figure 4.7B). However, addition of SSB to assays with RecA and Orf, with or without β, has a significant impact on Exo nuclease activity, alleviating all the effects of the additional proteins and returning the level and rate of degradation to that

observed when Exo was assayed alone. Thus under these conditions, the inhibitory effect of RecA, Orf and β are removed by addition of SSB. Overall the results indicate that the interaction of SSB with DNA is favourable for Exo nuclease activity and this compensates for the negative impact of other DNA binding proteins.

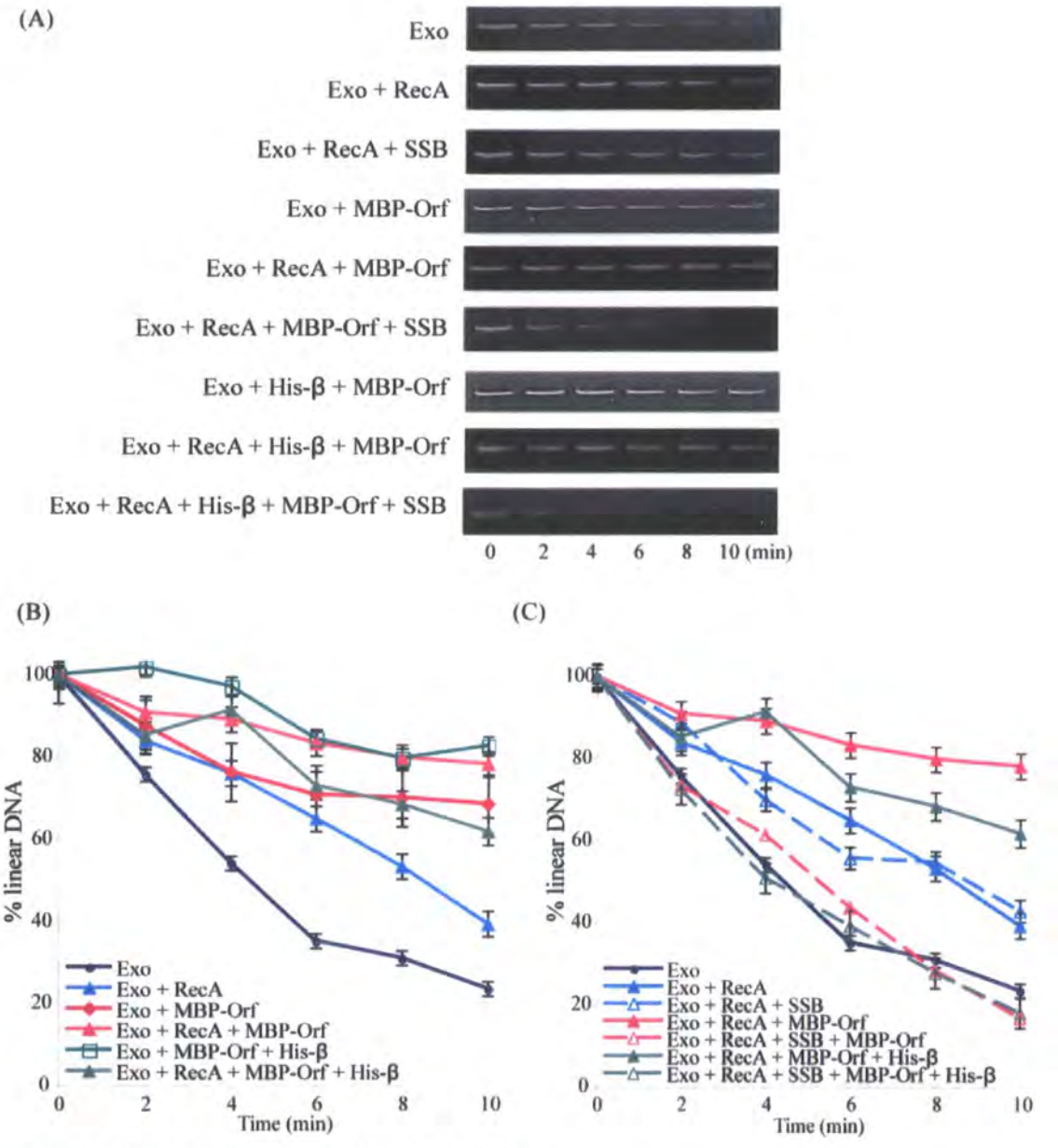

Figure 4.7. RecA modulates the nuclease activity of Exo.
A) Reactions contained $7.7x10^{-4}$ U/μl Exo, 5 μM λ DNA and 500 nM RecA (and 1 mM ATP), 200 nM SSB and 100 nM of Orf or β. B) and C) Effect of MBP-Orf, His-β and SSB on Exo-RecA reactions. Quantification of DNA degradation gels using Image J. Data are the mean of two independent experiments.

4.6 Discussion

In this chapter the effect of λ Orf and other proteins important in the initial steps of recombination, on λ Exo nuclease activity was investigated. Orf was shown to significantly reduce the level and speed of degradation by Exo. This inhibitory effect was enhanced when β was added suggesting that in the absence of other involved proteins, the combination of Orf and β helps preserve DNA from Exo nuclease activity, or at the very least serves to restrict the rate of degradation. Several Orf mutant proteins with defects in ssDNA binding, were found to have less of an adverse impact on Exo nuclease activity. OrfΔC19 and OrfR103E mutant proteins, which cannot bind DNA, have a significantly reduced impact compared to OrfΔC6 and OrfW141F, which retain a largely wild-type level of DNA binding. These results point to the DNA binding capacity of Orf being important for modulating Exo nuclease activity. It is not clear how binding to ssDNA tails released by Exo could reduce its processivity, although the combination of an Exo-Orf complex tethered to ssDNA by Orf could explain the results. The modulation of Exo activity mediated by β protein could occur in a similar fashion since Exo and β are known to interact (Tolun, 2007 *cited* Poteete, 2008) and β also binds ssDNA (Passy *et al*, 1999).

RecA protein also reduced Exo nuclease activity when ATP was included in the reactions. In this instance, it may be that strand-exchange between exposed ssDNA and any available homologous duplex interferes with the ability of Exo to continue strand degradation. It is also possible that annealing of ssDNA ends by β could also account for its inhibitory properties. RecA has a more substantial inhibitory effect on Exo nuclease activity when present in combination with either β or Orf. However, complex interactions between each of these proteins with each other and with DNA may lead to a variety of synergistic and compensatory effects.

In contrast to the effects noted with Orf, β and RecA, addition of SSB protein significantly enhanced Exo nuclease activity suggesting that the ssDNA binding properties of SSB encourage Exo action at DNA ends. This improvement in Exo activity may be due to SSB sequestering free 3'-tailed ssDNA that in some way interferes with the nuclease. SSB is known to antagonise inhibitory proteins involved in the initial exchange step of recombination (Baitin *et al*, 2008) and so *in vivo* SSB

may serve to substantially stimulate the rate of Exo end processing. Combining RecA and SSB in Exo nuclease assays resulted in a level of degradation similar to that observed with Exo alone. In this case, it may simply be a balance between the inhibitory and stimulatory activities of these two bacterial proteins. However, in reactions containing SSB, RecA, β and Orf, the level and rate of Exo nuclease activity returned to levels seen with Exo alone, suggesting that the presence of SSB is capable of removing entirely the negative influence of the three other proteins. It is clear from these results that a number of proteins fulfil inhibitory and stimulatory functions on the exonucleolytic processing of DNA ends by the λ exonuclease. Precisely how these competing factors participate in phage recombination reactions requires further study.

Chapter 5

Impact of Orf on RecA filament formation

5.1 Introduction

Genetic evidence suggests that Orf supplies an activity equivalent to the *E. coli* RecFOR proteins during λ recombination (Poteete, 2004, 2001; Sawitzke & Stahl, 1992). RecFOR stimulate assembly of RecA filaments on gapped DNA substrates coated with SSB protein and thereby accelerate the rate of DNA strand exchange (Morimatsu & Kowalczykowski, 2003). To determine the precise function of Orf in phage recombination the ATPase activity of RecA was exploited to monitor filament formation on ssDNA in the presence or absence of SSB protein. Orf is known to associate with SSB (Maxwell *et al*, 2005) and so the possibility that Orf interacts with RecA was also probed.

5.2 Orf interacts weakly with RecA

To assess any interaction between Orf and RecA, an ELISA was adopted as described in Chapter 2. RecA protein bound to an Immunlon plate was incubated with purified GST-Orf protein. After washing, any GST-Orf bound to RecA was detected with antibodies specific to the GST moiety. Some binding of GST-Orf to the RecA bound to the plate was evident (Figure 5.1). No interactions were detected in control reactions, either with RecA alone or with GST-Orf in the absence of RecA (Figure 5.1). Inclusion of a 51 -mer oligonucleotide had an inhibitory effect on the protein-protein interaction (Figure 5.1), indicating that DNA binding by either Orf or RecA, or both, can affect their stable association. Although the absorbance changes were relatively small, the results were reproducible suggesting that the Orf-RecA interaction is genuine and may be important during the initial stage of genetic exchange. Recent work has confirmed that Orf and RecA interact in far-western experiments (F.A. Curtis and G.J. Sharples, personal communication).

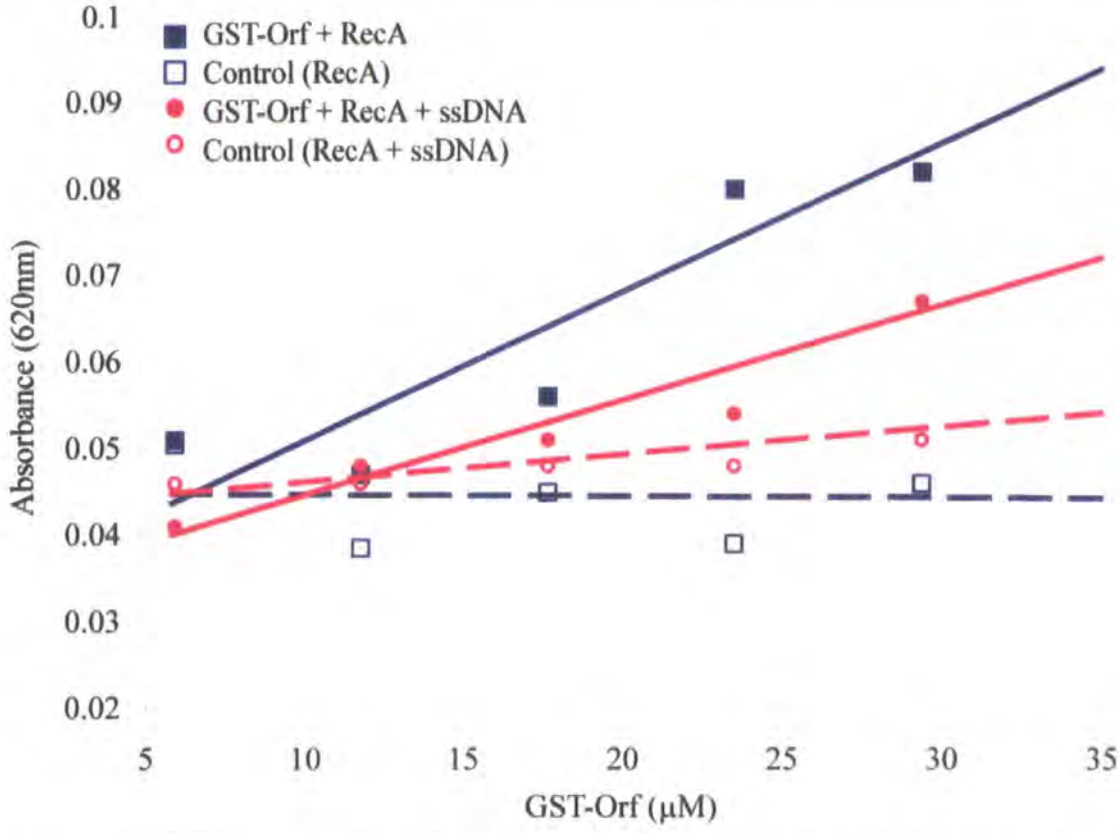

Figure 5.1. GST-Orf interacts with RecA. Binding mixtures contained 39.5 μM RecA and 5.87, 11.74, 17.61, 23.48, 29.35, 35.22 μM GST-Orf. A 51-nt ssDNA substrate was included at 0.5 μg/ml. Data are the mean of three experiments.

5.3 Orf promotes the assembly of RecA at ssDNA:dsDNA junctions

Formation of an active RecA-ssDNA filament requires hydrolysis of ATP (Brenner *et al*, 1987). The rate of ATP hydrolysis was therefore exploited to monitor the effects of Orf and SSB on RecA nucleoprotein assembly. Initial experiments utilised an NADH-oxidation-coupled assay (Chapter 2, section 2.6.1a) as employed by Morimatisu & Kowalczykowski, (2003) in studying RecA loading by RecFOR. The assay couples the formation of ADP, generated from the hydrolysis of ATP by RecA, to the oxidation of NADH to NAD^+. ϕX174 virion DNA (circular ssDNA) was used as a substrate since Orf binds preferentially to ssDNA (Maxwell *et al*, 2005). However, despite numerous protocol modifications, the results obtained lacked consistency. The overall RecA ATPase activity was low and inhibited by the presence of MBP-Orf (Figure 5.2). It is possible that Orf required gapped duplex DNA for assembly, as is the case for RecF and RecFOR (Morimatsu & Kowalczykowski, 2003; Hedge *et al*, 1996). A gapped duplex substrate containing four oligonucleotides annealed to ϕX174 was therefore constructed (Figure 5.3).

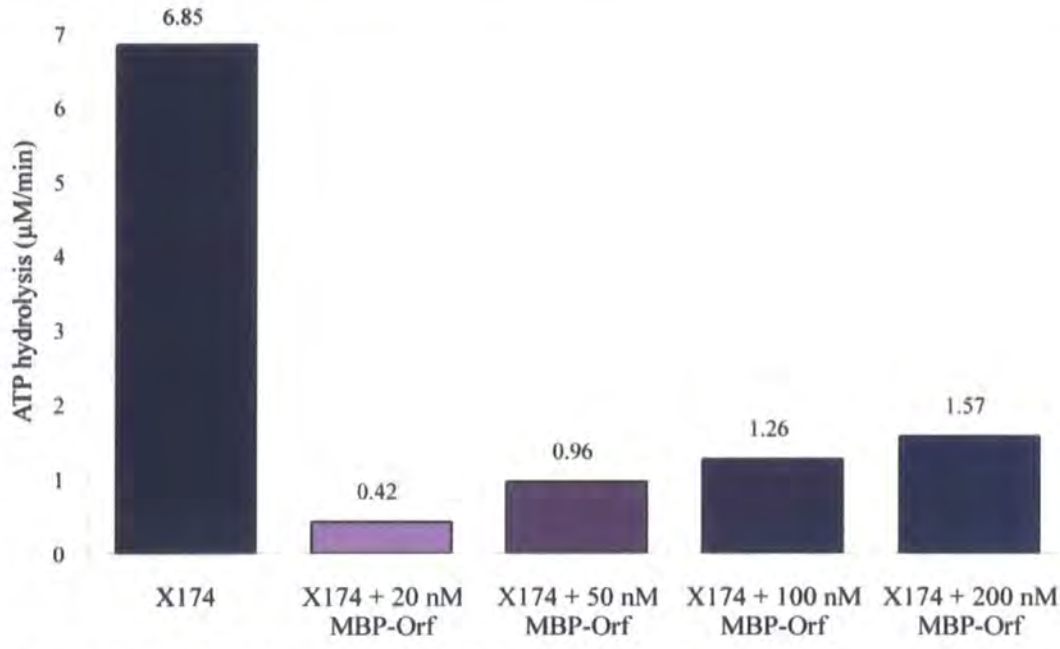

Figure 5.2. Effect of MBP-Orf on RecA ATPase activity in an NADH-oxidation coupled assay. All reactions contained 5 μM (N) ϕX174 DNA, 3.6 μM RecA and 1 mM ATP. MBP-Orf was added prior to the addition of RecA as indicated.

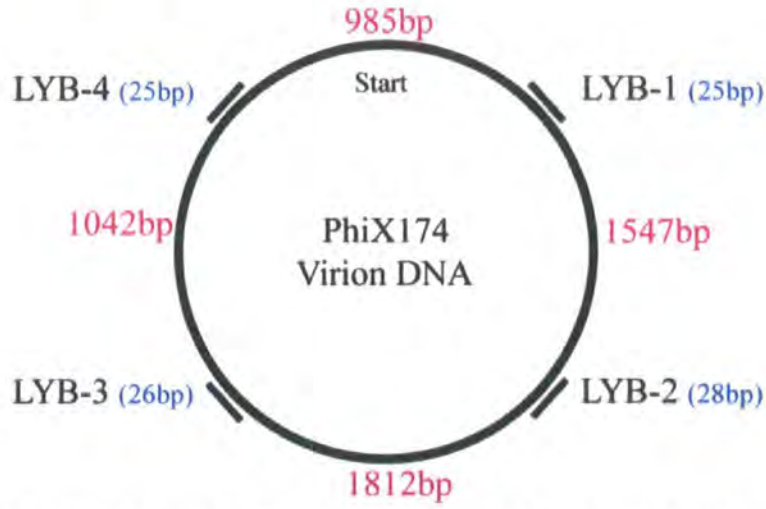

Figure 5.3. The LYB4000 gapped duplex DNA substrate. ϕX174 virion DNA was annealed to oligonucleotides LYB-1-4, to give a single-stranded circle with four short sections of duplex DNA.

The only structural difference between LYB4000 and ϕX174 is the presence of four short (25-28 bp) sections of duplex DNA providing ssDNA:dsDNA intersections. Each of the four oligonucleotides were designed to have a similar melting temperature to assist in annealing. Assays were performed with 5 μM (N) LYB4000, 3.6 μM RecA and 1 mM ATP. Appropriate control assays, performed in parallel, and published data (Iype *et al*, 1994) confirmed that none of the peripheral assay components, including the coupling system and protein storage buffer, limit or

enhance the rate of ATP hydrolysis (data not shown). The rate of ATP hydrolysed by RecA (i.e. protein assembly on ssDNA) on LYB4000 (Figure 5.4) was consistent with published data (Morimatsu & Kowalczykowski, 2003). Under the conditions used ATP hydrolysis by RecA was observed at 18.35 μM/min (Figure 5.4). Inclusion of MBP-Orf increased the rate of ATP hydrolysis observed; 2000 nM MBP-Orf enhanced the rate of ATP hydrolysis by 15% (21.12 μM/min) (Figure 5.4).

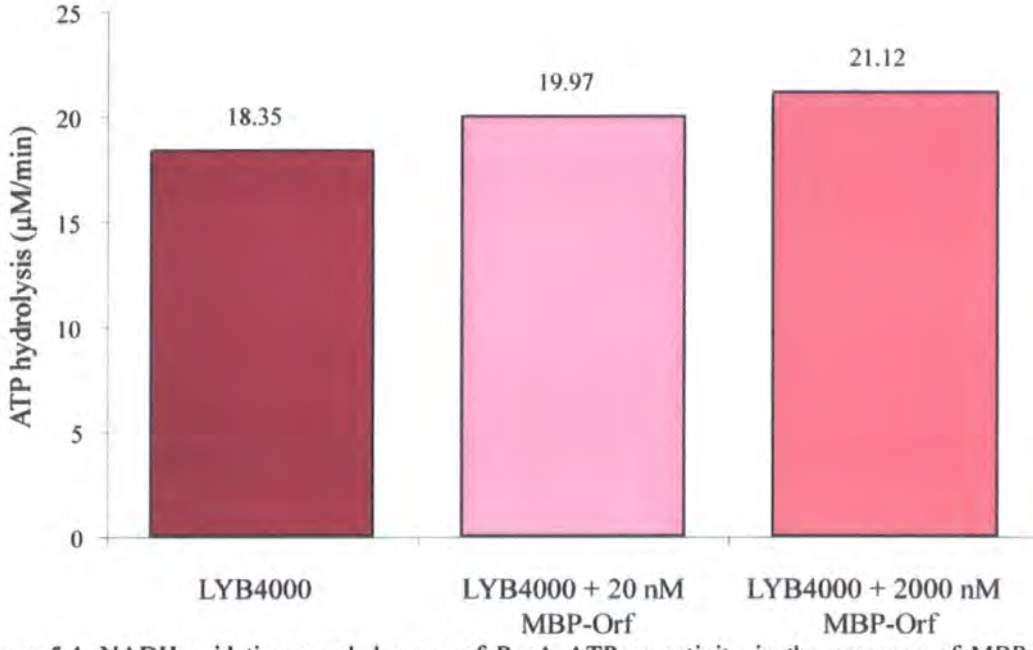

Figure 5.4. NADH-oxidation-coupled assay of RecA ATPase activity in the presence of MBP-Orf. Assays contained 5 μM (N) LYB4000 DNA, 3.6 μM RecA and 1 mM ATP and MBP-Orf at 20 or 2000 nM. MBP-Orf was added prior to the addition of RecA as indicated.

MBP-Orf also enhanced RecA ATPase with LYB4000 (Figure 5.5) in an MESG-phosphorolysis-coupled assay (Lee *et al*, 2007; Zhao *et al*, 2005; Cheng *et al*, 1995; Webb, 1992). No stimulation was apparent when ϕX174 or LYB2000, a ϕX174 substrate containing only two annealed oligonucleotides, were employed (Figure 5.5). Although the improvement in RecA ATPase activity mediated by MBP-Orf is limited, the results do suggest that providing ssDNA:dsDNA intersections is important and the number of these is also a critical factor.

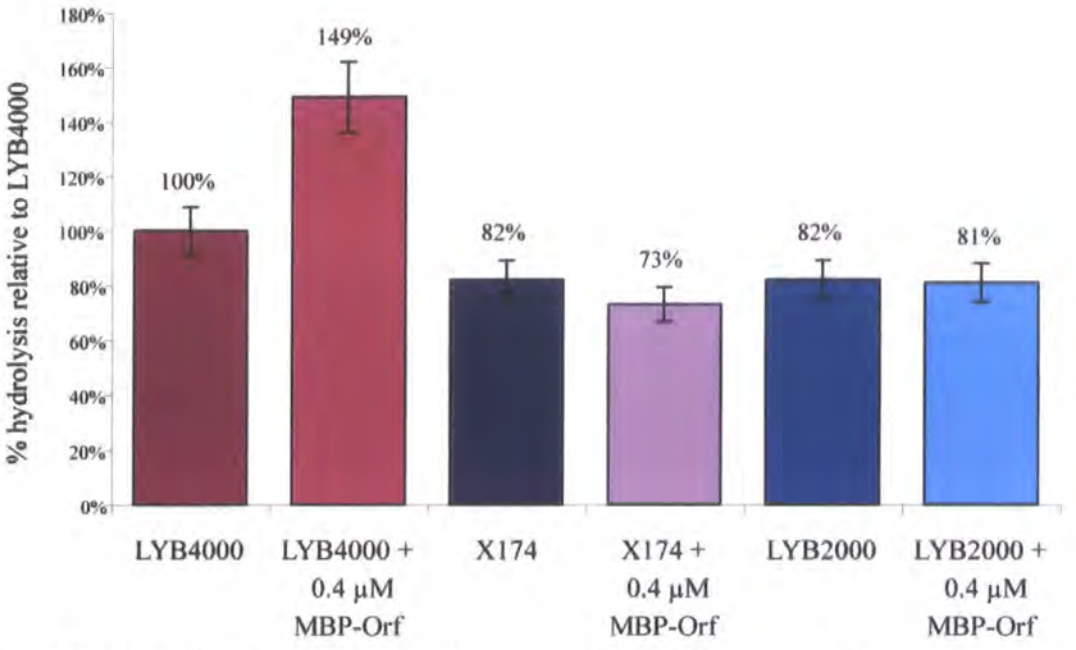

Figure 5.5. Effect of MBP-Orf on RecA ATPase activity in a MESG-phosphorolysis-coupled assay. All reactions contained 15 μM (N) LYB4000, ϕX174 or LYB2000 DNA, 0.5 μM RecA and 1 mM ATP. MBP-Orf was added prior to the addition of RecA as indicated. The rate of ATP hydrolysis for RecA alone was 3.77 μM/min.

5.4 Orf attenuates the inhibitory effect of SSB on RecA loading in an NADH-oxidation-coupled assay

The ability of Orf to replace the different functions of the RecFOR proteins in λ recombination is consistent with loading or unloading SSB or RecA at the ssDNA:dsDNA interface. The effect of *E. coli* SSB protein on RecA ATPase activity in the presence and absence of Orf was therefore investigated. No ATPase activity was detected when the LYB4000 substrate was incubated with SSB alone (data not shown). As expected, addition of SSB to NADH-oxidation-coupled assays resulted in significant inhibition of ATP hydrolysis mediated by RecA (Kowalczykowski & Krupp, 1987). Inclusion of 200 nM SSB led to a 3-fold reduction in ATP hydrolysis (Figure 5.6).

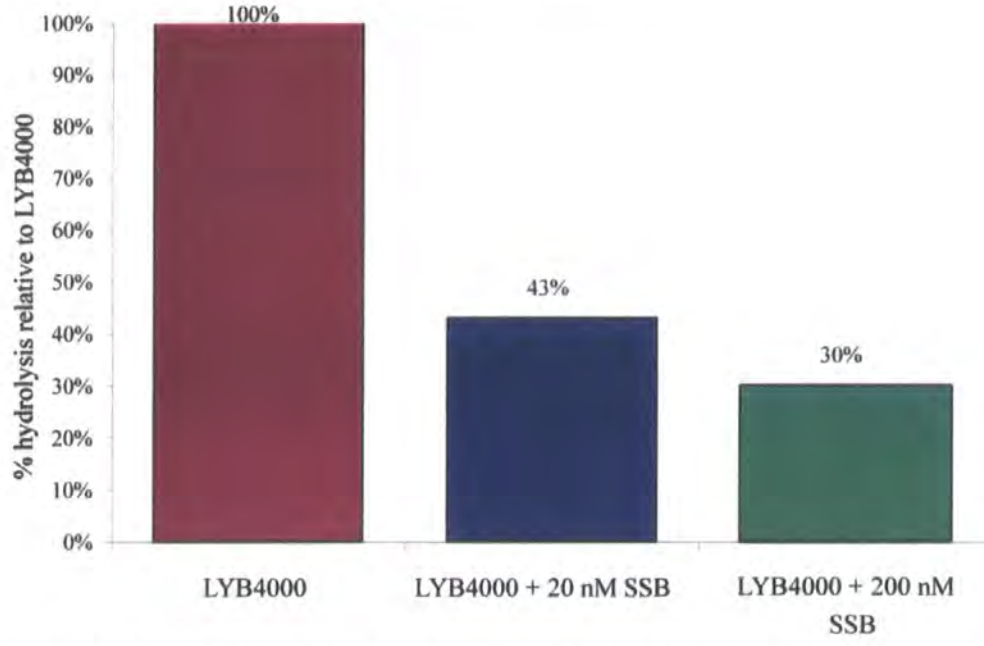

Figure 5.6. Inhibition of RecA ATPase activity by SSB in an NADH-oxidation-coupled assay. Assays contained 5 μM(N) LYB4000, 3.6 μM RecA, 1 mM ATP and 20 or 200 nM SSB. The rate of ATP hydrolysis for RecA alone was 27.76 μM/min.

Inclusion of MBP-Orf, in assays containing LYB4000 pre-bound with SSB, modulated the inhibitory effect of SSB on ATP hydrolysis. MBP-Orf at 2 and 20 nM further enhanced the inhibitory effect of SSB on ATP hydrolysis. However, addition of 200 nM MBP-Orf significantly alleviated the effect of SSB, reducing inhibition by 23% and thereby returning ATP hydrolysis to two-thirds of the un-inhibited rate (18.25 μM/min *vs* 27.76 μM/min) (Figure 5.7).

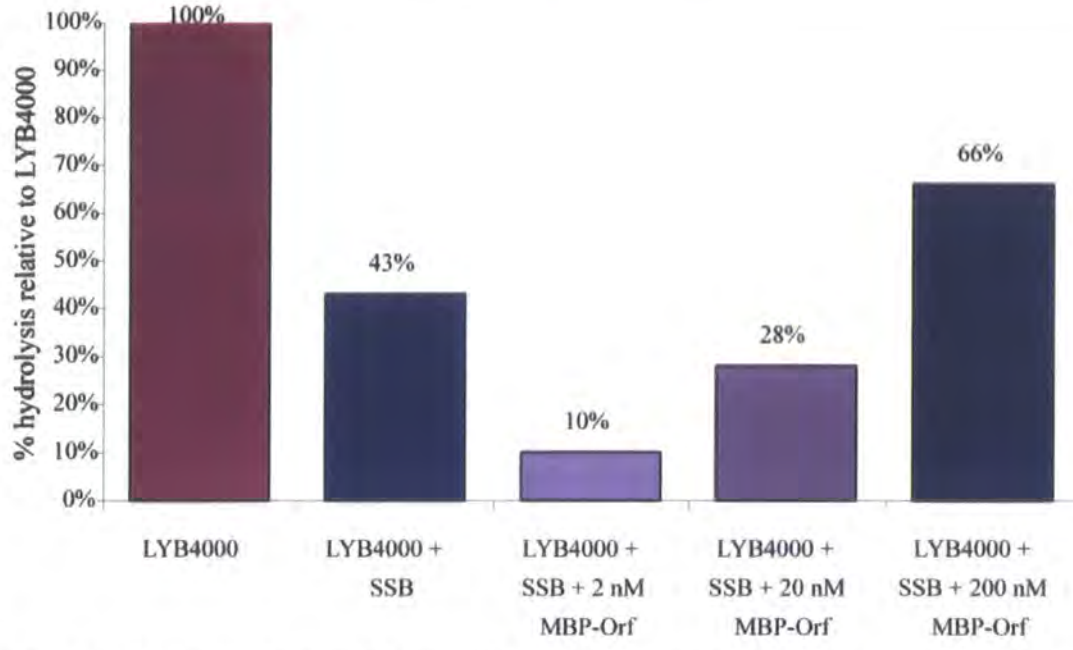

Figure 5.7. NADH-oxidation-coupled assay of RecA ATPase activity in the presence of MBP-Orf and SSB. Assays contained 5 μM(N) LYB4000, 3.6 μM RecA, 20 nM SSB, 1 mM ATP and 2, 20 and 200 nM MBP-Orf. The rate of ATP hydrolysis for RecA alone was 27.76 μM/min.

The results from the NADH-oxidation-coupled assay suggest that Orf facilitates the loading of RecA onto DNA at ssDNA:dsDNA intersections, alleviating the inhibitory effect of SSB. However, this assay protocol proved difficult to implement with the equipment available and, on occasions, the data obtained varied widely. Difficulties with reproducibility and robustness using this assay system have also been reported by Lee *et al*, (2007). As a consequence, alternative methods for monitoring ATP hydrolysis were pursued.

5.5 Orf attenuates the inhibitory effect of SSB on RecA loading in a colourimetric phosphate-detection assay

A colourimetric phosphate-detection assay (Lee *et al*, 2007; Martin *et al*, 1985) employing Biomol Green, an analog of Malachite Green, was used to study ATP hydrolysis by RecA directly rather than using an indirect enzyme-linked system. Utilising a non-enzymatic assay reduced the risk of false positive results due to interactions between proteins used in the study and enzymes, which formed the basis of the coupled system. However, to maintain the free phosphate concentration in the linear dynamic range of the assay reagent, reaction times were limited to 5 min. Discontinous assays were performed in 96-well microtitre plates with 0.5 μM RecA,

500 μM ATP and 2 μM (N) LYB4000. Reactions were terminated by addition of Biomol Green reagent and free phosphate measured by comparison with a phosphate standard curve. The rate of ATP hydrolysis rate was determined as described in Chapter 2, section 2.6.1(b).

Inclusion of 200 nM MBP-Orf in assays containing RecA and LYB4000 reduced the rate of ATP hydrolysis by half (Figure 5.8 A and B). In contrast, MBP-Orf at 2000 nM enhanced the rate of hydrolysis (Figure 5.8 A and B). The 13% enhancement of ATP hydrolysis rate by 2000 nM MBP-Orf detected by colourimetric phosphate assay is almost identical to the 15% enhancement observed using the NADH-oxidation-coupled assay (Figures 5.8 and 5.4).

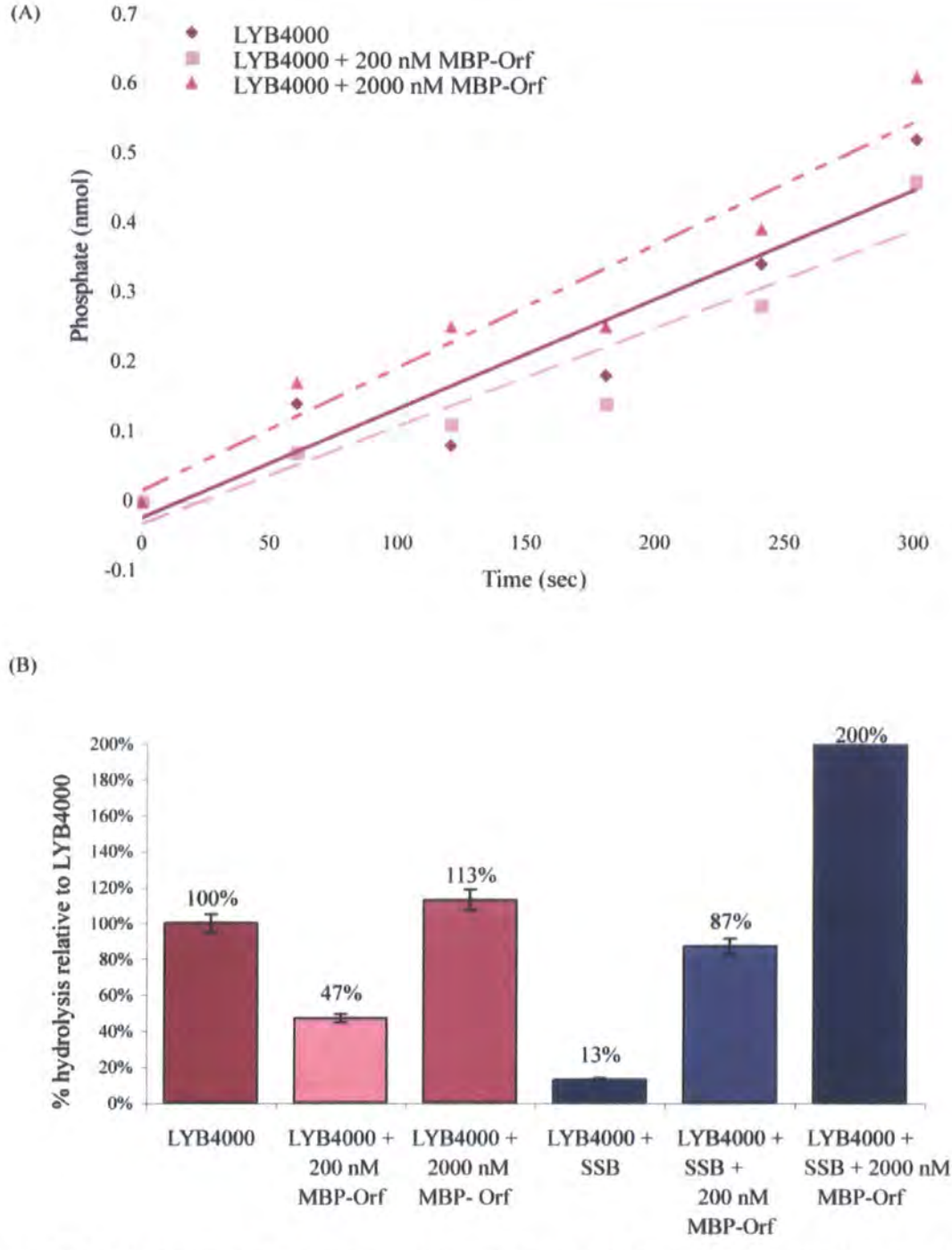

Figure 5.8. Colourimetric phosphate-detection assay, employing Biomol Green, for RecA ATPase activity in the presence of MBP-Orf and SSB. A) Time-course. B) Total hydrolysis over 5 min. Assays contained 2 μM (N) LYB4000, 0.5 μM RecA, 500 μM ATP and, where indicated, 20 μM SSB and 200 or 2000 nM MBP-Orf. The rate of ATP hydrolysis for RecA alone was 0.15 nmol/min.

As indicated in the NADH-oxidation-coupled assay, the colourimetric phosphate-detection method confirmed that SSB inhibits ATP hydrolysis by RecA (Figures 5.6 and 5.8). This inhibitory effect was alleviated by the presence of 200 nM MBP-Orf (Figures 5.6 and 5.8). Remarkably, given the weak stimulation seen in the RecA reaction with MBP-Orf, the rate of ATP hydrolysis doubled when 2000 nM MBP-Orf

was added. Taken together the data suggest that Orf, provided it is present at sufficient concentration, facilitates RecA loading, thereby alleviating the inhibition arising from SSB bound to ssDNA. This explanation is more likely than Orf titrating out SSB, since Orf can stimulate RecA in the absence of SSB and the enhancement of ATPase when all three proteins are present is greater than with RecA alone. To confirm these results, another method was adopted since colourimetric phosphate detection assays are single-point reactions and therefore also have limitations.

5.6 Orf attenuates the inhibitory effect of SSB on RecA loading in an MESG-phosphorolysis-coupled assay

The data obtained from the NADH-oxidation coupled and colourimetric-phosphate detection assays suggest that Orf facilitates the loading of RecA in the absence of SSB and has the potential to attenuate or alleviate the inhibitory effect of SSB depending on concentration ratio of SSB:Orf. A further assay system, an MESG-phosphorolysis-coupled assay, was employed to monitor inorganic phosphate released during the ATP hydrolysis reaction by RecA. The MESG-phosphorolysis-coupled assay was identified as being advantageous over the assays previously employed since it allows continuous monitoring of released free phosphate and can be performed in 96-well microtitre plates. Perhaps most importantly, detection of ATP hydrolysis is not dependent on an ADP-dependent enzyme (e.g. pyruvate kinase), therefore inhibition of RecA ATPase activity can be detected more reliably than is possible *via* the NADH-oxidation-coupled assay. Continuous assays were performed with 0.5 μM RecA, 15 μM (N) LYB4000 and 1 mM ATP as described in Chapter 2, section 2.6.1(c). Appropriate control assays, performed in parallel, confirmed the changes in the rate of hydrolysis were attributable to the proteins being investigated (Figure 5.9).

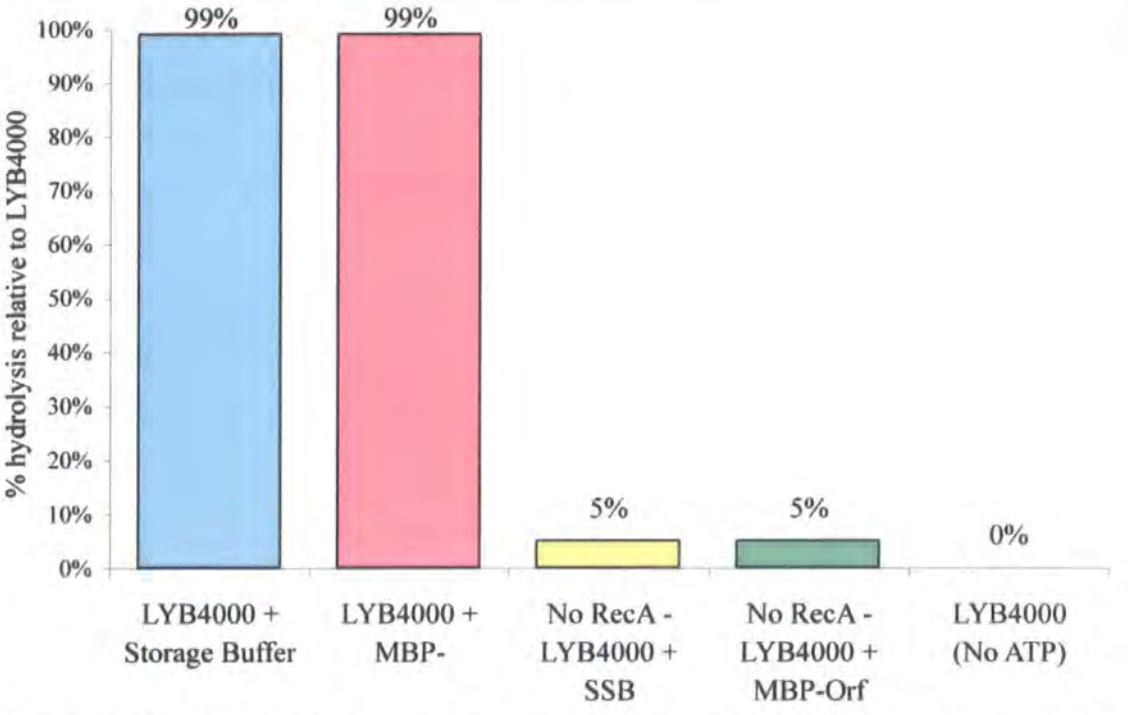

Figure 5.9. MESG-phosphorolysis-coupled assay of RecA ATPase activity in the presence of peripheral assay components. Assays contained 15 μM (N) LYB4000, 1 mM ATP and where indicated 0.5 μM RecA, 0.4 μM MBP or 2.04 μl protein storage buffer (2 mM Tris-HCl pH8, 0.1 mM EDTA, 0.05 mM DTT, 5% glycerol).

Under the conditions employed, RecA ATP hydrolysis rate was determined to be 5.02 μM/min (Figure 5.10). Inclusion of MBP-Orf modulated the rate of ATP hydrolysis; < 400 nM MBP-Orf was identified as inhibitory to RecA ATPase activity, with 100 nM MBP-Orf resulting in a 20% inhibition of hydrolysis, whereas 400 nM MBP-Orf returned ATP hydrolysis to the rate observed in the absence of Orf (Figure 5.10). This data suggests that the addition of high concentrations of Orf enhances RecA ATP hydrolysis in agreement with results from the NADH-oxidation-coupled and colourimetric phosphate detection assays.

As determined by both NADH-oxidation-coupled assays, colourimetric phosphate detection assays and published literature, SSB was again shown to inhibit RecA loading in the MESG-phosphorolysis-coupled assay. As in the NADH-oxidation-coupled assay, inclusion of MBP-Orf at lower concentrations, in combination with SSB, resulted in a further inhibition of RecA loading, whereas greater concentrations of MBP-Orf alleviated the inhibitory effect of SSB. MBP-Orf at 100 nM enhanced SSB inhibition by 6%, reducing the ATP hydrolysis rate to 72% of that with RecA alone (3.61 μM/min *vs* 5.02 μM/min). With MBP-Orf at 400 nM the inhibition of

SSB was alleviated by 14%, returning the rate of hydrolysis to 92% of that seen with RecA alone (4.63 μM/min *vs* 5.02 μM/min) (Figure 5.10).

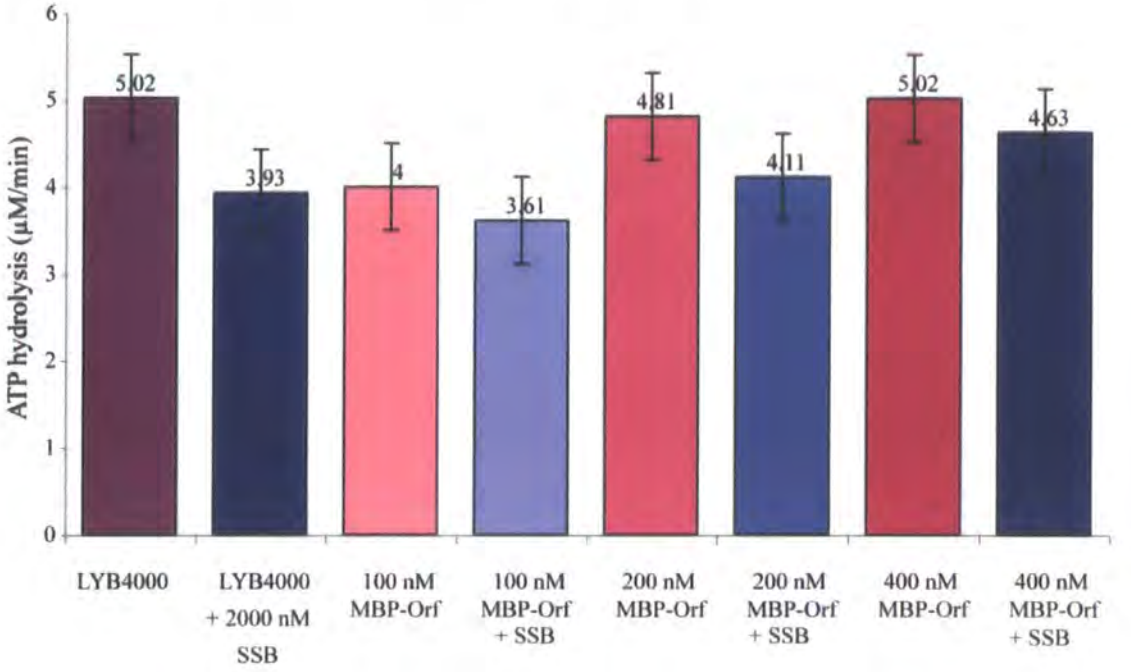

Figure 5.10. MESG-phosphorolysis-coupled assay of RecA ATPase activity in the presence of MBP-Orf and SSB. Assays contained 15 μM (N) LYB4000, 0.5 μM RecA, 1 mM ATP and, where indicated, 2000 nM SSB and 100, 200 or 400 nM MBP-Orf.

Consideration of the data from all three assays suggests that Orf plays a key role in modulating RecA loading onto SSB-coated ssDNA at ssDNA:dsDNA intersections, both alone and in concert with SSB. However, the nature of the effect of Orf on RecA loading appears to be dependent on the prevailing conditions, in particular the Orf:SSB ratio.

5.7 Orf mutants with defects in DNA binding show reduced capacity to alleviate the inhibitory effect of SSB on RecA

To examine the importance of Orf DNA binding on RecA loading and alleviating the negative effect of SSB, we analysed a number of MBP-Orf mutant proteins known to impair DNA binding. The nature of these mutations is discussed in Chapter 4. MESG-phosphorolysis-coupled assays were employed because they provide an efficient and reliable system for monitoring ATP hydrolysis. Inclusion of MBP-OrfΔC6 or MBP-OrfΔW141F mutant proteins (which confer a slightly reduced ssDNA binding capability relative to the wt Orf protein) were shown, in the absence of SSB, to exhibit similar modulatory effects on RecA ATPase activity as wt Orf (Figure 5.11).

However, addition of either mutant protein to assays incorporating LYB4000 pre-bound with SSB showed both MBP-OrfΔC6 and MBP-OrfW141F were incapable of alleviating the inhibitory effects of SSB. In contrast to wt Orf protein, addition of MBP-OrfΔC6 and MBP-OrfW141F enhanced the inhibitory effect of SSB (Figure 5.11). Mutant MBP-Orf proteins (MBP-OrfΔC19 and MBP-OrfR103E) that are unable to bind DNA significantly inhibited RecA ATPase activity in the absence of SSB. MBP-OrfΔC19 and MBP-OrfR103E at 200 nM further inhibited ATP hydrolysis beyond that seen with SSB, similar to the results obtained with MBP-OrfΔC6 and MBP-OrfW141F (Figure 5.11).

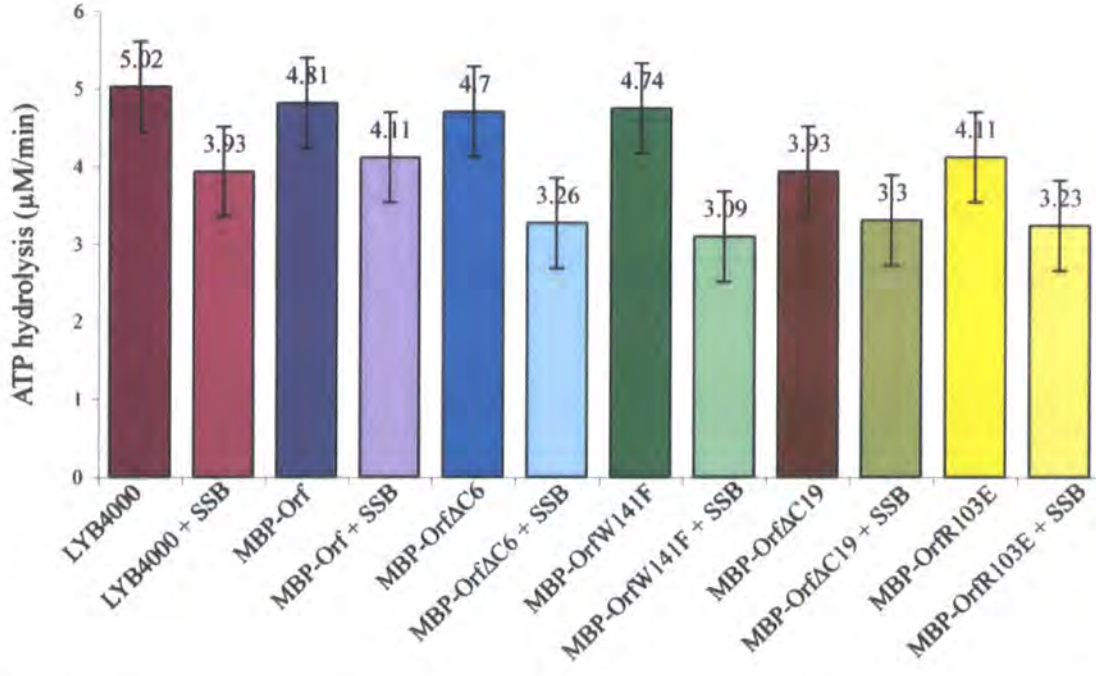

Figure 5.11. MESG-phosphorolysis-coupled assay of RecA ATPase activity in the presence of MBP-Orf C-terminal mutant proteins and SSB. Assays contained 15 μM (N) LYB4000, 0.5 μM RecA, 1 mM ATP, 200 nM MBP-Orf or MBP-Orf mutant and, where indicated, 2000 nM SSB.

The data obtained suggests that the Orf DNA binding capability is important in RecA loading in the presence or absence of SSB. It is also possible that these mutants show reduced binding to RecA or SSB and this accounts for the results observed. However, MBP-OrfΔC6, MBP-OrfΔC19 and MBP-OrfW141F are known to retain the capacity to bind SSB (F.A. Curtis and G.J. Sharples, personal communication). Only MBP-OrfR103E is known to show a curtailed interaction with RecA (L.A. Wilson and G.J. Sharples, personal communication); the other mutant proteins have not been tested as yet. The inhibitory effects of the C-terminal Orf mutant proteins could be explained

by the formation of an Orf-RecA complex, which is refractory to ATP hydrolysis unless Orf is bound to DNA.

5.8 Discussion

In this chapter the impact of Orf and SSB, on *E. coli* RecA loading onto ssDNA was investigated. Orf was shown to have a requirement for loading RecA at ssDNA:dsDNA intersections, an observation which correlates with a preference by the RecF protein for binding gapped DNA substrates and loading at ssDNA:dsDNA junctions (Hegde *et al*, 1996). Orf was detrimental to RecA loading when no or few ssDNA:dsDNA intersections were available.

The effect of Orf on ATP hydrolysis (i.e. RecA filament assembly) was also significantly influenced by the concentration of Orf in the assay. Lower MBP-Orf concentrations had an inhibitory effect, whereas higher concentrations tended to facilitate the loading of RecA onto ssDNA. It may be that this apparent concentration dependence may be due to Orf influencing the aggregation state of RecA. The quantity of Orf protein available and its ratio to the number of ssDNA:dsDNA intersections available may therefore be critical in determining whether RecA reactions are inhibited or stimulated by Orf. Significantly, MBP-Orf protein was able to alleviate the inhibition of RecA ATP hydrolysis exerted by SSB. This effect mirrors the results noted with *E. coli* RecFOR proteins (Morimatsu & Kowalczykowski, 2003).

Orf proteins with C-terminal mutations, conferring defects in ssDNA binding, adversely affected RecA loading and were unable to attenuate the inhibitory effect of SSB. MBP-OrfΔC19 and MBP-OrfR103E mutant proteins which cannot bind ssDNA had a significant negative effect on RecA loading and served only to enhance the inhibitory effect of SSB. These results point to the DNA binding capability of Orf being important for modulating RecA loading and crucial for attenuating SSB inhibition.

Overall these results are consistent with Orf interacting with RecA, SSB and DNA (preferentially at ssDNA:dsDNA intersections) during the initial stage of

recombination and thereby modulating the rate of RecA filament assembly according to the prevailing conditions. Precisely how Orf effects this modulation requires further study.

Chapter 6

Characterisation of the putative Orf homologues, Orf151 and ETA20

6.1 Introduction

A family of 42 Orf proteins, originating from diverse lambdoid phage and prophage sources, has been identified by position-specific iterative BLAST searches (F.A. Curtis and G.J. Sharples, unpublished results). Considerable sequence diversity is evident within this family. To confirm a functional relationship, two of the most dissimilar members of the family, Orf151 and ETA20, were purified and their *in vitro* properties examined.

Orf151, from the *E. coli* cryptic prophage DLP12, resembles several prophage-associated proteins (sharing 93% identity with an Orf homologue from *E. coli* O157:H7) but shares only 16% overall identity with λ Orf (F.A. Curtis and G.J. Sharples, unpublished results). However, structural prediction analyses indicate Orf151 and λ Orf share a similar architecture with the positively charged channel that traverses the dimer most highly conserved. The main differences between λ Orf and Orf151 are in the N-terminal region and C-terminal helix, the latter potentially influencing DNA-binding (F.A. Curtis and G.J. Sharples, unpublished results).

ETA20 from *Staphylococcus aureus* temperate phage ϕETA genome (Yamaguchi *et al*, 2000) has an Orf like domain with a C-terminal extension matching a zinc-finger motif from the HNH nuclease family (Mehta *et al*, 2004). It is possible that ETA20, in contrast to other Orf homologues, functions in a degradative capacity.

In this chapter the functional relationship between λ Orf and Orf151 is investigated using the assays described in Chapters 4 and 5. In addition, the ETA20 protein was probed for its ability to associate with and degrade DNA.

6.2 λ Orf and *E. coli* Orf151 share similar DNA and SSB binding properties

As part of this study, the *E. coli orf151* gene was cloned, and its product overexpressed and purified as a fusion to MBP (Chapter 3). Previously, purification of His-Orf or the wild-type protein had proved impossible due to its insolubility. Purified MBP-Orf151 protein was examined alongside MBP-Orf to confirm the potential functional relationship. Initial experiments focussed on their DNA binding properties and ability to interact with *E. coli* SSB (F.A. Curtis and G.J. Sharples, unpublished results). MBP-Orf151, like λ MBP-Orf, was shown to bind ssDNA in preference to dsDNA. However, Orf151, was also able to form a stable complex with a small proportion of present dsDNA (Figure 6.1. F.A. Curtis and G.J. Sharples, unpublished results). Far-western blotting indicated that Orf interacts with *E. coli* SSB, consistent with Orf functioning to facilitate the loading of RecA (Maxwell *et al*, 2005). MBP-Orf151 was also shown to bind SSB in far-western assays (Figure 6.2). ELISA and yeast two-hybrid analysis confirmed these results and suggest that Orf151 possesses a higher binding affinity for SSB than Orf (F.A. Curtis and G.J. Sharples, unpublished results).

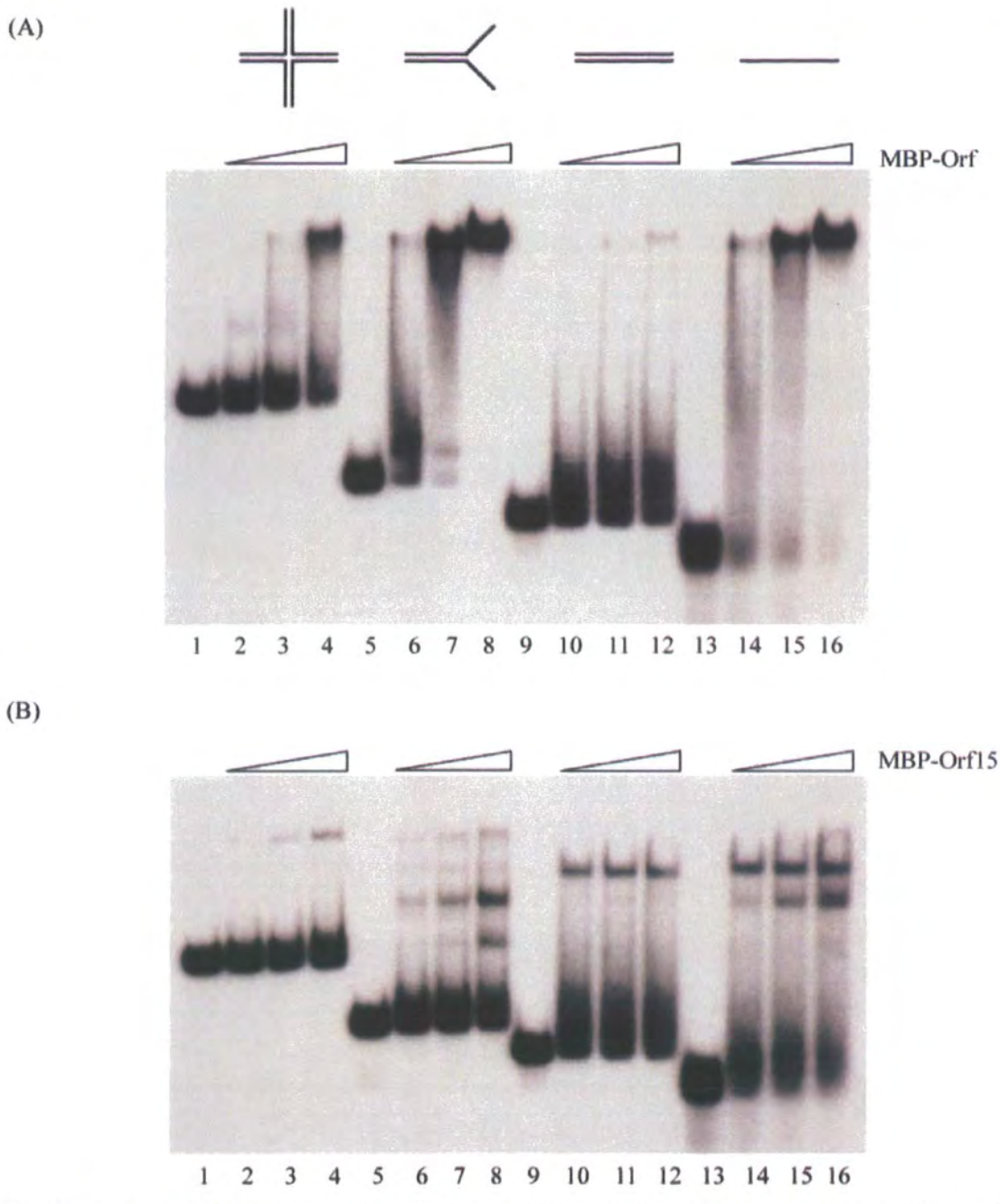

Figure 6.1. MBP-Orf and MBP-Orf151 binding to different DNA substrates in a gel mobility shift assay. Binding reactions contained 0, 125, 250 and 500 nM MBP-Orf (A) or MBP-Orf151 (B) and 0.3 nM of ^{32}P-labelled Holliday junction (lanes 1-4), Fork (lanes 5-8), dsDNA (lanes 9-12) and ssDNA (lanes 13-16). Experiments were performed by F.A. Curtis.

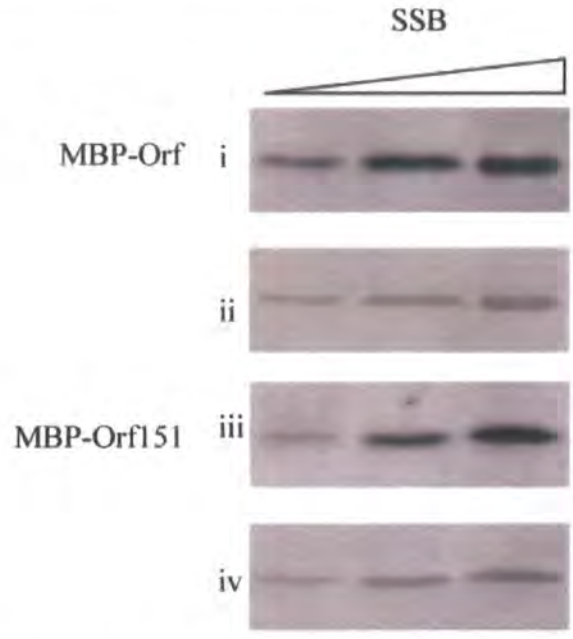

Figure 6.2. Interaction of MBP-Orf and MBP-Orf151 with SSB detected by far-western blotting. SSB (0.5, 1.9, 3.8 μg) was separated on 15% SDS-PAGE, blotted and probed with 20 μg MBP-Orf (i) or MBP-Orf151 (iii). Interactions were detected using antibodies specific for the MBP tag. Rows (ii) and (iv) demonstrate the efficiency of SSB transfer onto the blotted membranes (stained with amido black).

6.3 Orf151 interacts weakly with Exo

Experiments in Chapter 4 indicated that Orf and Exo may associate (Figure 4.1). An enzyme linked immunosorbent assay (ELISA) was employed to investigate any possible interaction between Orf151 and Exo using an N-terminal GST (glutathione-S-transferase) Orf151 fusion (Chapter 3, section 3.3). Following preliminary experiments to determine optimum conditions, assays were performed with 5 μg/ml Exo (10.42 μM) with purified GST-Orf151 at 0.367-11.74 μM. Antibodies to the GST moiety were used to detect GST-Orf151 binding to the untagged Exo protein bound to an Immunlon plate as described in Chapter 2 (section 2.6.2). A positive Orf151-Exo association was detected at GST-Orf151 concentrations greater than 0.734 μM (Figure 6.3). Inclusion of a 51-mer oligonucleotide enhanced the protein-protein interaction (Figure 6.3) indicating that DNA binding by Orf151 or Exo, or both, can affect their association.

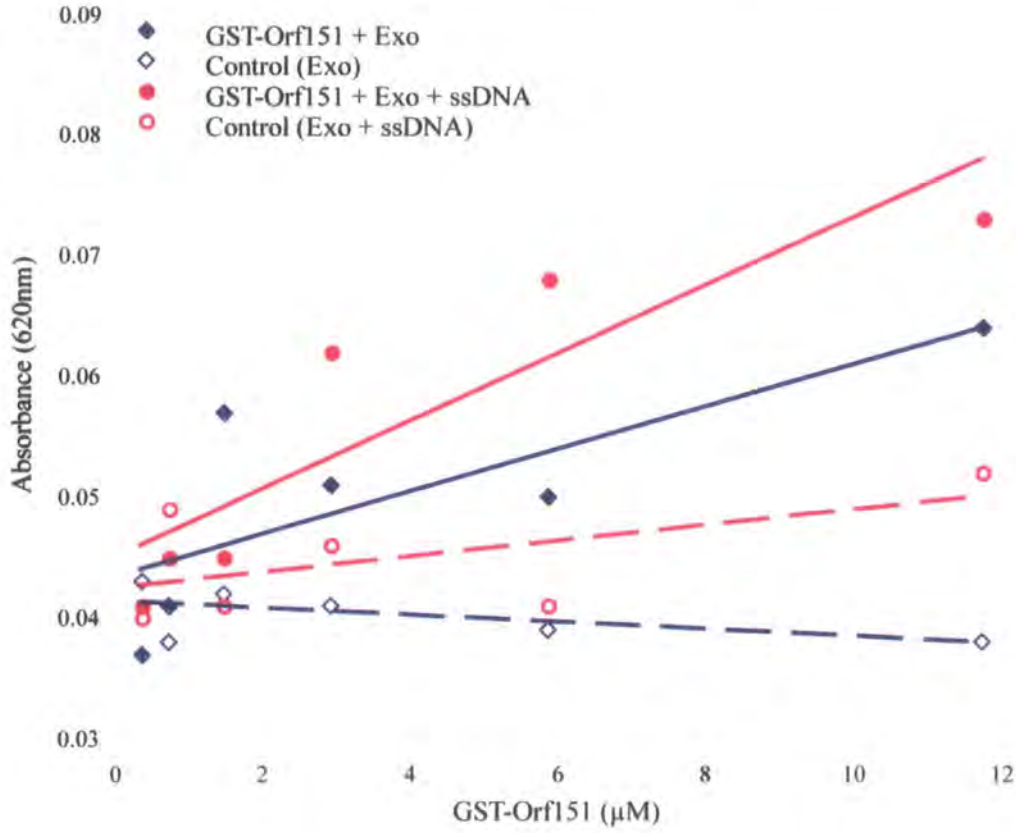

Figure 6.3. Interaction between GST-Orf151 and Exo in the presence or absence of DNA. Binding mixtures contained 10.42 μM Exo and 0.367, 0.734, 1.47, 2.93, 5.87 and 11.74 μM GST-Orf151. A 51-nt ssDNA substrate was included at 0.5 μg/ml. Data are the mean of three experiments.

6.4 Orf151 has no significant impact on Exo activity on linear λ DNA

To determine whether Orf151, like Orf (Chapter 4), modulates the degradative activity of Exo, nuclease assays were employed as described in Chapter 4. Assays were performed with 7.7×10^{-4} U/ml Exo and 5 μM (N) λ DNA and DNA degradation was quantified by densitometry as before. Appropriate control assays were performed in parallel, confirming that the observed degradation was solely due to Exo activity. Purified MBP-Orf151 did not exhibit any nuclease activity when incubated individually with DNA in the absence of Exo (data not shown). Inclusion of 100 nM MBP-Orf151 had no effect on Exo nuclease activity, with the linear λ DNA decreasing by approximately 5-fold in 10 min similar to those reactions with Exo alone (Figure 6.4).

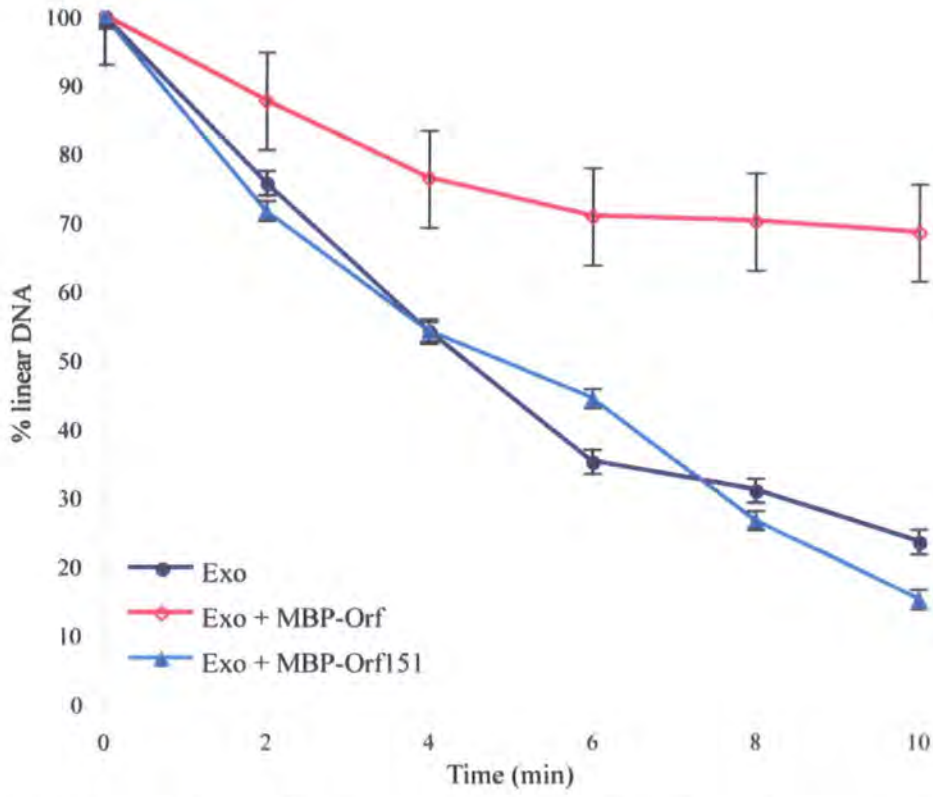

Figure 6.4. Exo nuclease assay in the presence of MBP-Orf and MBP-Orf151. Assays were performed at 37°C and contained $7.7x10^{-4}$ U/μl Exo and 5 μM (N) λ DNA with 100 nM MBP-Orf or MBP-Orf151 protein. The bands were analysed by densitometry. Data are the mean of two independent experiments.

6.5 Orf151 enhances RecA loading in the absence of SSB but has no effect in the presence of SSB

In Chapter 5, the interaction between Orf and RecA was investigated by studying RecA ATPase activity under various conditions. Orf appeared to stimulate RecA assembly on ssDNA in the absence of SSB and attenuated the inhibition of RecA activity associated with addition of SSB. In order to determine whether Orf151 behaves in a similar fashion, MESG-phosphorolysis-coupled assays were performed with MBP-Orf151, in the presence and absence of SSB. Appropriate control assays confirmed the changes in rate of ATP hydrolysis observed were solely due to the impact of the added proteins on RecA filament assembly.

Inclusion of 200 nM MBP-Orf151 enhanced RecA ATP hydrolysis by 5%, whereas 200 nM MBP-Orf was shown to result in a 4% inhibition of ATP hydrolysis (Figures 6.5 and 5.10). However, in the presence of SSB, MBP-Orf151 had little impact on RecA ATPase activity, with ATP hydrolysis recorded as only 0.03 μM/min greater

than the rate apparent with RecA and SSB together (Figure 6.5). Under the same conditions, MBP-Orf attenuated the inhibitory effect of SSB by 5%.

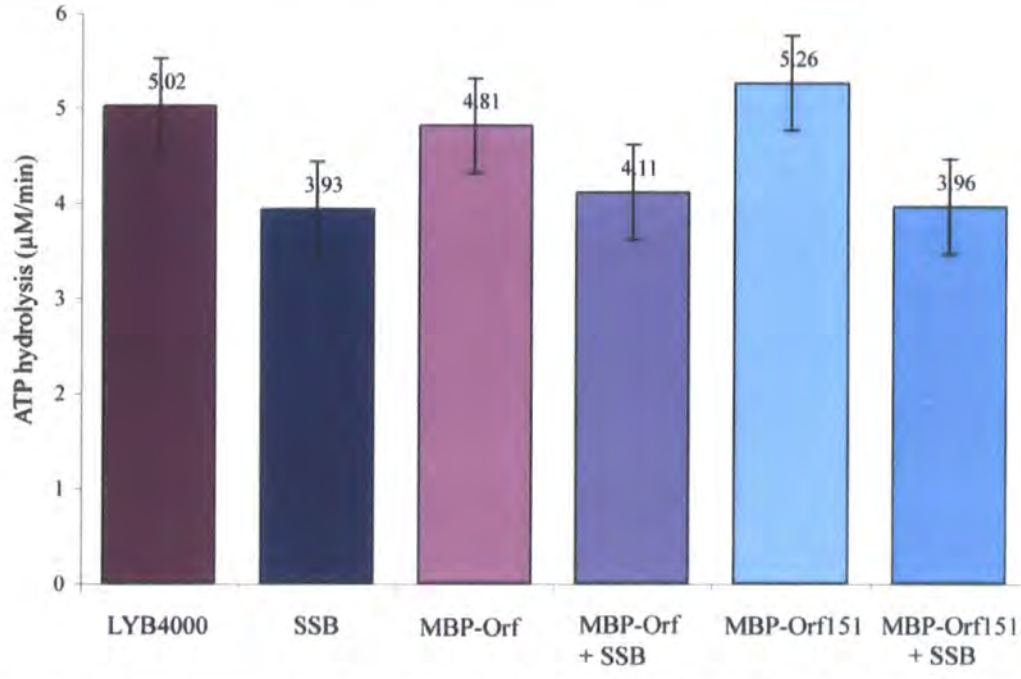

Figure 6.5. MESG-phosphorolysis-coupled assay of RecA ATPase activity with MBP-Orf, MBP-Orf151 and SSB. Assays contained 15 μM (N) LYB4000, 0.5 μM RecA, 1 mM ATP and, where indicated, 200 nM MBP-Orf or MBP-Orf151 and 2 μM SSB.

The results suggest that in the absence of SSB, Orf151 sequesters RecA monomers and enhances ATP hydrolysis, whereas in the presence of SSB, unlike Orf, Orf151 is unable to associate effectively with RecA and facilitate loading.

6.6 ETA20 binds DNA and the C-terminal domain is necessary for nuclease activity

Initial studies indicated that, like Orf and Orf151, ETA20 binds to DNA substrates (F.A. Curtis, personal communication). In addition, comparisons between MBP-ETA20 and a version lacking the C-terminal domain (MBP-ETA20ΔC82) suggested that the C-terminal region specifies a metal ion dependent nuclease activity (Figure 6.6).

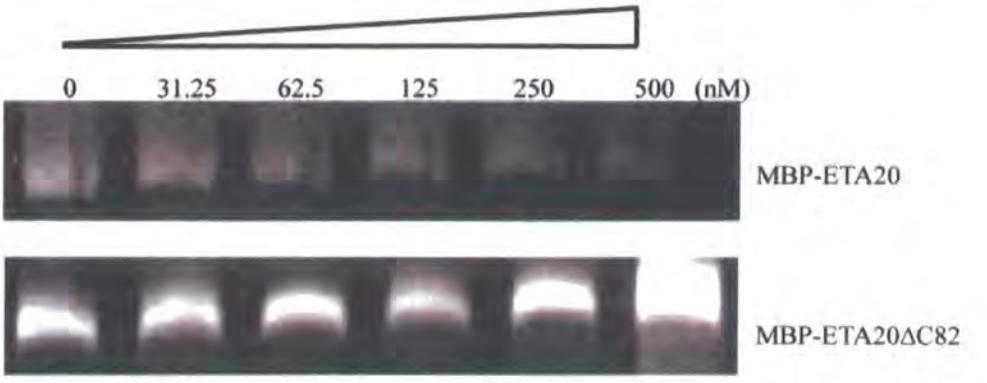

Figure 6.6. MBP-ETA20 and MBP-ETA20ΔC82 nuclease activity. Assays were performed with MBP-ETA20 or MBP-ETA20ΔC82 in buffer (50 mM Tris-HCl pH 8.0, 1 mM DTT, 100 μg/ml BSA) containing 1 mM $MgCl_2$ and single-stranded circular ϕX174 DNA (2 μg) at 37°C.

6.7 Possible preferential binding of ETA20 to dsDNA

To elucidate the DNA binding preferences of ETA20 and facilitate comparison with Orf and Orf151, electrophoretic mobility shift assays using range of branched and un-branched ^{32}P-labelled DNA substrates were employed. Unlike MBP-Orf and MBP-Orf151, which preferentially bind ssDNA over dsDNA (Figure 6.1), MBP-ETA20 exhibited a preference for binding dsDNA over ssDNA. MBP-ETA20 formed discrete complexes with both Holliday junction and 50 bp linear dsDNA, although only at high protein concentrations (Figure 6.7). It is possible that the limited binding observed is due to a contaminating non-specific DNA binding protein rather than ETA20. Time constraints prevented further analysis of the MBP-ETA20 and MBP-ETA20ΔC82 DNA binding and nuclease activities.

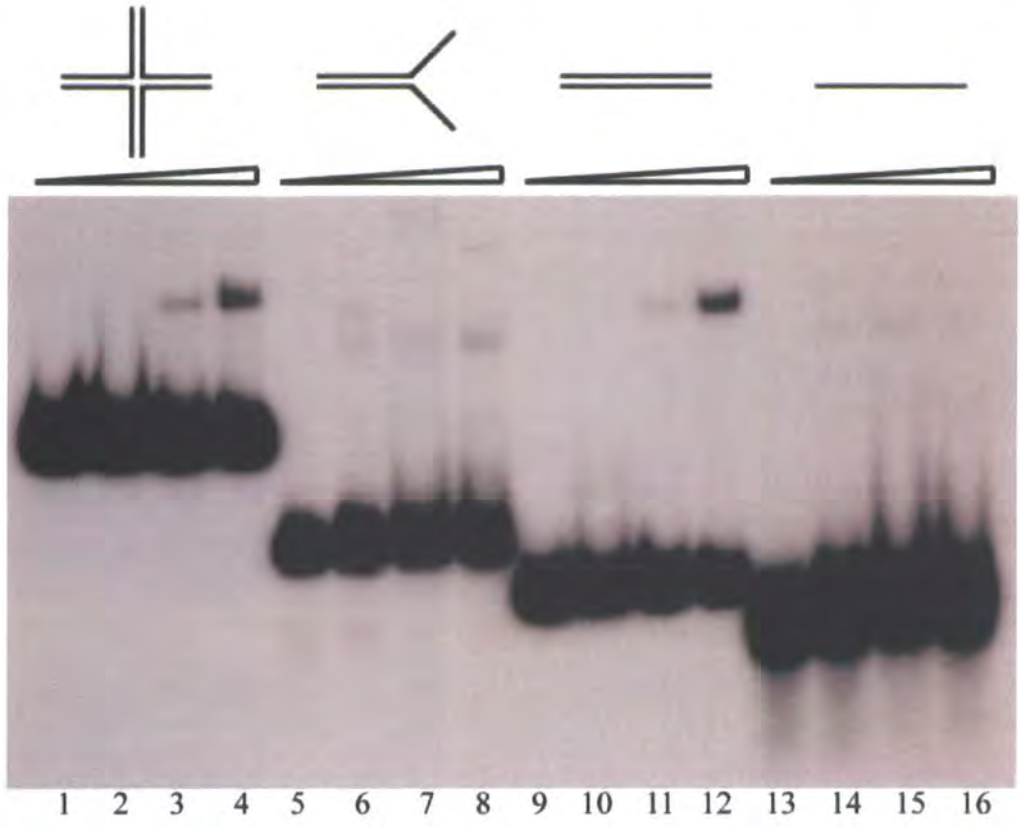

Figure 6.7. MBP-ETA20 binding to DNA substrates in gel mobility shift assays. Assays contained 0, 200, 400, 800 nM MBP-ETA20 and 0.3nM of ^{32}P-labelled Holliday junction (lanes 1-4), fork (lanes 5-8), dsDNA (lanes 9-12) and ssDNA (lanes 13-16).

6.8 Discussion

In this chapter, the properties and interactions of two Orf putative homologues, Orf151 and ETA20, were investigated to verify the functional relationship between diverse members of the 42 Orf protein family. Purified MBP-Orf151, from *E. coli* cryptic prophage DLP12, was shown to bind SSB with higher affinity than MBP-Orf protein in ELISA, yeast two-hybrid and far-western blots. MBP-Orf151 also showed a preference for binding ssDNA rather than dsDNA, although there were subtle differences in binding preferences compared to MBP-Orf. ELISA highlighted a potential Orf151-Exo interaction that was stimulated by addition of ssDNA. However, analysis of Exo nuclease activity in the presence of Orf151 suggests that, unlike Orf, it does not significantly affect Exo dsDNA degradation. ATPase assays suggest that Orf151 promotes RecA loading more effectively than Orf on LYB4000 (only 200 nM MBP-Orf151 was required to mimic the effect of >400 nM MBP-Orf). However, in RecA experiments with SSB, Orf151 was unable to alleviate the inhibitory effect on RecA loading.

The experiments suggest that the predicted similarities between Orf and Orf151 are genuine. However, differences between their effects on Exo and RecA activity indicate that Orf151 may not be fully active and would be unable to replace λ Orf in recombination. The apparent inactivity of Orf151 fits with its origins as part of a cryptic phage where selection for maintaining activity may no longer occur leading to loss of function. Alternatively, the structural differences noted between Orf and Orf151, particularly in α3 and β3, could affect the oligomeric interface, resulting in Orf151 being unable to interact effectively with other recombination proteins, such as Exo and RecA. The inability of Orf151 to attenuate the inhibitory effect of SSB on RecA loading could be due to the enhanced binding affinity of Orf151 for SSB reducing the efficiency of SSB removal required for RecA loading.

ETA20, from *S. aureus* phage φETA, possesses an endonuclease activity that depends on the presence of the C-terminal 82 residues, consistent with the presence of a zinc-finger motif belonging to the HNH family of nucleases in this region. ETA20 exhibited a weak binding preference for dsDNA rather than ssDNA, the reverse situation to that seen with Orf and Orf151. However, the ETA20 DNA binding activity required large amounts of protein possibly indicating that the DNA binding activity is due to a contaminant. Further experiments are required to determine any functional similarities and dissimilarities with λ Orf.

Chapter 7

Final Discussion

λ Orf protein exists as a dimer in solution, binds preferentially to ssDNA and associates with the SSB protein (Maxwell *et al*, 2005). Orf can substitute for the *E. coli* RecFOR complex in λ-λ recombination but not during host conjugational exchange (Sawitzke & Stahl, 1992, 1994) and partially substitutes for RecFOR in *E. coli* recombination when Exo and β are present (Poteete, 2004). As a consequence of the similarity of the Orf-SSB-ssDNA tripartite assemblies and those formed in phage T4 by UvsY, Gp32 and ssDNA (Liu *et al*, 2006), together with the known activities of RecFOR, Orf represents a convincing candidate for membership of the recombination/replication mediator protein family (Beernink & Morrical, 1999).

This study aimed to evaluate the role of λ Orf as a recombination/replication mediator protein in the initial stages of phage genetic recombination. The work presented describes the purification and biochemical analysis of the λ Orf protein and its interplay with other phage λ (Exo and β) and host recombinases (RecA and SSB). Two potential orthologues of λ Orf, *E. coli* DLP12 Orf151 and *S. aureus* ϕETA20, were also studied and their properties compared. The major findings are summarised and discussed here with possible future experiments proposed to address the questions that remain concerning the Orf function.

7.1 Potential homologues of λ Orf from the *E. coli* DLP12 cryptic prophage and *S. aureus* ϕETA

Sequence analysis suggested a family of diverse Orf-like proteins from lambdoid phages or prophages. Two distantly-related members of the family were selected, Orf151 from *E. coli* DLP12 and ETA20 from *S. aureus* phage ϕETA, for functional analysis. Both proteins were overexpressed as N-terminal MBP fusions and purified to near homogeneity. Although MBP-Orf151 retained the ability to bind ssDNA and SSB protein, it failed to act like its λ counterpart in combination with other λ and bacterial recombinases. These deficiencies may be due to it residing in a cryptic prophage where selection pressures may have rendered it inactive. Alternatively, the apparent structural differences between Orf and Orf151 may be sufficient to prevent

Orf151 from interacting with other recombinases effectively. The *S. aureus* phage ϕETA Orf homologue, ETA20, carries an additional C-terminal extension resembling HNH family nucleases. Both full-length protein and a deletion derivative missing this putative nuclease domain were studied. Preliminary experiments indicated that ETA20 may function as an endonuclease active on circular ssDNA. The deletion derivative, ETA20ΔC82, lacked this activity. ETA20 may be an example where the Orf DNA binding domain has been recruited for targeting of a nuclease for DNA end processing.

7.2 Orf interacts with λ and *E. coli* recombinases involved in the initial exchange step of recombination

The Orf protein exists as a dimer in solution, binds preferentially to ssDNA and associates with the SSB protein (Maxwell *et al*, 2005). Orf can substitute for the *E. coli* RecFOR complex in λ crosses but not during host conjugational exchange (Sawitzke & Stahl, 1992, 1994). Orf also partially substitutes for RecFOR in *E. coli* recombination when Exo and β are present (Poteete, 2004). The similarities of the Orf-SSB-ssDNA tripartite assemblies and those formed in phage T4 by UvsY, Gp32 and ssDNA (Liu *et al*, 2006), together with the known activities of RecFOR, suggest Orf may be a member of the recombination/replication mediator protein family (Beernink & Morrical, 1999).

a) Orf attenuates Exo nuclease activity

Phage λ Red recombination is initiated by Exo binding and degrading 5' ended DNA strands, thus exposing 3' ssDNA overhangs bound by either RecA or β (Little, 1967; Radding *et al*, 1966). An ELISA indicated a physical interaction between Orf and Exo and initial studies therefore focussed on the impact of Orf on Exo 5'-3' exonuclease activity. Assays were also conducted with other proteins important in the exchange step of recombination, namely β, SSB and RecA (Figure 7.1). Orf protein on its own significantly inhibited exonuclease activity, suggesting that Orf may be important in regulating end processing during lambda recombination. Addition of β protein slightly decreased Exo nuclease activity, however, the presence of both β and Orf, significantly inhibited Exo nuclease activity. Analysis of mutant Orf proteins with defects in DNA binding identified a correlation between the loss of DNA binding

capacity and a lack of inhibition of Exo nuclease activity. The modulation of Exo activity by Orf may therefore be a consequence of Orf interacting with DNA rather than directly with Exo, although, both features may be important. Exo and β are known to associate and both are required for efficient Red recombination (Tolun, 2007 *cited* Poteete, 2008). It is possible that Orf and β combine to halt Exo nuclease progression and encourage exchanges mediated by β annealing.

The strand invasion recombination pathway in phage λ is dependent on the RecA recombinase (Stahl *et al*, 1997). RecA alone inhibited Exo nuclease activity and this inhibition was enhanced by addition of Orf (Figure 7.1). The inhibition by RecA could be due to the assembly of the nucleoprotein filament or because strand invasion prevents Exo loading effectively or continuing in its degradation. Inclusion of β, Orf and RecA resulted in Exo nuclease activity halfway between that observed with RecA alone and RecA with Orf, i.e. addition of β (100 nM) in combination with RecA (500 nM) reduced the inhibitory effect of Orf (100 nM) on Exo by approximately 50%. RecA may sequester Orf protein, restricting its ability to bind ssDNA or Exo and reducing its inhibitory activity. Preferential binding of Orf to RecA or Exo could dictate pathway choices, facilitating β assembly for strand annealing or RecA assembly for strand invasion.

Surprisingly, SSB was found to stimulate Exo nuclease activity. Binding of exposed ssDNA by SSB may somehow permit faster Exo progress, perhaps by preventing inter or intra-molecular strand annealing. Addition of both Orf and SSB to Exo nuclease reactions returned degradation to the level evident when Exo was studied alone (Figure 7.1), i.e. their enhancing and inhibitory effects cancelled each other. Addition of SSB to a reaction comprising RecA and Exo had minimal effect on Exo activity, however, SSB in the presence of RecA and Orf (±β) alleviated the effects of the additional protein returning nuclease activity to that observed when Exo was assayed alone. The alleviation of inhibitory effects of the other recombinases by SSB suggests that *in vivo* its presence antagonises protein(s), which inhibit Exo activity. SSB is known to antagonise RecA protein assembly in any case (Kowalczykowski & Krupp, 1987). One could envisage that *in vivo,* SSB binds ssDNA produced by Exo, stabilising the nucleic acid structure, and also preventing binding by RecA. SSB

removal is facilitated by the actions of Orf, which, as a result of DNA binding, slows Exo and encourages loading of RecA or β to initiate strand invasion or strand annealing exchange pathways.

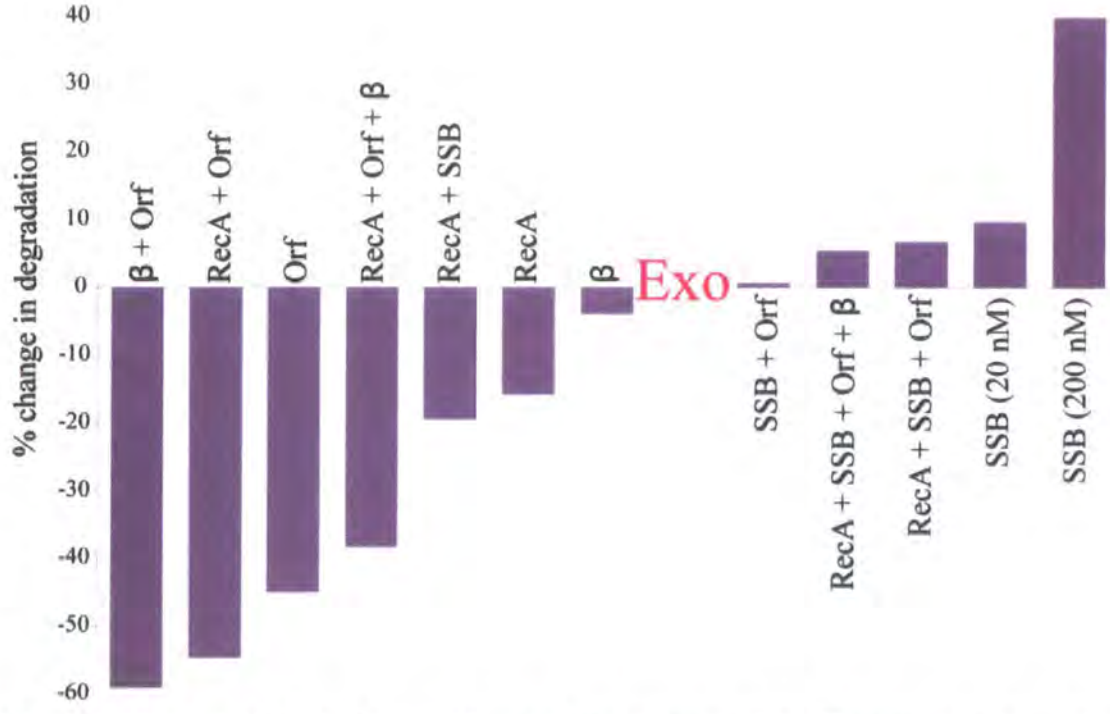

Figure 7.1. Impact of Orf and other recombinases on Exo nuclease activity. The percentage degradation observed at 10 min in the reaction of Exo alone ($7.7x10^4$ U/μl) is subtracted from the equivalent value for each reaction mix to give the percentage change in degradation level (i.e. Exo nuclease activity). Protein concentrations were Orf (100 nM), β (100 nM), RecA (500 nM), SSB (200 nM when in combination with RecA and 20 nM otherwise).

b) ssDNA:dsDNA intersections are required for optimal interaction between λ Orf and RecA

Previous investigations failed to distinguish any difference in Orf affinity for single-stranded, tailed and gapped substrates (Maxwell *et al*, 2005). However, in this study, a gapped duplex was found to be essential for Orf-mediated assembly of RecA onto ssDNA pre-incubated with SSB. Experiments with Orf binding to gapped duplex DNA suggested that the DNA was accommodated within a shallow U-shaped cleft running perpendicular to the central cavity (Maxwell *et al*, 2005). However, this conclusion failed to take into account the possibility that Orf is a hinge protein with the dimeric ring opening to permit ssDNA access to the central channel (Reed, 2006). The central cavity is lined with positively charged residues and the identification of a new DNA binding fold in the N-terminal portion of the Orf structure is consistent with DNA binding here. The novel DNA binding domain, termed RAGNYA (Balaji

& Aravind, 2007), is composed of two α-helices (αA from each Orf monomer) and four β-strands (β1 and β2 from each Orf monomer). The DNA binding surface is predicted to cross the face of the β sheet region. Analysis of the hydrogen bonding within the Orf structure also supports the idea of Orf being a hinge protein, as the N-terminal intertwined β-sheet region of the Orf dimer, which corresponds to the RAGNYA motif, has extensive hydrogen bonding whereas in the C-terminal section hydrogen bonding is much less extensive (Reed, 2006). The hydrogen bonding in the N-terminal region of the dimer combined with stable packing would allow the Orf dimer to act as a hinge, with the dimer opening in the C-terminal region between the anti-parallel β sheets (Figure 7.2). The ssDNA:dsDNA intersection could be accommodated at the widest portion of the cavity with the ssDNA threaded through the middle. This clamp model shows structural congruity with the dimeric RecF protein (Koroleva *et al*, 2007), one of the subunits in the RecFOR complex, which can be functionally replaced by Orf.

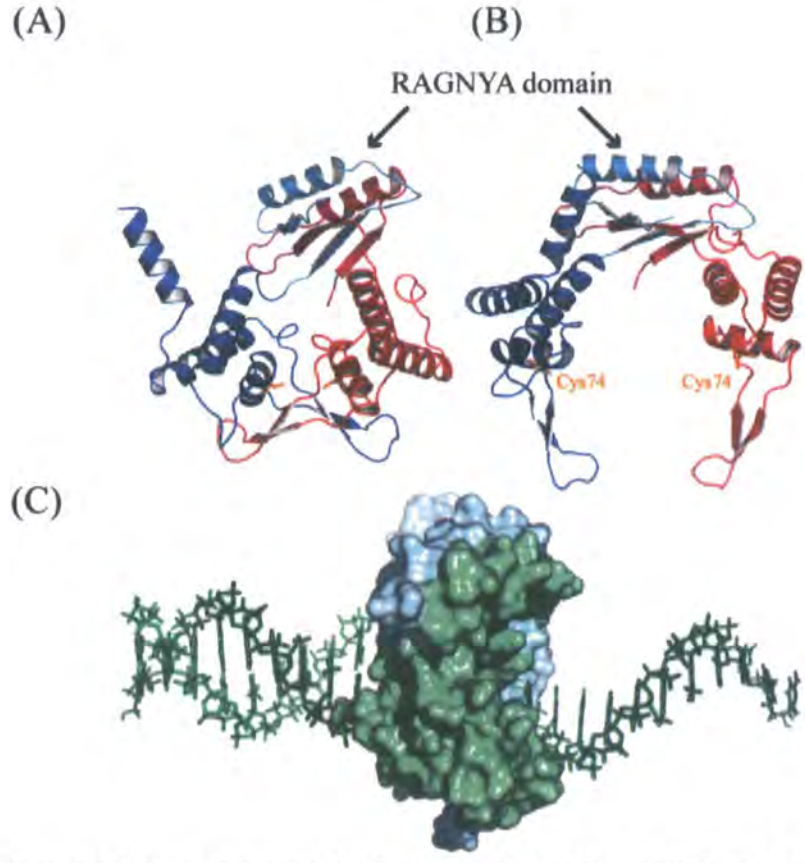

Figure 7.2. Proposed Orf DNA binding modes (figure provided by G.J. Sharples and P. Reed).
A) and B) Ribbon representation of the structure of Orf in closed and proposed open conformations. The Cys74 residue is highlighted as a possible target for FRET analysis. C) Model for Orf binding at the ssDNA:dsDNA intersection. The dsDNA is accommodated in the widest end of the central cavity with the ssDNA threaded through the narrow channel.

c) λ Orf modulates RecA loading

In order to assess how protein-protein interactions between Orf and RecA promote the establishment of RecA nucleoprotein filaments on ssDNA pre-bound with SSB, ATP hydrolysis assays were conducted. The RecA nucleoprotein filament hydrolyses ATP when bound to DNA allowing the kinetics of filament formation to be monitored (Brenner *et al*, 1987).

Orf stimulated the rate of ATP hydrolysis, consistent with it helping RecA assemble on ssDNA, although some inhibition was detected at lower Orf concentrations. It is possible that high levels of Orf promote the formation of RecA monomers, which could potentially bind DNA more rapidly, whereas low levels of Orf may encourage RecA filament formation, which recycles only slowly on ssDNA. This hypothesis is supported by work showing increased BRCA2 produces more Rad51 monomers, while decreased BRCA2 leads to Rad51 filaments (Pellegrini *et al*, 2002). RecA and Rad51, the human homologue of RecA, are both strand-exchange recombinases with topologically identical catalytic domains. Loading of both RecA and Rad51 requires recombination mediator proteins (RMPs), which recognise cognate SSB proteins bound to ssDNA and facilitate recombinase assembly (Pellegrini *et al*, 2002; Beernink & Morrical, 1999). In eukaryotes, several accessory proteins are involved in assembly and stabilisation of the Rad51-ssDNA complex. These include Rad52 (Figure 1.5(B)), which stimulates pre-synaptic filament assembly by Rad51 onto ssDNA bound with RPA, the eukaryotic equivalent of SSB (New *et al*, 1998) and BRCA2, the tumour suppressor protein, which supplies a recombination mediator active in Rad51 filament assembly (Sung *et al*, 2003; Singleton *et al*, 2002). Addition of Orf to reactions involving ssDNA pre-bound with SSB, indicated that Orf alleviates the inhibitory effect of SSB on RecA loading, with higher Orf concentrations having the potential to completely annul the effects of SSB. Hence evidence for Orf recombination mediator activity *in vitro* has been obtained.

Experiments with mutant Orf proteins impaired in DNA binding revealed that DNA binding by Orf was critical for overcoming the inhibitory effect of SSB in RecA loading. Orf mutants, OrfΔC6 and OrfW141F, with only slightly reduced DNA binding ability (G.J. Sharples, unpublished results), exhibited little difference in their ability to promote RecA loading when compared to wild-type Orf. However, both

mutant proteins were unable to alleviate the inhibitory effects of SSB. In contrast, OrfΔC19 and OrfR103E, which are unable to bind DNA (G.J. Sharples, unpublished results), inhibited RecA loading and, in the presence of SSB, served only to enhance the inhibitory effect of SSB. Orf's requirement for ssDNA:dsDNA intersections to overcome SSB inhibition and facilitate RecA loading is analogous to the activities seen with RecFOR and BRCA2, where mediator activity requires sections of duplex DNA adjacent to ssDNA (Yang *et al*, 2005; Morimatisu & Kowalczykowski, 2003).

In addition to the interactions identified between Orf, DNA and SSB, Orf has also been shown to associate with RecA in far-western assays (F.A.Curtis, unpublished results) and in an ELISA. An OrfΔC19 mutant also binds RecA indicating the interaction is independent of the C-terminal helix of Orf (F.A.Curtis, unpublished results). The ability of Orf to bind RecA and evidence that Orf facilitates the assembly of RecA onto gapped DNA suggests the binding of Orf to RecA may be fundamental for its recombination mediator function. Comparisons between Orf and RecA identified a stretch of seven residues (102-108 in Orf and 25-31 in RecA), which show significant similarity (G.J. Sharples, personal communication). The 102-108 region of Orf protrudes from either side of the dimer and the 25-31 region in RecA lies at the interface between adjacent monomers and is instrumental in oligomerisation of the helical nucleoprotein filament (Figure 7.3). It is plausible therefore that Orf may act by mimicking a RecA monomer, with the regions of homology functioning as nucleation sites for polymer assembly. This notion is supported by evidence that a similar situation is apparent in BRCA2-mediated assembly of Rad51, where the interaction has been matched to the conserved sequence repeats, BRC repeats, within the central domain of BRCA2 (residues 900-2100 in human BRCA2), interacting with the oligomerisation domain of Rad51 (Spies & Kowalczykowski, 2006; Pellegrini *et al*, 2002). The conserved motif in Orf and RecA has been identified as a precise structural match to the interface between BRCA2 and Rad51 (Figure 7.3). If the hypothesis that Orf is a hinge protein is correct, the Orf-BRC-like peptide is ideally positioned to direct RecA assembly on only one face of the ring, where ssDNA exits the channel (Figure 7.2).

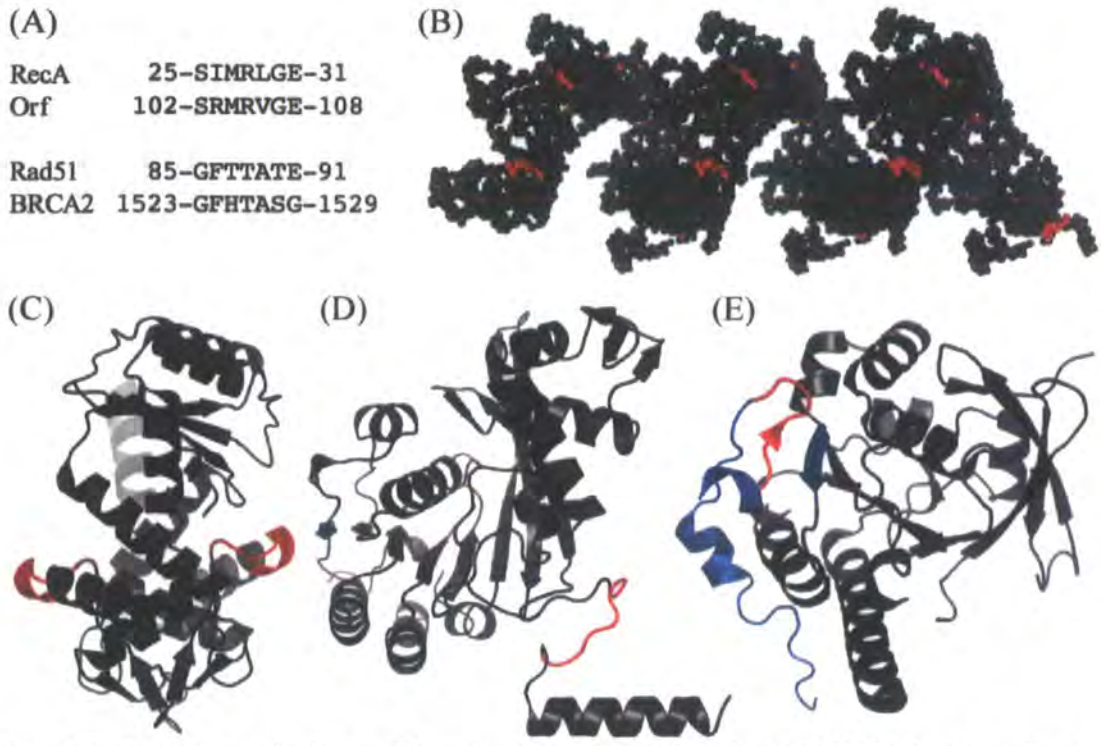

Figure 7.3. BRC/oligomerisation motif location in RecA, Orf, Rad51 and BRCA2 (figure provided by G.J. Sharples). A) Sequence homology of BRC-like peptides. B) Representation of the RecA filament with the BRC-like heptad highlighted (red) at the subunit interface. C) Location of the BRC-like sequence (red) on the crystal structure of Orf. D) Structure of RecA showing the BRC-like motif and the region it recognises in neighbouring subunits (teal). E) The Rad51-BRC4 complex. The BRC4 heptad (red) contacts a region of Rad51 involved in filament polymerisation. Helices in BRC4 (blue) stabilise this interaction.

In addition to regulating Rad51 activity, BRCA2 controls the aggregation state of Rad51. Physiological modification of several of the BRC repeat residues influences complex formation, suggesting a mechanism by which pathways responsible for signalling DNA damage may regulate Rad51-BRCA2 interaction (Pellegrini *et al*, 2002; Davies *et al*, 2001). The nature of the similarities between the Rad51-BRCA2 and RecA-Orf interactions suggests a comparable means of regulating the deployment of different recombinases either from the phage or from the host.

7.3 Role of Orf in λ recombination

This study has shown that Orf can modulate λ Exo nuclease activity in combination with other λ and host recombinases and, when present at sufficient concentration, facilitate RecA loading onto SSB-coated ssDNA at the junction between single and double stranded DNA. The precise role of Orf in genetic recombination remains to be elucidated, however the results do suggest a possible mechanism of action for Orf in the initial stages of λ genetic exchange (Figure 7.4).

Recombination commences with Exo degrading DNA ends, exposing 3' ssDNA overhangs, which are rapidly coated with SSB. The activity of Exo is modulated, possibly by both β and Orf, to prevent the 48 kb λ genome from being completely destroyed by Exo (Poteete, 2008; Matsuura *et al*, 2001). Interactions between Exo and β should allow β protein to load directly onto the exposed ssDNA with formation of a multimeric ring potentially halting Exo progression. Orf may promote loading of β and the two together stimulate strand annealing at the point of Exo stalling. This scenario fits with the observation that phage λ lacking Orf can still recombine *via* the Red pathway, although exchanges occur further from the dsDNA break (Tarkowski *et al*, 2002). The finding that lower concentrations of Orf are inhibitory to RecA loading suggests strand annealing is the dominant pathway for λ recombination with strand invasion occurring only when a threshold level of Orf protein is reached.

The RecA-dependent strand invasion pathway is required when a homologous partner ssDNA is unavailable. It is not yet known whether β participates in this pathway because, although it has been shown to promote strand exchange under certain circumstances, it cannot initiate the duplex strand invasion reactions performed by RecA (Li *et al*, 1998). Additionally, the involvement of β in strand invasion seems unlikely because were β to be loaded onto the ssDNA following Exo degradation, RecA would have to displace β before the presynaptic filament could form. The results obtained here suggest that, if present together, RecA and β compete for Orf, indicating the binding sites for these proteins may overlap and Orf may not be able to facilitate removal of β and loading of RecA simultaneously.

The primary role of Orf in λ recombination is presumed to favour the strand invasion pathway, particularly as it can substitute for the function of the RecFOR proteins (Maxwell *et al*, 2005; Sawitzke & Stahl, 1992, 1997). Orf promotes RecA loading onto SSB-coated ssDNA at ssDNA:dsDNA intersections, potentially by acting as a molecular mimic of RecA as depicted in Figure 7.4. Orf may be required in these reactions rather than RecFOR, because it favours end-mediated exchanges rather than the gaps preferred by RecFOR.

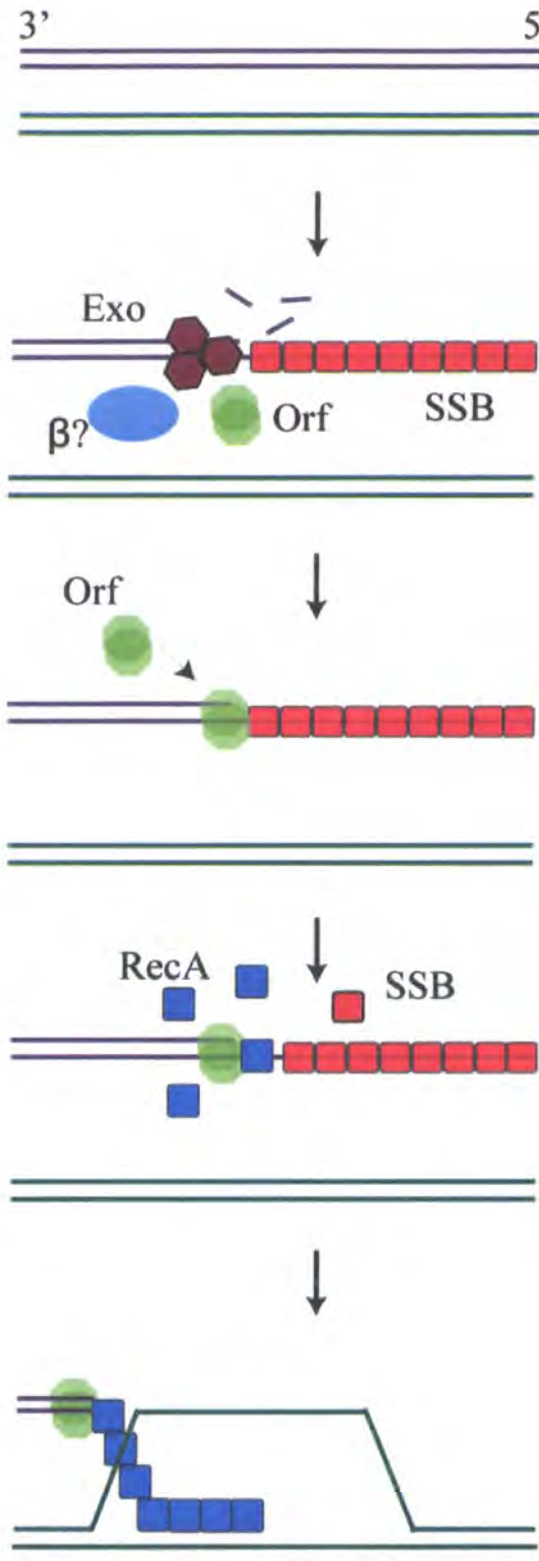

Figure 7.4. Model for the role of Orf in the Red-mediated strand invasion recombination pathway. Exo recognises DNA and degrades dsDNA ends 5'-3' forming 3' ssDNA overhangs which become coated in SSB. The activity of Exo may be regulated by interaction with β and/or Orf to limit extensive degradation and stimulate recombination. Orf recognises and binds the SSB-ssDNA complex at the ssDNA:dsDNA intersection and acts as a molecular mimic of a RecA monomer to facilitate nucleoprotein filament formation, resulting in displacement of SSB. The RecA-coated ssDNA invades an intact homologous duplex and either *E. coli* RuvABC, RecG or λ Rap, a structure-specific endonuclease, resolve the branched intermediates.

7.4 Future Directions

This study investigated the role Orf plays in the initial stages of genetic exchange in phage λ. However, further work is required to confirm the precise mechanism of action and possible options are discussed below.

a) Involvement of Orf in RecA loading and filament formation

The ATPase assays performed as part of this study have the potential to provide further significant insights into the role of Orf in RecA loading. It would also be possible to employ a fluorescence based RecA-DNA assay as a more direct measure of nucleoprotein filament formation (Lee *et al*, 2007). The effect of Orf on RecA-mediated recombination could also be investigated in an *in vitro* strand exchange assay, similar to that utilised by Morimatsu & Kowalczykowski, 2003 and Shan *et al*, 1996. These groups employed a gapped duplex analogous to that used to study RecFOR loading of RecA (Morimatsu & Kowalczykowski, 2003) and Brh2 (a BRCA2 homologue) loading of Rad51 (Brenner *et al*, 1987). It is important to analyse the importance of stoichiometry in the reaction allowing determination of K_{cat} for RecA and Orf in concert with SSB (K_i) and employment of various DNA substrates to further define the requirements for RecA loading. The current assay model provides an opportunity to probe the impact of Orf mutations affecting the motif thought to serve as a nucleation site for RecA. Two mutants, R103E and V106E, located in the BRC-like motif, are already available for testing. Short peptides matching the Orf BRC-like motif can also be assayed for their impact on RecA polymerisation (see below).

Further study on the nature of the Orf-SSB interaction by far-western blotting, affinity chromatography and size exclusion chromatography would be appropriate. Moreover, inclusion of SSB mutant proteins in RecA ATPase assays, in particular the C-terminal mutant, SSBΔC10, would extend our understanding of how Orf loads RecA in the context of SSB-coated ssDNA. Other known recombination/replication mediator proteins tend to utilise the acidic C-terminus of ssDNA binding proteins for targeting.

The interactions between Orf and RecA, observed in ELISA and far-western blotting assays need to be confirmed before further study into the role of the Orf BRC-like

motif is undertaken. Affinity pull-down or immunoprecipitation experiments and yeast two-hybrid analysis would be appropriate. Generating additional site-directed mutants in the proposed RecA-interacting region of Orf would help define residues important in the Orf-RecA interaction. This feature could also be tested using synthetic peptides based on the Orf (SRMRVGE) or RecA (SIMRLGE) BRC-like signatures. Biotin-tagged peptides attached to streptavidin-conjugated agarose beads could be used in pull-down experiments or affinity columns. Competition experiments with non-biotinylated peptides would allow the specificity of interactions to be confirmed. Alternatively, a fluorescent dye attached to the peptides would allow visualisation of RecA or Orf peptide interactions to be monitored by gel filtration chromatography.

RecA filaments in combination with ssDNA, SSB, Orf and Orf mutants could be visualised by transmission electron microscopy (TEM). Assembly and integrity of RecA nucleoprotein filaments when Orf and SSB are present may help uncover how Orf prevails over SSB to facilitate RecA loading.

b) Orf DNA binding

Precisely how Orf binds to DNA has yet to be determined. Current models suggest that Orf may be a hinge protein that opens and then clamps onto the intersection between ssDNA and dsDNA (Reed, 2006). DNA binding by Orf was important in attenuating the nuclease activity of λ Exo. Orf assembly at this site could displace Exo or block its access to the 5' terminus of the resected dsDNA.

The ATPase assays highlighted the requirement for ssDNA:dsDNA junctions for Orf loading of RecA. This specificity could be further investigated by incorporating gapped duplex substrates containing a single-region of duplex with unpaired flaps at either 5' or 3' ends. If Orf fulfils a similar role to that of RecFOR, it should only load RecA at a gapped duplex containing a fully base paired 5' terminus, in keeping with the substrates typically recognised *in vivo*.

Electron microscopy, TEM or scanning electron microscopy (SEM) could potentially be used to visualise Orf-DNA complexes on substrates with 5' or 3' ssDNA overhangs. This may allow discrimination of its preferred DNA substrates. In

addition, 3D single particle reconstruction of negative stained samples, might distinguish between the proposed open (without ssDNA) and closed (with ssDNA) conformations of Orf (Reed, 2006).

The clamp model of Orf binding to ssDNA could be further investigated by analysing the conformational changes in Orf by circular dichroism and site-directed mutagenesis of residues in the regions predicted to be involved in DNA binding (e.g. the C-terminus) or RecA binding (e.g. the N-terminal RAGNYA domain). Cross-linking with bis-maleimidoethane between Cys74 (Figure 7.2) to force the Orf dimer into a permanently locked state and fluorescence resonance energy transfer studies (FRET) to study its conformational states in the presence of various DNA substrates have been proposed in a recent grant application (G.J. Sharples, personal communication). The data obtained from electron microscopy and biochemical analysis should provide valuable information in elaborating the detailed mechanism of action of Orf in genetic recombination.

c) The Orf151 and ETA20 homologues of λ Orf

Results suggest Orf and Orf151 share a functional relationship, however Orf151 may not be fully active relative to the λ protein. Future investigations could focus on determining whether Orf151 retains residual activities furthering RecA ATPase and Exo nuclease assays. Structural studies by X-ray crystallography and visualisation of Orf151 binding to DNA by electron microscopy would be profitable approaches.

Similarly, further work is needed to examine the DNA binding properties and exonuclease activities of ETA20. The protein samples may require further purification to eliminate potential contaminants. The nuclease activity needs to be characterised in detail to define its substrate and cofactor requirements. The quaternary structure of ETA20 is not known and this could be analysed by protein cross-linking and gel filtration. Investigations into the structure and function of ETA20 could be followed by an *in vivo* model system to examine its role in recombination.

7.5 Conclusions

This study has contributed significantly to our understanding of phage λ Orf function in the initial stages of genetic exchange. Two putative Orf orthologues, and various λ and host recombinases were purified and their properties, alone and in combination, examined. A model has been proposed that envisages Orf loading RecA onto SSB-coated ssDNA at ssDNA:dsDNA junctions. The results provide the foundation for future study of phage recombination in the context of the bacterial host cell and elucidating the mechanisms responsible for the genomic rearrangements that lead to the emergence of new pathogens.

References

Amundsen, S.K. Taylor, A.F. Smith, G.R. (2000). The RecD subunit of the *Escherichia coli* RecBCD enzyme inhibits RecA loading, homologous recombination and DNA repair. *Proc. Natl. Acad. Sci.* **97**: 7399-404

Amundsen, S.K. & Smith, G.R. (2003). Interchangable parts of the *Escherichia coli* recombination machinery. *Cell.* **112**: 741-44

Amundsen, S.K. Taylor, A.F. Reddy, M. Smith, G.R. (2007). Intersubunit signalling in RecBCD enzyme, a complex protein machine regulated by Chi hot spots. *Genes & Dev.* **21**: 3296-307

Anand, S.P. Zheng, H. Bianco, P.R. Leuba, S.H. Khan, S.A. (2007). DNA helicase activity of PcrA is not required for the displacement of RecA protein from DNA or inhibition of RecA-mediated strand exchange. *J. Bacteriol.* **189**: 4502-9

Anderson, D.G. Churchill, J.J. Kowalczykowski, S.C. (1997). Chi-activated RecBCD enzyme possesses 5'-3' nucleolytic activity, but RecBC enzyme does not: evidence suggesting that the alteration induced by Chi is not simply ejection of the RecD subunit. *Genes to Cells.* **2**: 117-28

Anderson, D.G. & Kowalczykowski, S.C. (1997a). The recombination hot spot χ is a regulatory element that switches the polarity of DNA degradation by the RecBCD enzyme. *Genes & Dev.* **11**: 571-81

Anderson, D.G. & Kowalczykowski, S.C. (1997b). The translocating RecBCD enzyme stimulates recombination by directing RecA protein onto ssDNA in a χ-regulated manner. *Cell.* **90**: 77-86

Anderson, D.G. Churchill, J. J. Kowalczykowski, S.C. (1999). A single mutation, $RecB_{D1080A}$, eliminates RecA protein loading but not Chi recognition by RecBCD enzyme. *J. Biol. Chem.* **274**: 27139-44

Arnold, D.A. & Kowalczykowski, S.C. (2000). Facilitated loading of RecA protein is essential to recombination by RecBCD enzyme. *J. Biol. Chem.* **275**: 12261-5

Bachman, B.J. (1996). Derivations and genotypes of some mutant derivatives of *Escherichia coli* K-12, p2460-2488. *In* F.C. Neidhardt, R. Curtiss III, J.L. Ingraham, E.C.C. Lin, K.B. Low, B. Magasanik, W.S. Reznikoff, M. Riley, M. Schaechter, and H.E. Umbarger (ed.), *Escherichia coli* and *Salmonella*: cellular and molecular biology, 2nd ed. ASM Press, Washington D.C.

Baitin, D.M. Gruenig, M.C. Cox, M.M. (2008). SSB antagonizes RecX-RecA interaction. *J. Biol. Chem.* **283**: 14198-204

Balaji, S. & Aravind, L. (2007). The RAGNYA fold: a novel fold with multile topological variants found in functionally diverse nucleic acid, nucleotide and peptide-binding proteins. *Nucleic Acids Research.* **35**: 5658-71

Bazemore, L.R. Folta-Stogniew, E. Takahashi, M. Radding, C.M. (1997). RecA tests homology at both pairing and strand exchange. *Proc. Natl. Acad. Sci.* **94**: 11863-8

Beernink, H.T.H. & Morrical. S.W. (1999). RMPs: recombination / replication mediator proteins. *TIBS.* **24**: 385-9

Bianco, P.R. & Kowalczykowski, S.C. (1997). The recombination hotspot Chi is recognized by the translocating RecBCD enzyme as the single strand of DNA containing the sequence 5'-GCTGGTGG-3'. *Proc. Natl. Acad. Sci.* **94**: 6706-11

Bianco. P.R. Brewer, L.R. Corzett, M. Balhorn, R. Yeh, Y. Kowalczykowski, S.C. Baskin, R.J. (2001). Processive translocation and DNA unwinding by individual RecBCD enzyme molecules. *Nature.* **409**: 374-8

Bidnenko, V. Seigneur, M. Penel-Colin, M. Bouton, M-F. Ehrlich, S.D. Michel, B. (1999). *sbcB sbcC* null mutations allow RecF-mediated repair of arrested replication forks in *rep recBC* mutants. *Mol. Micro.* **33**: 846-57

Biet, E. Sun, J-S. Dutreix, M. (1999). Conserved sequence preference in DNA binding among recombination proteins: an effect of ssDNA secondary structure. *Nucleic Acids Research.* **27**: 596-600

Bork, J.M. Cox, M.M. Inman, R.B. (2001). RecOR proteins modulate RecA protein function at 5' ends of single-stranded DNA. *EMBO J.* **20**: 7313-22

Brenner, S.L. Mitchell, R.S. Morrical, S.W. Neuendorf, S.K. Schutte, B.C. Cox, M.M. (1987). recA Protein-promoted ATP hydrolysis occurs throughout recA nucleoprotein filaments. *J. Biol. Chem.* **262**: 4011-6

Breusegem, S.Y. Clegg, R.M. Lootiens, F.G. (2002). Base-sequence specificity of Hoechst 33258 and DAPI binding to five (A/T_4) DNA sites with kinetic evidence for more than one high-affinity Hoechst 33258-AATT complex. *J. Mol. Biol.* **315**: 1049-61

Brussow, H. Canchaya, C. Hardt, W-D. (2004). Phages and the evolution of bacterial pathogens: from genomic rearrangements to lysogenic conversion. *Microbiol. Mol. Biol. Rev.* **68**: 560-602

Cadman, C.J. & McGlynn, P. (2004). PriA helicase and SSB interact physically and functionally. *Nucleic Acids Research.* **32**: 6378-87

Carter, D.M. & Radding, C.M. (1971). The role of exonuclease and β protein of phage λ in genetic recombination. II. Substrate specificity and the mode of action of λ exonuclease. *J. Biol. Chem.* **246**: 2502-12

Cassuto, E. & Radding, C.M. (1971). Mechanism for the action of λ exonuclease in genetic recombination. *Nature New Biology.* **229**: 13-16

Cassuto, E. Lash, T. Sriprakash, K.S. Radding, C.M. (1971). The role of exonuclease and β protein of phage lambda in genetic recombination V. Recombination *in vitro*. *Proc. Natl. Acad. Sci.* **68**: 1639-43

Chang, H.W. & Julin, D.A. (2001). Structure and function of the *Escherichia coli* RecE protein, a member of the RecB nuclease domain family. *J. Biol. Chem.* **276**: 46004-10

Cheetham, B.F. & Katz, M.E. (1995). A role for bacteriophages in the evolution and transfer of bacterial virulence determinants. *Mol. Micro.* **18**: 201-8

Chen, Z. Yang, H. Pavletich, N.P. (2008). Mechanism of homologous recombination from the RecA-ssDNA/dsDNA structures. *Nature*. **453**: 489-96

Cheng, Q. Wang, Z-X. Killilea, S.D. (1995). A continuous spectrophotometric assay for protein phosphatases. *Analytical Biochem.* **226**: 68-73

Churchill, J.J. & Kowalczykowski, S.C. (2000). Identification of the RecA protein-loading domain of RecBCD enzyme. *J. Mol. Biol.* **297**: 537-42

Clark, A.J. & Margulies, A.D. (1965). Isolation and characterisation of recombination-deficient mutants of *Escherichia coli* K12. *Genetics*. **53**: 451-9

Clark, A.J. (1971). Toward a metabolic interpretation of genetic recombination of *E. coli* and its phages. *Annu. Rev. Microbiol.* **25**: 437-64

Clark, A.J. (1973). Recombination deficient mutants of *E. coli* and other bacteria. *Annu. Rev. Genet.* **7**: 67-86

Court, D.L. Sawitzke, J.A. Thomason, L.C. (2002). Genetic engineering using homologous recombination. *Annu. Rev. Genet.* **36**: 361-88

Court, D.L. Oppenheim, A.B. Adhya, S.L. (2007). A new look at bacteriophage λ genetic networks. *J. Biol.* **189**: 298-304

Court, R. Cook, N. Saikrishnan, K. Wigley, D. (2007). The crystal structure of λ-Gam protein suggests a model for RecBCD inhibition. *J. Mol. Biol.* **371**: 25-33

Cox, J.M. Tsodikov, O.V. Cox, M.M. (2005). Organised unidirectional waves of ATP hydrolysis within a RecA filament. *PLoS Biology*. **3**: 231-43

Cox, M.M. McEntree, K. Lehman, I.R. (1981). A simple and rapid procedure for the large scale purification of the recA protein of *Escherichia coli*. *J. Biol. Chem.* **256**: 4676-8

Cox, M.M. (1998). A broadening view of recombinational DNA repair in bacteria. *Genes Cells*. **3**: 65-78

Cox, M.M. Goodman, M.F. Kreuzer, K. N. Sherratt, D.J. Sandler, S.J. Marians, K.J. (2000). The importance of repairing stalled replication forks. *Nature*. **404**: 37-41

Cox, M.M. (2007). Regulation of bacterial RecA protein function. *Crit. Rev. Biochem. & Mol. Biol.* **42**: 41-63

Cromie, G.A. Connelly, J.C. Leach, D.R.F. (2001). Recombination at double-strand breaks and DNA ends: conserved mechanisms from phage to humans. *Mol. Cell.* **8**: 1163-74

DasGupta, C. & Radding, C.M. (1982). Polar branch migration promoted by RecA protein: effect of mismatched base pairs. *Proc. Natl. Acad. Sci.* **79**: 762-6

Davies, A.A. Masson, J-Y. McIlwraith, M.J. Stasiak, A.Z. Stasiak, A. Venkitaraman, A.R. West, S.C. (2001). Role of BRCA2 in control of the Rad51 recombination and DNA repair protein. *Mol. Cell.* **7**: 271-82

Davison, J. (1999). Genetic exchange between bacteria in the environment. *Plasmid.* **42**: 73-91

Dillingham, M.S. Spies, M. Kowalczykowski, S.C. (2003). RecBCD enzyme is a bipolar DNA helicase. *Nature.* **423**: 893-7

Dixon, D.A. & Kowalczykowski, S.C. (1993). The recombination hotspot χ is a regulatory sequence that acts by attenuating the nuclease activity of the *E. coli* RecBCD enzyme. *Cell.* **73**: 87-96

Dixon, D.A. & Kowalczykowski, S.C. (1995). Role of *Escherichia coli* recombination hotspot, χ, in RecABCD-dependent homologous pairing. *J. Biol. Chem.* **270**: 16360-70

Drees, J.C. Lusetti, S.L. Chitteni-Pattu, S. Inman, R.B. Cox, M.M. (2004)a. A RecA filament capping mechanism for RecX protein. *Mol. Cell.* **15**: 789-98

Drees, J.C. Lusetti, S.L. Cox, M.M. (2004)b. Inhibition of RecA protein by the *Escherichia coli* RecX Protein. *J. Biol. Chem.* **279**: 52991-7

Drees, J.C. Chitteni-Pattu, S. McCaslin, D.R. Inman, R.B. Cox, M.M. (2006). Inhibition of RecA protein function by the RdgC protein from *Escherichia coli*. *J. Biol. Chem.* **281**: 4708-17

Dutreix, M. (1997). (GT_n) repetitive tracts affect several stages of RecA-promoted recombination. *J. Mol. Biol.* **273**: 105-13

Echolas, H. & Gingery, R. (1968). Mutants of bacteriophage lambda defective in vegetative genetic recombination. *J. Mol. Biol.* **34**: 239-49

Echols, H. & Murialdo, H. (1978). Genetic map of bacteriophage lambda. *Microbiol. Rev.* **42**: 577-91

Eggler, A.L. Lusetti, S.L. Cox, M.M. (2003). The C terminus of the *Escherichia coli* RecA protein modulates the DNA binding competition with single-stranded DNA-binding protein. *J. Biol. Chem.* **278**: 16389-96

Franklin, N.C. (1967). Extraordinary recombinational events in *Escherichia coli*. Their independence of the *rec*$^{+}$ function. *Genetics.* **55**: 699-707

Friedman, D.I. & Court, D.L. (2001). Bacteriophage lambda: alive and well and still doing its thing. *Curr. Opin. Microbiol.* **4**: 201-7

Giese, K.C. Michalowski, C.B. Little, J.W. (2008). RecA-dependent cleavage of LexA dimers. *J. Mol. Biol.* **377**: 148-51

Griffin, T.J. & Kolodner, R.D. (1990). Purification and preliminary characterisation of the *Escherichia coli* K12 RecF protein. *J. Bacteriol.* **172**: 6291-9

Gupta, R.C. Golub, E.I. Wold, M.S. Radding, C.M. (1998). Polarity of DNA strand exchange promoted by recombination proteins of the RecA family. *Proc. Natl. Acad. Sci.* **95**: 9843-8

Hambly, E. & Suttle, C.A. (2005). The viriosphere, diversity and genetic exchange within phage communities. *Curr. Opin. Microbiol.* **8**: 444-50

Hanahan, D. (1983). Studies on transformation of *Escherichia coli* with plasmids. *J. Mol. Biol.* **166**: 557-80

Handa, N. Bianco, P.R. Baskin, Kowalczykowski, S.C. (2005). Direct visualisation of RecBCD movement reveals cotranslocation of the RecD motor after χ recognition. *Mol. Cell.* **17**: 745-50

Handa, N. & Kowalczykowski, S.C. (2006). A RecA mutant, RecA^{730}, suppresses the recombination deficiency of the RecBC^{1004}D-χ^{*} interaction *in vitro* and *in vivo*. *J. Mol. Biol.* **365**: 1314-25

Harmon, F.G. & Kowalczykowski, S.C. (1998). RecQ helicase, in concert with RecA and SSB proteins, initiates and disrupts DNA recombination. *Genes & Dev.* **12**: 1134-44

Hatch, K. Danilowicz, C. Coljee, V. Prentiss, M. (2008). Measurement of the salt-dependent stabilisation of partially open DNA by *Escherichia coli* SSB protein. *Nucleic Acids Research.* **36**: 294-9

Hedge, S.P. Rajagopalan, M. Madiraju, M.V.V.S. (1996a). Preferential binding of *Escherichia coli* RecF protein to gapped DNA in the presence of Adenosine (γ-Thio) Triphosphate. *J. Bacteriol.* **178**: 184-90

Hedge, S.P. Qin, M-H. Li, X-H. Atkinson, M.A.L. Clark, A.J. Rajagopalan, M. Madiraju, M.V.V.S. (1996b). Interactions of RecF protein with RecO, RecR and single-stranded DNA binding protein reveal roles for the RecF-RecO-RecR complex in DNA repair and recombination. *Proc. Natl. Acad. Sci.* **93**: 14468-73

Hendrix, R.W. Smith, M.C.M. Burns, R.N. Ford, M.E. Hatfull, G.F. (1999). Evolutionary relationships among diverse bacteriophages and prophages: All the world's a phage. *Proc. Natl. Acad. Sci.* **96**: 2192-7

Hendrix, R.W. (2002). Bacteriophages: evolution of the majority. *Theor. Popul. Biol.* **61**: 471-80

Hill, S.A. Stahl, M.M. Stahl, F.W. (1997). Single-strand DNA intermediates in phage lambda's Red recombination pathway. *Proc. Natl. Acad. Sci.* **94**: 2951-6

Holliday, R. (1964). A mechanism for gene conversion in fungi. *Genet. Res.* **5**: 282-304

Hollifield, W.C. Kaplan, E.N. Huang, H.V. (1987). Efficient RecABC-dependent, homologous recombination between coliphage lambda and plasmids requires a phage *ninR* region gene. *Mol. Gen. Genet.* **210**: 248-55

Honda, M. Inoue, J. Yoshimasu, M. Ito, Y. Shibata, T. Mikawa, T. (2006). Identification of the RecR Toprim Domain as the Binding Site for both RecF and RecO. *J. Biol. Chem.* **281**: 18549-59

Horii, Z-I. & Clark, A.J. (1973). Genetic analysis of the RecF pathway to genetic recombination in *Escherichia coli* K12: Isolation and characterisation of mutants. *J. Mol. Biol.* **80**: 327-44

Inoue, J. Honda, M. Ikawa, S. Shibata, T. Mikawa, T. (2008). The process of displacing the single-stranded-DNA-binding protein from single-stranded DNA by RecO and RecR proteins. *Nucleic Acids Res.* **36**: 94-109

Iyer, L. Koonin, E.V. Aravind, L. (2002). Classification and evolutionary history of the single-strand annealing proteins, RecT, Redβ, ERF and RAD52. *BMC Genomics.* **3**: 8-19

Iype, L.E. Wood, E.A. Inman, R.B. Cox, M.M. (1994). RuvA and RuvB proteins facilitate the bypass of heterologous DNA insertions during RecA protein-mediated DNA strand exchange. *J. Biol. Chem.* **269**: 24967-78

Joo, C. McKinney, S.A. Nakamura, M. Rasnik, I. Myong, S. Ha, T. (2006). Real-time observation of RecA filament dynamics with single monomer resolution. *Cell.* **126**: 515-27

Juhala, R.J. Ford, M.E. Duda, R.L. Youlton, A. Hatfull, G.F. Hendrix, R.W. (2000). Genomic sequences of bacteriophages HK97 and HK022: Pervasive genetic mosaicism in the Lambdoid bacteriophages. *J. Mol. Biol.* **299**: 27-51

Kantake, N. Madiraju, M.V.V.M. Sugiyama, T. Kowalczykowski, S.C. (2002). *Escherichia coli* RecO protein anneals ssDNA complexed with its cognate ssDNA-binding protein: A common step in genetic recombination. *Proc. Natl. Acad. Sci.* **99**: 15327-32

Karakousis, G. Ye, N. Li, Z. Chiu, S.K. Reddy, G. Radding, C.M. (1998). The β protein of phage λ binds preferentially to an intermediate in DNA renaturation. *J. Mol. Biol.* **276**: 721-31

Karu, A.E. Sakaki, Y. Echols, H. Linn, S. (1975). The γ protein specified by bacteriophage λ. *J. Biol. Chem.* **250**: 7377-87

Kmiec, E. & Holloman, W.K. (1981). β protein of bacteriophage λ promotes renaturation of DNA. *J. Biol. Chem.* **256**: 12636-9

Kolodner, R. Fishel, R.A. Howard, M. (1985). Genetic recombination of bacterial plasmid DNA: effect of RecF pathway mutations on plasmid recombination in *E. coli*. *J. Bacteriol.* **163**: 1060-6

Koonin, E.V. Makarova, K.S. Aravind, L. (2001). Horizontal gene transfer in prokaryotes: Quantification and Classification. *Annu. Rev. Microbiol.* **55**: 709-42

Korangy, F. & Julin, D.A. (1994). Efficiency of ATP hydrolysis and DNA unwinding by the RecBC enzyme from *Escherichia coli*. *Biochemistry*. **33**: 9552-60

Koroleva, O. Makharashvili, N. Courcelle, C.T. Courcelle, J. Korolev, S. (2007). Structural conservation of RecF and Rad50: implications for DNA recognition and RecF function. *EMBO J.* **26**: 867-77

Kovall, R. & Matthews, B.W. (1997). Toroidal structure of λ-exonuclease. *Science*. **277**: 1824-7

Kovall, R. & Matthews, B.W. (1998). Structural, functional, and evolutionary relationships between λ-exonuclease and the type II restriction endonucleases. *Proc. Natl. Acad. Sci.* **95**: 7893-7

Kowalczykowski, S.C. & Krupp, R.A. (1987). Effects of Escherichia coli SSB protein on the single-stranded DNA-dependent ATPase activity of *Escherichia coli* RecA protein. *J. Mol. Biol.* **193**: 97-113

Kowalczykowski, S.C. Dixon, D.A. Eggleston, A.K. Lauder, S.D. Rehrauer, W.M. (1994). Biochemistry of Homologous Recombination in *Escherichia coli*. *Microbiol. Rev.* **58**: 401-65

Kowalczykowski, S.C. (2000). Initiation of genetic recombination and recombination-dependent replication. *TIBS*. **25**: 156-65

Kreuzer, K.N. (2005). Interplay between DNA replication and recombination in prokaryotes. *Annu. Rev. Microbiol.* **59**: 43-67

Kroger, M. & Hobom, G. (1982). A chain of interlinked genes in the *ninR* region of bacteriophage lambda. *Gene*. **20**: 25-38

Kubota, Y. Kubota, K. Tani, S. (2000). DNA binding properties of DAPI (4'6'-diamindino-2-phenylindole) analogs having an imadazoline ring or a terahydropyrimidine ring: Groove binding and intercalation. *Nucleic Acids Symposium Series*. **44**: 53-4

Kulkarni, S.K. & Stahl, F.W. (1989). Interaction between the *sbc*C gene of *Escherichia coli* and the *gam* gene of phage λ. *Genetics*. **123**: 249-53

Kushner, S.R. Nagaishi, H. Templin, A. Clark, A.J. (1971). Genetic recombination in *Escherichia coli*: The role of exonuclease I. *Proc. Natl. Acad. Sci.* **68**: 824-7

Kuzminov, A. Schabtach, E. Stahl, F.W. (1994). χ sites in combination with RecA protein increase the survival of linear DNA in *Escherichia coli* by inactivating exoV activity of RecBCD nuclease. *EMBO J.* **13**: 2764-76

Kuzminov, A. (1999). Recombinational Repair of DNA Damage in *Escherichia coli* and Bacteriophage λ. *Microbiology and Molecular Biology Reviews*. **63**: 751-813

Lam, S.T. Stahl, M. McMilin, K.D. Stahl, F.W. (1974). Rec-mediated recombinational hot spot activity in bacteriophage lambda. II. A mutation which causes hot spot activity. *Genetics*. **77**: 425-33

Lavery, P.E. & Kowalczykowski, S.C. (1992). Biochemical basis of the constitutive repressor cleavage activity of recA730 protein. A comparison to recA441 and rec803 proteins. *J. Biol. Chem.* **267**: 20648-58

Lederberg, E. (1951). Lysogenicity in *E. coli* K12. *Genetics*. **36**: 560-69

Lee, A.M. Wigle, T.J. Singleton, S.F. (2007). A complementary pair of rapid molecular screening assays for RecA activities. *Analytical Biochem.* **367**: 247-58

Lee, B.I. Kim, K.H. Park, S.J. Eom, S.H. Song, H.K. Suh, S,W. (2004). Ring-shaped architecture of RecR: implications for its role in homologous recombinational DNA repair. *EMBO J.* **23**: 2029-38

Leiros, I. Timmins, J. Hall, D.R. McSweeney, S. (2005). Crystal structure and DNA-binding analysis of RecO from *Deinococcus radiodurans*. *EMBO J.* **24**: 906-18

Li, Z. Karakousis, G. Chiu, S.K. Reddy, G. Radding, C.M. (1998). The beta protein of phage λ promotes strand exchange. *J. Mol. Biol.* **276**: 733-44

Little, J.W. (1967). An exonuclease induced by bacteriophage λ: II. Nature of the enzymatic reaction. *J. Biol. Chem.* **242**: 679-86

Little, J.W. (1984). Autodigestion of LexA and phage Lambda repressors. *Proc. Natl. Acad. Sci.* **81**: 1375-9

Little, J.W. (1991). Mechanism of specific LexA cleavage: autodigestion and the role of RecA coprotease. *Biochimie*. **73**: 411-22

Liu, J. Bond, J.P. Morrical, S.W. (2006). Mechanism of presynaptic filament stabilisation by the bacteriophage T4 UvsY recombination mediator protein. *Biochemistry.* **45**: 5493-502

Lloyd, R.G. & Buckman, C. (1985). Identification and genetic analysis of *sbcC* mutations in commonly used *recBC sbcB* strains of *Escherichia coli* K-12. *J. Bacteriol.* **164**: 836-44

Lovett, S.T. & Kolodner, R.D. (1989). Identification and purification of a single-stranded-DNA-specific exonuclease encoded by the *recJ* gene of *Escherichia coli*. *Proc. Natl. Acad. Sci.* **86**: 2627-31

Luisi-DeLuca, C. & Kolodner, R.D. (1994). Purification and Characterisation of the *Escherichia coli* RecO protein. *J. Mol. Biol.* **236**: 124-38

Luisi-DeLuca, C. (1995). Homologous pairing of single-stranded DNA and superhelical double-stranded DNA catalysed by RecO protein from *Escherichia coli*. **177**: 566-72

Lusetti, S.L. Hobbs, M.D. Stohl, E. A. Chitteni-Pattu, S. Inman, R.B. Seifert, H.S. Cox, M.M. (2006). The RecF Protein Antagonizes RecX Function via Direct Interaction. *Mol. Cell.* **21**: 41-50

Madiraju, M.V. V.S. & Clark, A.J. (1991). Effect of RecF protein on reactions catalysed by RecA protein. *Nucleic Acids Research.* **19**: 6295-300

Madiraju, M.V.V.S. & Clark, A.J. (1992). Evidence for ATP binding and double-stranded DNA binding by *Escherichia coli* RecF protein. *J. Bacteriol.* **174**: 7705-10

Mahdi, A.A. & Lloyd, R.G. (1989). The *rec*R locus of *Escherichia coli* K12: molecular cloning, DNA sequencing and identification of the gene product. *Nucleic Acids Res.* **17**: 6781-94

Maiden, M. (1998). Horizontal genetic exchange, evolution and spread of antibiotic resistance in bacteria. *Clin. Infect. Dis.* **27**: S12-20

Makharashvili, N. Koroleva, O. Bera, S. Grandgenett, D.P. Korolev, S. (2004). A novel structure of DNA repair protein RecO from *Deinococcus radiodurans*. *Structure.* **12**: 1881-9

Martin, B. Pallen, C.J. Wang, J. H. Graves, D.J. (1985). Use of fluorinated tyrosine phosphates to probe the substrate specificity of the low molecular weight phosphatase activity of calcineurin. *J. Biol. Chem.* **260**: 14932-7

Matsuura, S-I. Komatsu, J. Hirano, K. Yasuda, H. Takashima, K. Katsura, S. Mizuno, A. (2001). Real-time observation of a single DNA digestion by λ exonuclease under a fluorescence microscope field. *Nucleic Acids Research.* **29**: No.16 e79

Maxwell, K.L. Reed, P. Zhang, R-G. Beasley, S. Walmsley, A.R. Curtis, F.A. Joachimiak, A. Edwards, A.M. Sharples, G.J. (2005). Functional similarities between phage λ Orf and *Escherichia coli* RecFOR in initiation of genetic exchange. *Proc. Natl. Acad. Sci.* **102**: 11260-5

Mazin, A.V. & Kowalczykowski, S.C. (1999). A novel property of the RecA nucleoprotein filament: activation of double-stranded DNA for strand exchange in trans. *Genes & Dev.* **13**: 2005-16

McMilin, K.D. Stahl, M. Stahl, F.W. (1974). Rec mediated recombinational hot spot activity in bacteriophage lambda. I. Hot spot activity associated with Spi deletions and *bio* substitutions. *Genetics.* **77**: 409-23

Meselson, M.S. & Radding, C.M. (1975). A General Model for Genetic Recombination. *Proc. Natl. Acad. Sci.* **72**: 358-61

Mehta, P. Katta, K. Krishnaswamy, S. (2004). HNH damily subclassification leads to identification of commonality in the His-Me endonuclease superfamily. *Protein Sci.* **13**: 295-300

Miao, E.A. & Miller, S.I. (1999). Bacteriophages in the evolution of pathogen-host interactions. *Proc. Natl. Acad. Sci.* **96**: 9452-4

Mitsis, P.G. & Kwagh, J.G. (1999). Characterization of the interaction of lambda exonuclease with the ends of DNA. *Nucleic Acids Research.* **27**: 3057-63

Morimatsu, K. & Kowalczykowski, S.C. (2003). RecFOR proteins load RecA protein onto gapped DNA to accelerate DNA strand exchange: A universal step of recombinational repair. *Mol. Cell.* **11**: 1337-47

Muniyappa, K. Shaner, S.L. Tsang, S.S. Radding, C.M. (1984). Mechanism of the concerted action of recA protein and helix-destabilising proteins in homologous recombination. *Proc. Natl. Acad. Sci.* **81**: 2757-61

Muniyappa, K. & Radding, C.M. (1986). The homologous recombination system of phage λ. *J. Biol. Chem.* **261**: 7472-8

Murphy, K.C. (1991). λ Gam protein inhibits the helicase and χ-stimulated recombination activities of *Escherichia coli* RecBCD enzyme. *J. Bacteriol.* **173**: 5808-21

Murphy, K.C. (1998). Use of bacteriophage λ recombination functions to promote gene replacement in *Escherichia coli*. *J. Bacteriol.* **180**: 2063-71

Murphy, K.C. (2007). The λ Gam protein inhibits RecBCD binding to dsDNA ends. *J. Mol. Biol.* **371**: 19-24

Murray, N. E. & Gann, A. (2007). What has phage lambda ever done for us? *Curr. Biol.* **17**: 989-93

Muyrers, J.P.P. Zhang, Y. Buchholz, F. Stewart, A.F. (2000). RecE/RecT and Redα/β initiate double-stranded break repair by specifically interacting with their respective partners. *Genes & Dev.* **14**: 1971-82

Myers, R. Kuzminov, A. Stahl, F. (1995). The recombination hot spot χ activates RecBCD recombination by converting *Escherichia coli* to a *recD* mutant phenocopy. *Proc. Natl. Acad. Sci.* **92**: 6244-8

Mythili, E. Kumar, A. Muniyappa, K. (1996). Characterisation of the DNA-binding domain of β protein, a component of phage λ Red-pathway, by UV catalysed cross-linking. *Gene.* **182**: 81-7

New, J.H. Sugiyama, T. Zaitseva, E. Kowalczykowski, S.C. (1998). Rad52 protein stimulates DNA strand exchange by Rad51 and replication protein A. *Nature.* **391**: 407-10

New England Biolabs (www.neb.com) (2005). pMALc2 product information.

Passy, S.I. Yu, X. Li, Z. Radding, C.M. Egelman, E.H. (1999). Rings and filaments of β protein from bacteriophage λ suggest a superfamily of recombination proteins. *Proc. Natl. Acad. Sci.* **96**: 4279-84

Pellegrini, L. Yu, D.S. Lo, T. Anand, S. Lee, M. Blundell, T.L. Venkitaraman, A.R. (2002). Insights into DNA recombination from the structure of a Rad51-BRCA2 complex. *Nature.* **420**: 287-93

Perkins, T.T. Dalal, R.V. Mitsis, P.G. Block, S.M. (2003). Sequence-dependent pausing of single lambda exonuclease molecules. *Science.* **301**: 1914-8

Poteete, A.R. & Fenton, A.C. (1993). Efficient double-strand break stimulated recombination promoted by the general recombination systems of phages λ and P22. *Genetics.* **134**: 1013-21

Poteete, A.R. (2001). What makes the bacteriophage λ Red system useful for genetic engineering: molecular mechanism and biological function. *FEMS Microbiology Letters.* **201**: 9-14

Poteete, A.R. (2004). Modulation of DNA Repair and Recombination by the Bacteriophage λ Orf Function in *Escherichia coli* K-12. *J. Bacteriol.* **186**: 2699-707

Poteete, A.R. (2008). Involvement of DNA replication in phage lambda Red-mediated homologous recombination. *Mol. Micro.* **68**: 66-74

Pratt, T.S. Steiner, T. Feldman, L.S. Walker, K.A. Osuna, R. (1997). Deletion Analysis of the *fis* Promoter Region in *Escherichia coli*: Antagonistic Effects of Integration Host Factor and Fis. *J. Bacteriol.* **179**: 6367-77

Radding, C.M. Szpirer, J. Thomas, R. (1966). The structural gene for λ exonuclease. *Proc. Natl. Acad. Sci.* **57**: 277-83

Rajan, R. Wisler, J.W. Bell, C.E. (2006). Probing the DNA sequence specificity of *Escherichia coli* RecA protein. *Nucleic Acids Research.* **34**: 2463-71

Rangarajan, S. Woodgate, R. Goodman, M.F. (2002). Replication restart in UV-irradiated *Escherichia coli* involving pols II, III, V, PriA, RecA and RecFOR proteins. *Mol. Micro.* **43**: 617-28

Reed, P. (2006). Function of bacteriophage Orf recombinases in genetic exchange. PhD thesis. University of Durham.

Renzette, N. Gumlaw, N. Sandler, S.J. (2006). DinI and RecX modulate RecA-DNA structures in *Escherichia coli* K-12. *Mol. Micro.* **63**: 103-15

Renzette, N. & Sandler, S.J. (2008). Requirements for ATP binding and hydrolysis in RecA function in *Escherichia coli. Mol. Micro.* **6716**: 1347-59

Roman, L.J. Eggleston, A.K. Kowalczykowski, S.C. (1992). Processivity of the DNA helicase activity of *Escherichia coli* RecBCD enzyme. *J. Biol. Chem.* **267**: 4207-14

Rybalchenko, N. Golub, E.I. Bi, B. Radding, C.M. (2004). Strand invasion promoted by recombination protein β of coliphage λ. *Proc. Natl. Acad. Sci.* **101**: 17056-60

Safo, M.K. Yang,W.Z. Corselli, L. Cramton, S.E. Yuan, H.S. Johnson, R.C. (1997). The transactivation region of the Fis protein that controls site-specific DNA inversion contains extended mobile β-hairpin arms. *EMBO J.* **16**: 6860-73

Sambrook, J. & Russell, D.W. (2001). Molecular Cloning. A Laboratory Manual. Cold Spring Harbor Laboratory, New York, 2nd Ed.

Sandler, S.J. Chackerian, B. Li, J.T. Clark, A.J. (1992). Sequence and complementation analysis of *recF* genes from *Escherichia coli*, *Salmonella typhimurium*, *Pseudomonas putida* and *Bacillus subtilis*: evidence for an essential phosphate binding loop. *Nucleic Acids Research.* **20**: 839-45

Sandler, S.J. (1996). Overlapping functions for *recF* and *priA* in cell viability and UV-inducible SOS expression are distinguished by *dnaC809* in *Escherichia coli* K12. *Mol. Micro.* **19**: 871-80

Sawitzke, J.A. & Stahl, F.W. (1992). Phage λ Has an Analog of *Escherichia coli* *rec*O, *rec*R and *rec*F Genes. *Genetics.* **130**: 7-16

Sawitzke, J.A. & Stahl, F.W. (1994). The Phage λ *orf* Gene Encodes a *trans*-Acting Factor That Suppresses *Escherichia coli* *rec*O, *rec*R and *rec*F Mutations for Recombination of λ but Not of *E.coli. J. Bacteriol.* **176**: 6730-7

Sawitzke, J.A. & Stahl, F.W. (1997). Roles for λ Orf and *Escherichia coli* RecO, RecR and RecF in λ recombination. *Genetics.* **147**: 357-69

Serra-Moreno, R. Acosta, S. Hernalsteens, J.P. Jofre, J. Muniesa, M. (2006). Use of lambda Red recombinase system to produce recombinant prophages carrying antibiotic resistance genes. *BMC Mol. Biol.* **7**: 31-43

Shan, Q. Cox, M.M. Inman, R.B. (1996). DNA strand exchange promoted by RecA K72R. *J. Biol. Chem.* **271**: 5712-24

Shan, Q. Bork, J.M. Webb, B.L. Inman, R.B. Cox, M.M. (1997). RecA protein filaments: end-dependent dissociation from ssDNA and stabilisation by RecO and RecR proteins. *J. Mol. Biol.* **265**: 519-40

Sharples, G.J. Corbett, L.M. Graham, I.R. (1998). λ Rap protein is a structure-specific endonuclease involved in phage recombination. *Proc. Natl. Acad. Sci.* **95**: 13507-12

Sheridan, S.D. Yu, X. Roth, R. Heuser, J.E. Sehorn, M.G. Sung, P. Egelman, E.H. Bishop, D.K. (2008). A comparative analysis of Dmc1 and Rad51 nucleoprotein filaments. *Nucleic Acids. Research.* **36**: 4057-66

Sherratt, D.J. (2003). Bacterial chromosome dynamics. *Science*. **301**: 780-5

Shibata, T. Cunningham, R.P. DasGupta, C. Radding, C.M. (1979a). Homologous pairing in genetic recombination: complexes of RecA protein and DNA. *Proc. Natl. Acad. Sci.* **76**: 5100-4

Shibata, T. DasGupta, C. Cunningham, R.P. Radding, C.M. (1979b). Purified *Escherichia coli* RecA protein catalyses homologous pairing of superhelical DNA and single-stranded fragments. *Proc. Natl. Acad. Sci.* **76**: 1638-42

Shibata, T. DasGupta, C. Cunningham, R.P. Radding, C.M. (1980). Homologous pairing in genetic recombination: formation of D-loops by combined action of RecA protein and a helix-destabilising protein. *Proc. Natl. Acad. Sci.* **77**: 2606-10

Shivashankar, G.V. Feingold, M. Krichevsky, O. Libchaber, A. (1999). RecA polymerisation on double-stranded DNA by using single-molecule manipulation: The role of ATP hydrolysis. *Proc. Natl. Acad. Sci.* **96**: 7916-21

Sigal, N. Delius, H. Kornberg, T. Gefter, M.L. Alberts, B. (1972). A DNA-unwinding protein isolated from *Escherichia coli*: its interaction with DNA and DNA polymerases. *Proc. Natl. Acad. Sci.* **69**: 3537-41

Singleton, M.R. Wentzell, L.M. Liu, Y. West, S.C. Wigley, D.B. (2002). Structure of the single-strand annealing domain of human RAD52 protein. *Proc. Natl. Acad. Sci.* **99**: 13492-7

Singleton, M.R. Dillingham, M.S. Gaudier, M. Kowalczykowski, S.C. Wigley, D.B. (2004). Crystal structure of RecBCD enzyme reveals a machine for processing DNA breaks. *Nature*. **432**: 187-93

Spies, M. Bianco, P.R. Dillingham, M.S. Handa, N. Baskin, R.J. Kowalczykowski, S.C. (2003). A molecular throttle: The recombination hotspot χ controls DNA translocation by the RecBCD helicase. *Cell.* **114**: 647-54

Spies, M. Dillingham, M.S. Kowalczykowski, S.C. (2005). Translocation by the RecB motor is an absolute requirement for χ-recognition and RecA protein loading by RecBCD enzyme. *J. Biol. Chem.* **280**: 37078

Spies, M. & Kowalczykowski, S.C. (2006). The RecA binding locus of RecBCD is a general domain for recruitment of DNA strand exchange proteins. *Molecular Cell.* **21**: 573-80

Spies, M. Amitani, I. Baskin, R.J. Kowalczykowski, S.C. (2007). RecBCD enzyme switches lead motor subunits in response to χ recognition. *Cell.* **131**: 694-705

Sriprakash, K.S. Lundh, N. Huh, M.M-O. Radding, C.M. (1975). The specificity of λ exonuclease: Interactions with single-stranded DNA. *J. Biol. Chem.* **250**: 5438-45

Stahl, F.W. McMilin, K.D. Stahl, M. Crasemann, J.M. Lam, S. (1974). The distribution of crossovers along unreplicated lambda bacteriophage chromosomes. *Genetics.* **77**: 395-408

Stahl, F.W. Fox, M.S. Faulds, D. Stahl, M.M. (1990). Break-join recombination in phage λ. *Genetics.* **125**: 463-74

Stahl, F.W. (1998). Recombination in phage λ: one geneticist's historical perspective. *Gene.* **223**: 95-102

Stahl, M.M. Thomason, L. Poteete, A.R. Tarkowski, T. Kuzminov, A. Stahl, F.W. (1997). Annealing *vs.* Invasion in Phage λ Recombination. *Genetics.* **147**: 961-77

Story, R.M. & Steitz, T.A. (1992). Structure of the RecA protein-ADP complex. *Nature.* **355**: 374-6

Story, R.M. Weber, I.T. Steitz, T.A. (1992). The structure of the *E. coli recA* protein monomer and polymer. *Nature.* **355**: 318-25

Studier, F.W. & Moffatt, B.A. (1986). Use of bacteriophage T7 RNA polymerase to direct selective high-level expression of cloned genes. *J. Mol. Biol.* **189**: 113-30

Subramanian, K. Rutvisuttinunt, W. Scott, W. Myers, R.S. (2003). The enzymatic basis of processivity in λ exonuclease. *Nucleic Acids Research.* **31**: 1585-96

Sung, P. Krejci, L. Van Komen, S. Sehorn, M.G. (2003). Rad51 recombinase and recombination mediators. *J. Biol. Chem.* **278**: 42729-32

Sutherland, J.H. Cheng, B. Liu, I-F. Tse-Dinh, Y-C. (2008). SOS induction by stabilised topoisomerase IA cleavage complex occurs via the RecBCD pathway. *J. Bacteriol.* **190**: 3399-403

Szabo, M. Kiss, J. Kotany, G. Olasz, F. (1999). Importance of illegitimate recombination and transposition in IS*30*-associated excision events. *Plasmid.* **42**: 192-209

Szostak, J.W. Orr-Weaver, T.L. Rothstein, R.J. (1983). The Double-Strand-Break Repair Model for Recombination. *Cell.* **33**: 25-35

Tabor, S. & Richardson, C.C. (1985). A bacteriophage T7 RNA polymerase/promoter system for controlled exclusive expression of specific genes. *Proc. Natl. Acad. Sci USA.* **82**: 1074-8

Takahashi, M. Maraboeuf, F. Morimatsu, K. Selmane, T. Fleury, F. Norden, B. (2007). Calorimetric analysis of binding of two consecutive DNA strands to RecA protein illuminates mechanism for recognition of homology. *J. Mol. Biol.* **365**: 603-11

Takahashi, N. & Kobayashi, I. (1990). Evidence for the double-strand break repair model of bacteriophage lambda recombination. *Proc. Natl. Acad. Sci.* **87**: 2790-4

Tarkowski, T.A. Mooney, D. Thomason, L.C. Stahl, F.W. (2002). Gene products encoded in the *ninR* region of phage λ participate in Red-mediated recombination. *Genes to Cells.* **7**: 351-63

Taylor, A.F. & Smith, G.R. (1985). Substrate specificity of the DNA unwinding activity of the RecBC enzyme of *Escherichia coli. J. Mol. Biol.* **185**: 431-43

Taylor, A.F. & Smith, G.R. (1992). RecBCD enzyme is altered upon cutting at a Chi recombination hotspot. *Proc. Natl. Acad. Sci.* **89**: 5226-30

Taylor, A.F. & Smith, G.R. (1999). Regulation of homologous recombination: Chi inactivates RecBCD enzyme by disassembly of the three subunits. *Genes & Dev.* **13**: 890-900

Taylor, A.F. & Smith, G.R. (2003). RecBCD enzyme is a DNA helicase with fast and slow motors of opposite polarity. *Nature.* **423**: 889-93

Thaler, D.S. Stahl, M.M. Stahl, F.W. (1987). Evidence that the normal route of replication-allowed Red-mediation involves double-chain ends. *EMBO J.* **6**:3171-6

Thaler, D.S. Stahl, M.M. Stahl, F.W. (1987b). Double-chain-cut sites are recombination hotspots in the Red pathway of phage λ. *J. Mol. Biol.* **195**: 75-87

Tracy, R.B. & Kowalczykowski, S.C. (1996). *In vitro* selection of preferred DNA pairing sequences by the *Escherichia coli* RecA protein. *Genes & Dev.* **10**: 1890-1903

Tracy, R.B. Baumohl, J.K. Kowalczykowski, S.C. (1997). The preference for GT-rich DNA by the yeast Rad51 protein defines a set of universal pairing sequences. *Genes & Dev.* **11**: 3423-31

Umezu, K. Nakayama, K. Nakayama, H. (1990). *Escherichia coli* RecQ protein is a DNA helicase. *Proc. Natl. Acad. Sci.* **87**: 5363-7

Umezu, K. Chi, N.W. Kolodner, R.D. (1993). Biochemical interaction of the *Escherichia coli* RecF, RecO and RecR proteins with RecA protein and single-stranded DNA binding protein. *Proc. Natl. Acad. Sci.* **90**: 3875-9

Umezu, K. Kolodner, R.D. (1994). Protein interactions in genetic recombination in *Escherichia coli. J. Biol.Chem.* **269**: 30005-13

Venkatesh, R. Ganesh, N. Guhan, N. Sreedhar Reddy, M. Chandrasekhar, T. Muniyappa, K. (2002). RecX protein abrogates ATP hydrolysis and strand exchange promoted by RecA: Insights into negative regulation of homologous recombination. *Proc. Natl. Acad. Sci.* **99**: 12091-6

Wagner, P.L. & Waldor, M.K. (2002). Bacteriophage control of bacterial virulence. *Infect. Immun.* **70**: 3985-93

Webb, M.R. (1992). A continuous spectrophotometric assay for inorganic phosphate and for measuring phosphate release kinetics in biological systems. *Proc. Natl. Acad. Sci.* **89**: 4884-7

Webb, B.L. Cox, M.M. Inman, R.B. (1995). An Interaction between the *Escherichia coli* RecF and RecR proteins dependent on ATP and double-stranded DNA. *J. Biol. Chem.* **270**: 31397-404

Webb, B.L. Cox, M.M. Inman, R.B. (1997). Recombinational DNA repair – the RecF and RecR proteins limit the extension of RecA filaments beyond single-stranded DNA gaps. *Cell.* **91**: 347-56

Webb, B.L. Cox, M.M. Inman, R.B. (1999). ATP hydrolysis and DNA binding by the *Escherichia coli* RecF protein. *J. Biol. Chem.* **274**: 15367-74

Weiner, M.P. Anderson, C. Jerspeth, B. Wells, S. Johnson-Browne, B. *et al.* (1994). Strategies Newsletter (Stratagene). *Strategies.* **7**: 41-43

Weinstock, G.M. (1996). General recombination in *Escherichia coli.* p1034. *In* F.C. Neidhardt, R. Curtiss III, J.L. Ingraham, E.C.C. Lin, K.B. Low, B. Magasanik, W.S. Reznikoff, M. Riley, M. Schaechter, and H.E. Umbarger (ed.), *Escherichia coli* and *Salmonella*: cellular and molecular biology, 2nd ed. ASM Press, Washington D.C.

Whitby, M.C. Vincent, S.D. Lloyd, R.G. (1994). Branch migration of Holliday junctions: identification of RecG protein as a junction specific DNA helicase. *EMBO J.* **13**: 5220-8

Wigley, D. (2007). RecBCD: The supercar of DNA repair. *Cell.* **131**: 651-3

Wu, A.M. Bianchi, M. DasGupta, C. Radding, C.M. (1983). Unwinding associated with synapsis of DNA molecules by RecA protein. *Proc. Natl. Acad. Sci.* **80**: 1256-60

Wu, Z. Xing, X. Bohl, C.E. Wisler, J.W. Dalton, J.T. Bell, C.E. (2006). Domain structure and DNA binding regions of β protein from bacteriophage λ. *J. Biol. Chem.* **281**: 25205-14

Xu, L.W. & Marians, K.J. (2003). PriA mediates DNA replication pathway choice at recombination intermediates. *Mol. Cell.* **11**: 817-26

Yamaguchi, T. Hayashi, T. Takami, H. Nakasone, K. Ohnishi, M. Nakayama, K. Yamada, S. Komatsuzawa, H. Sugai, M. (2000). Phage conversion of exfoliative toxin A production in *Staphylococcus aureus*. *Mol. Micro.* **38**: 694-705

Yang, H. Li, Q. Fan, J. Holloman, W.K. Pavletich, N.P. (2005). The BRCA2 homologue Brh2 nucleates Rad51 filament formation at a dsDNA-ssDNA junction. *Nature*. **433**: 653-7

Zaitsev, E.N. & Kowalczykowski, S.C. (1998). Binding of double-stranded DNA by *Escherichia coli* RecA protein monitored by a fluorescent dye displacement assay. *Nucleic Acids Research*. **26**: 650-4

Zhao, J. Wang, W-N. Tan, Y-C. Zheng, Y. Wang, Z-X. (2002). Effect of Mg^{2+} on the kinetics of guanine nucleotide binding and hydrolysis by Cdc42. *Biochem. Biophys. Res. Comms*. **297**: 653-8

Ziebuhr, W. Ohlsen, K. Karch, H. Korhonen, T. Hacker, J. (1999). Evolution of bacterial pathogenesis. *Cell. Mol. Life. Sci.* **56**: 719-28